

Temperature buffer test

**Sensors data report
(Period 030326–100301)
Report No: 13**

Reza Goudarzi, Mattias Åkesson, Ulf Nilsson
Clay Technology AB

December 2010

Svensk Kärnbränslehantering AB
Swedish Nuclear Fuel
and Waste Management Co
Box 250, SE-101 24 Stockholm
Phone +46 8 459 84 00



ISSN 1651-4416

SKB P-12-03

ID 1334653

Temperature buffer test

Sensors data report (Period 030326–100301) Report No: 13

Reza Goudarzi, Mattias Åkesson, Ulf Nilsson
Clay Technology AB

December 2010

Keywords: Field test, Buffer, Bentonite, Temperature, Relative humidity, Pore pressure, Total pressure, Displacement.

This report concerns a study which was conducted for SKB. The conclusions and viewpoints presented in the report are those of the authors. SKB may draw modified conclusions, based on additional literature sources and/or expert opinions.

Data in SKB's database can be changed for different reasons. Minor changes in SKB's database will not necessarily result in a revised report. Data revisions may also be presented as supplements, available at www.skb.se.

A pdf version of this document can be downloaded from www.skb.se.

Résumé

TBT (Test de Barrière ouvragée en Température) est un projet mené par SKB et l'ANDRA, soutenu par ENRESA (en modélisation) et DBE (en instrumentation) qui vise à comprendre et modéliser le comportement thermo-hydro-mécanique de barrières ouvragées à base d'argile gonflante soumises à des températures élevées (> 100°C) pendant leur hydratation.

L'essai est conduit dans le HRL d'Äspö dans une alvéole verticale de 8 m de profondeur et 1.76 m de diamètre. Deux sondes chauffantes (chacune de 3 m de long et 0.6 m de diamètre) sont entourées d'argile gonflante, une bentonite MX-80 qui est confinée par un bouchon ancré dans la roche par 9 câbles. L'essai fonctionne depuis le printemps 2003.

Deux types de barrières ouvragées sont étudiés:

- La sonde inférieure est, de manière traditionnelle, directement entourée de bentonite dont la température peut localement largement excéder 100°C.
- La sonde supérieure est elle entourée par un anneau de sable formant écran thermique pour la bentonite disposée autour dont la température est maintenue en deçà de 100°C.

Les sondes ont été chauffées chacune à la puissance de 1,500 W du 15^{ème} au 1,171^{ème} jour et à 1,600 W ensuite. Autour du 1,700^{ème} jour, les puissances ont été portées par paliers à 2,000 W pour la sonde inférieure et à 1,000 W pour la sonde supérieure.

Ce rapport présente les données de TBT enregistrées depuis son début le 26 mars 2003 jusqu'au premier mars 2010.

Dans la bentonite la pression totale est mesurée en 29 points, la pression de pore en 8 points et l'humidité relative en 35 points. La température est mesurée en 92 points et aussi à l'emplacement de chaque capteur dont la mesure nécessite d'être compensée en température.

Des mesures additionnelles sont faites : température en 40 points dans la roche alentour, en 11 points à la surface et 6 à l'intérieur des sondes. La force de confinement est mesurée sur trois des neuf câbles. Le déplacement vertical du bouchon est mesuré en trois points. Le débit et la pression d'eau fournie au système sont également mesurés.

Des mesures de température et de pression dans les zones chaudes du test obtenues par des capteurs à fibres optiques installés par DBE sont rapportées dans l'Appendix B.

Globalement, le système de mesure et de transmission des données fonctionne bien et les capteurs fournissent des valeurs fiables. Une exception concerne la mesure d'humidité relative au droit de la sonde inférieure où plusieurs capteurs ne fonctionnent plus.

La densité des dispositifs de mesure de température par thermocouples à mi-hauteur de chaque sonde chauffante s'est révélée utile pour observer de façon qualitative les cycles saturation - désaturation. Dans la section du bas des indications claires de désaturation sont apparues très tôt dans l'expérience sur une zone annulaire de 0.15 m autour de la sonde chauffante. Cette partie se resature très lentement à l'heure actuelle.

Dans la bentonite, la plupart des mesures d'humidité ne sont plus significatives, car le matériau est désormais trop proche de la saturation. Cependant dans la section supérieure (au Ring 9), le fait que les pressions de pore s'équilibrent avec la pression d'eau du filtre de sable indique une saturation de l'argile.

Ce filtre de sable disposé entre la roche et la colonne de bentonite permet une alimentation artificielle du système en eau. Plus de la totalité de l'eau théoriquement nécessaire au remplissage du filtre et à la saturation de la bentonite a été injectée, ce qui montre que le système n'est pas hydrauliquement clos mais fuit dans l'environnement rocheux (EDZ). La pression croissante nécessaire pour maintenir le débit d'injection prouvait la fragilité du système d'injection (colmatage des embouts des injecteurs).

De ce fait, une action de décolmatage a été entreprise en 2007 avec injection d'eau déminéralisée à la place de l'eau du site utilisée depuis le début du test. L'action a porté ses fruits et rendu possible le contrôle de la pression hydraulique dans le filtre de sable et son maintien à 4 bars.

La baisse de pression totale et la hausse de la succion observées entre le 225^{ème} et le 370^{ème} jour autour de la sonde supérieure ont été provoquées par un déficit en eau inattendu du haut du filtre de sable. Lorsque ce filtre a été de nouveau rempli, la pression totale dans la bentonite s'est rétablie et la succion s'est remise à décroître.

Le fait d'hydrater l'anneau de sable autour de la sonde supérieure et de modifier la puissance électrique a influencé les pressions totales et les pressions interstitielles. Six mois après ces événements, les pressions totales ont retrouvé leurs valeurs antérieures et les pressions interstitielles atteignent enfin des valeurs significatives.

Abstract

TBT (Temperature Buffer Test) is a joint project between SKB/ANDRA and supported by ENRESA (modeling) and DBE (instrumentation), which aims at understanding and modeling the thermo-hydro-mechanical behavior of buffers made of swelling clay submitted to high temperatures (over 100°C) during the water saturation process. The test was dismantled during the winter of 2009/2010, and this sensors data report is thereby the last one.

The test was carried out in Äspö HRL in a 8 meters deep and 1.76 m diameter deposition hole, with two heaters (3 m long, 0.6 m diameter), surrounded by a MX-80 bentonite buffer and a confining plug on top anchored with 9 rods. It was installed during spring 2003. Two buffer arrangements have been investigated:

- The lower heater was surrounded by bentonite in the usual way, allowing the temperature of the bentonite to exceed 100°C locally.
- The higher heater was surrounded by a ring of sand acting as thermal protection for the bentonite, the temperature of which is kept below 100°C.

The heaters were powered with 1,500 W from day 15 to day 1,171, when the power was raised to 1,600 W. Around day 1,700, the power was raised by steps in the lower heater to 2,000 W and reduced in the upper heater to 1,000 W. The power output was terminated on day 2,347.

This report presents data from the measurements in the Temperature Buffer Test from 030326 to 100301 (26 March 2003 to 01 March 2010).

The following measurements have been made in the bentonite: Temperature was measured in 92 points, total pressure in 29 points, pore water pressure in 8 points and relative humidity in 35 points. Temperature was also measured by all gauges as an auxiliary measurement used for compensation.

The following additional measurements have been made: temperature was measured in 40 points in the rock, in 11 points on the surface of each heater and in 6 points inside each heater. The force on the confining plug was measured in 3 of the 9 rods and its vertical displacement was measured in three points. The water inflow and water pressure in the outer sand filter was also measured.

A general conclusion is that the measuring systems and transducers have worked well and almost all sensors have delivered reliable values. An exception is the Relative Humidity sensors in the high temperature area around the lower heater, where some sensors have failed.

The dense arrays of thermocouples at the mid-height of the two heaters appear to be useful for examining the dehydration/hydration process qualitatively. In the lower section there were clear signs of early dehydration in a 0.15 m annular zone around the heater. The resaturation of this part has been followed during the test period.

Most humidity sensors measurements in the bentonite buffer have been insignificant during the second half of the test period, indicating that the material was close to saturation. However in the upper section (Ring 9), the fact that the pore pressure started to equilibrate with the water pressure in the sand filter indicated that fill water saturation was reached in this part.

This sand slot between the bentonite column and the surrounding rock has been used for artificial wetting. More than the water theoretically needed to fill up the sand slot and to saturate the bentonite has been injected, which proves that the system was not hydraulically closed but leaked towards the rock (EDZ). The high sand slot injection pressure required to maintain the inflow shows the weakness of the injection system (clogging of the filter tips). An unclogging action was therefore performed by injecting demineralised water instead of ground water, as it was done since the beginning of the experiment. This action proved successful, and after this modification it was possible to maintain a hydraulic pressure in the filter around 4 bar absolute.

The decrease in total pressure and increase in suction that was recorded around the upper heater from day 225 to day 370 has been caused by an unexpected lack of water supply in the upper part of the sand slot. When this slot got filled again with water, the total pressure resumed and increased and the suction decreased again.

The hydration of the sand shield surrounding the upper heater, and the change in power output, which were implemented during the second half of 2007, influenced the total pressures and the pore pressures. Half a year after these activities, the total pressures had in general recovered to their original levels. Moreover, all measured pore pressures displayed significant values at that time. However, the total pressure and the pore pressure at the innermost sensors in Ring 3 decreased considerably during the autumn of 2008. Among these, the total pressure recovered to some degree before the termination of the heaters in August 2009, whereas the pore pressure never recovered.

Sammanfattning

TBT (TBT (Temperature Buffer Test) är ett gemensamt SKB/ANDRA projekt med deltagande av ENRESA (modellering) och DBE (instrumentering). Syftet är att öka förståelsen för de termiska, hydrauliska och mekaniska processerna i en buffert gjord av svällande lera som utsätts för höga temperaturer (över 100 °C) under vattenmättnadsfasen och att kunna modellera dessa processer. Testet bröts under vintern och denna sensor data rapport är därmed den sista.

Försöket utfördes i Äspö HRL i ett 8 m djupt deponeringshål med diametern 1,76 m, där två värmare, omgivande MX-80 bentonitbuffert och en ovanliggande plugg, som förankrats med 9 stag, installerades våren 2003. Två olika buffertarrangemang har undersökts:

- Den nedre värmaren omgavs på konventionellt sätt av bentonit, vilket medgav att temperaturen i bentoniten lokalt kunde överstiga 100 °C.
- Den övre värmaren omgavs av en ring av sand, vilket fungerade som ett termiskt skydd för bentoniten, varför temperaturen i denna var lägre än 100 °C.

Värmarna belastades med en effekt på 1 500 W från dag 15 till dag 1 171. Effekten på värmarna ökades till 1 600 W dag 1 171. Från ungefär dag 1 700 ökades effekten stegvis i den nedre värmaren till 2 000 W och samtidigt minskades effekten från den övre till 1 000 W. Effekten stängdes av dag 2 347.

I denna rapport presenteras data från mätningar i TBT under perioden 030326–100301.

Följande mätningar har gjorts i bentoniten: Temperaturen mättes i 92 punkter, totaltryck i 29 punkter, porvattentryck i 8 punkter och relativa fuktigheten i 35 punkter. Temperaturen mättes även i alla relativa fuktighetsmätare, detta för att kompensera för temperaturens inverkan på mätresultaten.

Följande övriga mätningar gjordes: Temperaturen mättes i 40 punkter i berget, i 11 punkter på ytan av varje värmare och i 6 punkter inne i vardera värmare. Kraften på den ovanliggande pluggen mättes i 3 av de 9 stagen och vertikala förskjutningen av pluggen mättes i tre punkter. Vatteninflödet och vattentrycket i den yttre sandfyllda spalten har också mätts.

En generell slutsats är att mätsystemen och givarna fungerade bra och i stort sett alla givare levererade pålitliga mätvärden. Ett undantag är mätningarna av relativa fuktigheten i högttemperaturområdet runt den nedre värmaren, där ett flertal givare inte fungerade.

De täta linjerna av termoelement vid de två värmarnas höjdcentrum visar sig vara användbara för att undersöka torkning/mättnadsprocessen kvalitativt. I den undre sektionen fanns det tydliga tecken på uttorkning inom ett avstånd av 0,15 m från värmerytan. En långsam återmättnad av denna zon har kunnat följas under projektets gång.

Resultaten från de flesta relativ fuktighetsmätarna har varit mindre signifikanta under andra halvan av testperioden, eftersom bentonitbufferten är för nära mättnad. Portrycksgivarna i Ring 9 började emellertid komma i jämvikt med vattentrycket i sandfiltret, vilket indikerade att full mättnad har uppnåtts i denna del.

Sandfiltret mellan bentonitblocken och omgivande berg användes för artificiell bevätning. Mer vatten än den teoretiska mängden som behövs för att mätta hela systemet hade tillförts i ett ganska tidigt skede. Detta visar att systemet inte var hydrauliskt stängt, utan att det finns ett läckage (sannolikt ut i berget). Det injekteringstryck i sandspalten som fordrades för att upprätthålla inflödet visar på en svaghet hos injekteringssystemet. Detta berodde sannolikt på en igensättning av filterspetsarna. Detta har åtgärdats genom att injektera avjoniserat vatten. Detta ersatte således det formationsvatten som tidigare användes för den artificiella bevätningen. Denna åtgärd visade sig vara framgångsrik och det var därefter möjligt att upprätthålla ett filtertryck kring 4 bar (absolut).

Den sänkning av totaltrycket och höjning av buffertens *suction* som noterats runt den översta kapseln mellan dag 225 och dag 370 orsakades av en brist på vattentillgång i övre delen av sandfiltret. När sandfiltret vattenfylldes och trycksattes höjdes totaltrycket åter medan buffertens *suction* minskade.

Bevätningen av sandskölden och den effektförändring som implementerades under andra halvan av 2007 påverkade såväl totaltryck som portryck. Ett halvår efter dessa aktiviteter hade totaltrycken i allmänhet återställts till sina ursprungliga nivåer. Dessutom uppvisade samtliga portryck signifikanta värden. Däremot minskade total- och portrycket vid de innersta sensorerna i Ring 3 markant under hösten 2008. Bland dessa återhämtade sig totaltrycket i viss utsträckning innan avstängningen av värmarna i Augusti 2009. Portrycket återhämtade sig däremot aldrig.

Contents

1	Introduction	11
2	Comments	13
2.1	General	13
2.2	Total pressure, Geokon (App. A, pages 45–53)	13
2.3	Suction, Wescore Psychrometers (App. A, pages 54–58)	15
2.4	Relative humidity, Vaisala and Rotronic (App. A, pages 59–64)	15
2.5	Pore water pressure, Geokon (App. A, pages 65–66)	15
2.6	Water flow and water pressure in the sand (App. A, pages 67–69)	15
2.7	Forces on the plug (App. A, page 70)	16
2.8	Displacement of the plug (App. A, page 71)	16
2.9	Heater power (App A, page 72–73)	16
2.10	Temperature in the buffer (App. A, pages 74–79)	16
2.11	Temperature in the rock (App. A, pages 80–83)	17
2.12	Temperature on the heater surface (App. A, pages 84–85)	17
2.13	Temperature inside the heater (App. A, pages 86–87)	17
3	Coordinate system	19
4	Location of instruments	21
4.1	Brief description of the instruments	21
4.2	Strategy for describing the position of each device	22
4.3	Position of each instrument in the bentonite	23
4.4	Instruments in the rock	28
4.5	Instruments in the heaters	29
4.6	Instruments on the plug	31
5	Discussion of results	33
5.1	General	33
5.2	Total inflow of water	33
5.3	Temperatures	35
5.4	Relative humidity/suction	38
5.5	Pore pressure	41
5.6	Total pressure	41
	References	43
	Appendix A Measured data	45
	Appendix B Sensor validation	89

1 Introduction

The installation of the Temperature Buffer Test was made during spring 2003 in Äspö Hard Rock Laboratory, Sweden.

The Temperature Buffer Test, TBT, is a full-scale experiment that ANDRA and SKB carry out at the SKB Äspö Hard Rock Laboratory. In addition ENRESA supports TBT with THM modelling and DBE has installed a number of optic pressure sensors.

The test aims at understanding and modelling the thermo-hydro-mechanical behaviour of buffers made of swelling clay submitted to high temperatures (over 100°C) during the water saturation process. No other full scale tests have been carried out with buffer temperatures exceeding 100°C so far. The test was dismantled during the winter of 2009/2010, and this sensors data report is thereby the last one.

The test consisted of a full-scale KBS-3 deposition hole, 2 steel heaters equipped with electrical heating elements simulating the power of radioactive decay and a mechanical plug at the top. Figure 1-1 shows the layout and denomination of blocks and heaters. The heaters were embedded in dense clay buffer consisting of blocks (cylindrical and ring shaped) of compacted bentonite powder.

An artificial water pressure was applied in the outer slot between the buffer and the rock, which was filled with compacted sand and functioned as a filter.

The upper heater was surrounded by sand in order to reduce the temperature in the bentonite.

The buffer material was instrumented with pressure cells (total and water pressure), thermocouples and moisture gauges. Thermocouples are also installed in the rock.

A retaining plug was built in order to confine the buffer swelling.

Measured results and general comments concerning the collected data are given in Chapter 2. A test overview with the positions of the measuring points and a brief description of the instruments are presented in Chapters 3 and 4. Finally analyses and discussions of the results are given in Chapter 5.

In general the data in this report are presented in diagrams covering the time period 030326 to 100301¹. The time axis in the diagrams represents days from 030326. The diagrams are attached in Appendix A.

Results for the sensor function control, performed on instrument collected during the dismantling operation, are attached in Appendix B.

¹ YYMMDD (Swedish way of expressing dates implying that the first two numbers are the year, the next two numbers are the month and the final two numbers are the date).

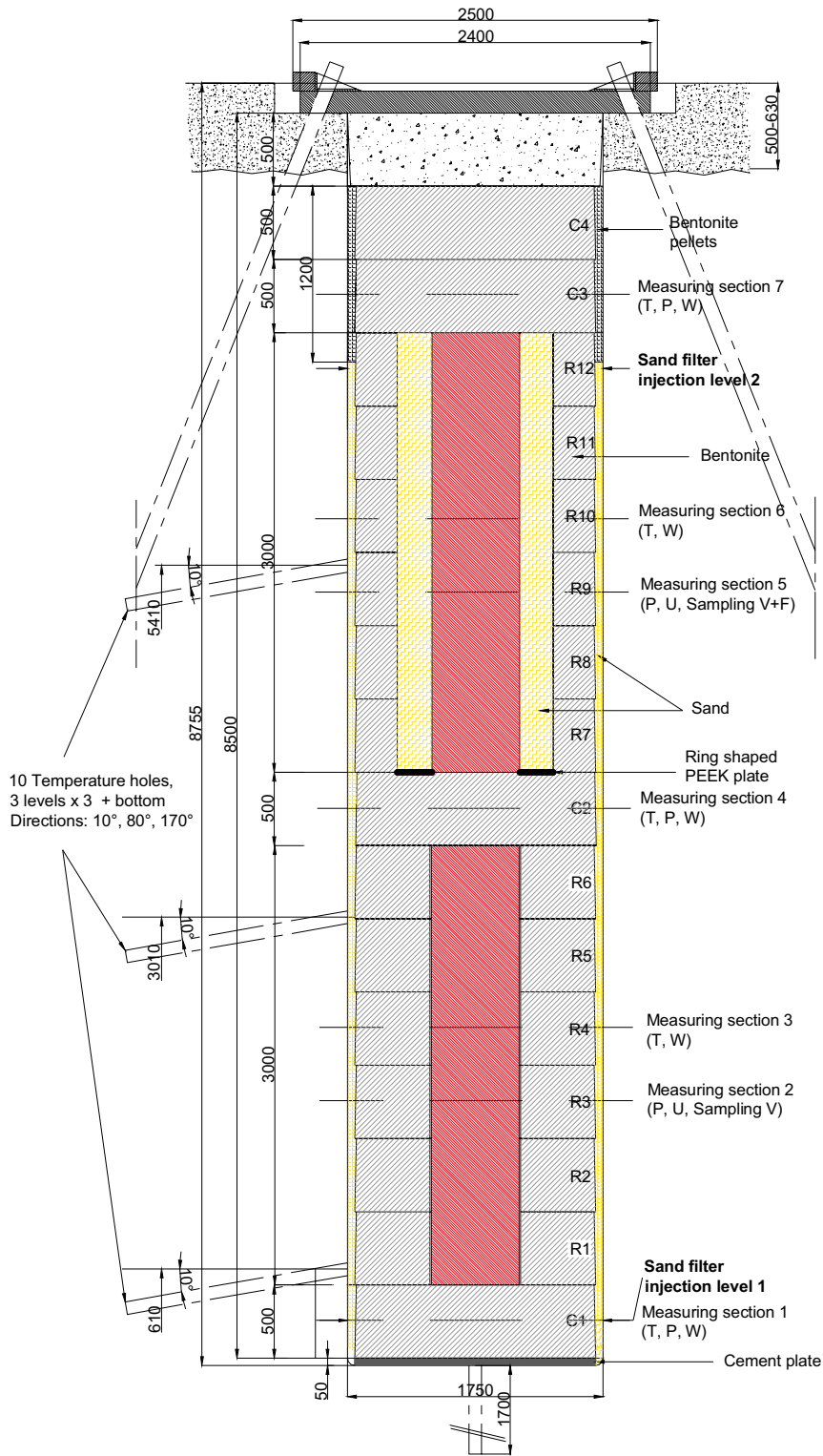


Figure 1-1. Schematic view showing the layout of the experiment and the numbering of bentonite blocks. The lower heater is denominated No. 1 and the upper heater is No. 2.

2 Comments

2.1 General

In this chapter short comments on general trends in the measurements are given. Sensors that are not delivering reliable data or no data at all are noted and comments on the data in general are given but no evaluation or comparison with predictions will be given here.

The heating of both heaters started with an initially applied constant power of 900 W on 030326. This date is also marked as start date. The power was raised to 1,200 W on 030403. The power was further raised to 1,500 W on 030410. Several power failures have occurred. The power was raised to 1,600 W on 060609 (day 1,171).

The power in Heater 1 was raised to 2,000 W during three weeks (100 W/week) from 071115 to 071206 (day 1,695–1,716).

The power in Heater 2 was decreased to 1,000 W during five weeks (100 W/week) from 071115 to 071220 (day 1,695–1,730).

The power in Heater 1 and Heater 2 has been switched off on 090828 (day 2,347).

Important events and dates are shown in Table 2-1.

The water filling was done through four tubes leading to the bottom of the sand filter. The filling was slow due to flow resistance in the sand (or the filter tips) and the rate was increased by pressurizing the water (see section 2.6). The filling was completed after 60–80 days. The water pressure in the bottom of the sand filter has been kept with periodical interruptions (see section 2.6) but the valves to the 4 upper tubes leading out water from the top of the sand filter was open at all times until 040406.

On day 377 (040406) water was supplied to the sand filter also through the tubes leading to the top of the sand filter and a small pressure applied. On days 448–449 the filters were flushed and a water pressure of 160 kPa was applied on the sand filter through both the top tubes and the bottom tubes.

This report is the 13th and last one and covers the results up to 20100301, (i.e. during the sampling and removal of Ring 4).

2.2 Total pressure, Geokon (App. A, pages 45–53)

The measured pressure ranges were from 5.1 to 9.3 MPa on 090817 (day 2,336) when the power on Heater 1 has started to switch off in step.

The start of the pressure increase takes place shortly after the water filling has reached the level of the different transducer.

Notable is that all transducers in ring 9 around Heater 2 except the one at the rock are recording decreasing total pressure in a period between day ~230 and day ~370.

The pressure increase by sensor placed in Cyl.3 on 051209 (day 989) due to water filling of the filter mats between Cyl.3 and Cyl.4.

Fifteen transducers were out of order on 090817 when the power on Heater 1 was switched off.

During the dismantling operation, it was found that the outermost radial pressure sensor in Ring 9 (PB226) was located approximately 1 m below the position given in Table 4-2 and the diagram shown on page 50.

Table 2-1. Key dates for TBT.

Activity	Date (time)	Day No.
900 W power applied.	030326	0
Start water filling of filter.	030327	1
1,200 W power applied.	030403	8
1,500 W power applied.	030410	15
Finished water filling.	~030604	~70
Power failure Heater 1.	030423 (~20.00)–030424 (~10.00)	27–28
Power failure Heater 1.	030527 (~01.00)–030527 (~12.00)	62
Power failure Heater 1.	030603 (~12.00)–030603 (~14.00)	69
Power failure Heater 1.	030606 (~19.00)–030609 (~10.00)	72–75
Power failure Heater 1.	030612 (~12.00)–030612 (~14.00)	78
Power failure Heaters 1 and 2.	030923 (~12.00 ¹⁾)–030923 (~18.00 ¹⁾)	181
Power failure Heaters 1 and 2.	031028 (~18.00 ¹⁾)–031029 (~11.00 ¹⁾)	216
Injection pump replaced by gas tube.	031104	223
Power failure Heater 1.	040120 (~16.00)–040120 (~19.00)	300
Power failure Heater 2.	040120 (~18.00)–040120 (~20.00)	300
Filling and pressurisation of the sand filter also through the upper tubes.	040406	377
Flushing and pressurisation of filters through both upper and lower tubes (160 kPa).	040615–040616	448–449
Pressurisation of filters through both upper and lower tubes.	041011–041014	565–568
Filling and pressurisation of the sand filter through AS205 and AS207.	041014	568
Filling and pressurisation of the sand filter through AS201, AS202, AS204, AS205, AS206 and AS208.	041110	595
Power failure Heater 2. 50 w more power.	050629–050706	826–833
Filling and pressurisation of the sand filter through AS201, AS203, AS204, AS205, AS207 and AS208.	050728	856
Water filling of filter mats.	051209	989
Airvents AS212–AS215 closed.		
AS209 connected to artificial saturation.		
AS210 connected to artificial saturation.	051212	992
Back flushing of filters through both upper and lower tubes. Only AS203 is still closed.	060517–060614	1,148–1,176
1,600 W power applied.	060609–	1,171–
Power failure Heater 1.	060903–060904	1,257–1,258
Change in water quality for injection.	070417	1,483
1,700 W power applied Heater 1.	071115–071122	1,695–1,702
1,500 W power applied Heater 2.	071115–071122	1,695–1,702
1,800 W power applied Heater 1.	071122–071129	1,702–1,709
1,400 W power applied Heater 2.	071122–071129	1,702–1,709
1,900 W power applied Heater 1.	071129–071206	1,709–1,716
1,300 W power applied Heater 2.	071129–071206	1,709–1,716
2,000 W power applied Heater 1.	071206–090817	1,716–2,336
1,200 W power applied Heater 2.	071206–071213	1,716–1,723
1,100 W power applied Heater 2.	071213–071220	1,723–1,730
1,000 W power applied Heater 2.	071220–090824	1,730–2,343
Stop water inflow to sand shield.	090409	2,206
Power in Heater 1 switches off.	090817–090828	2,336–2,347
Power in Heater 2 switches off.	090824–090828	2,343–2,347
Stop water filling of filter.	090828	2,347
Start dismantling.	091028	2,408
Last sensors data (removal of Ring 4).	100301	2,532

1) The duration of the power loss is not known since no data was recorded between the times noted.

2.3 Suction, Wescor Psychrometers (App. A, pages 54–58)

Wescor psychrometers are only working at suction below $\sim 7,000$ kPa, which correspond to high relative humidity (higher than 95%).

Notable is that two transducers around Heater 2 (Ring 10) yielded increasing suction values (drying) concurrently with the decreasing total pressures in Ring 9 mentioned above.

All transducers have at some point yielded interpretable values. However, during the last measuring period (i.e. since 080701) no transducer has yielded any interpretable values.

2.4 Relative humidity, Vaisala and Rotronic (App. A, pages 59–64)

Relative humidity and temperature measured with Vaisala and Rotronic transducers are shown on pages 64–69. For most transducers RH starts to increase just after the filling of water has reached the sensor level

7 of 23 sensors have failed for other reasons than high degree of saturation during the test period. Four of them were placed in ring 4. All remaining sensors have shown 100%.

2.5 Pore water pressure, Geokon (App. A, pages 65–66)

The measured pressure ranges of sensors placed in Ring 9 were from 0.0 to 0.4 MPa on 090817 (day 2,336) when the power on Heater 1 has started to switch off in steps.

The measured pressure ranges of sensors placed in Ring 3 were from 0.0 to 0.2 MPa on 090824 (day 2,343) when the power on Heater 2 has started to switch off in steps.

One transducer (UB201) was out of order on 090817.

2.6 Water flow and water pressure in the sand (App. A, pages 67–69)

Water filling and measurement of water inflow into the sand started on 030327. The total inflow to the sand has since that date been 4,199 litres. The total volume of voids in the sand filter was initially about 790 litres. The inflow rate has been in average about 1.3 l/day since day 110. The inflow has been stopped on 090828 (day2,347).

There was also an outflow that started after completed filling since the valves from the top of the sand filter was kept open. The outflow stopped rather early and the total outflow of water has been 44 litres.

The water injection pressure upstream the filter tips is shown on page 68. The water pressure was increased to 800–900 kPa during the first 50 days and then kept “constant” until day ~ 370 . However, problems with the water pump have lead to many interruptions in the applied pressure. On day 377 the water pressure was reduced in connection with the start of water supply also from the tubes leading to the top of the filter.

It should be noted that the actual water pressure in the sand filter is only measured at those injection points that are closed to the atmosphere and not pressurized, on 090828 points AS203 and AS207.

The water inflow into the sand shield started on 070509, and stopped on 090409. The total inflow into the sand shield was 548 litre.

2.7 Forces on the plug (App. A, page 70)

The forces on the plug have been measured since 030404. The total force was about 14,940 kN on 090821 when the power had started to switch off in steps.

The influence of the additional water supply from the upper tubes after ~370 days was clearly noticeable.

During the first about 15 days the plug was only fixed with 3 rods. When the total force exceeded 1,100 kN the rest of the 9 rods were fixed in a prescribed manner. This procedure took place 10–11 April 2003 that is 15–16 days after test start. From that time only every third anchor is measured and the results should thus be multiplied with 3. The diagram shows both the actual measurements and after multiplication with 3.

One of the force transducers displayed some irregular trends from day 1,478.

The last measuring of total forces was about 13,905 kN on 091026, i.e. just before the start of the dismantling.

2.8 Displacement of the plug (App. A, page 71)

The three displacement gauges were placed and started to measure displacements from 030409 (day 14) (except for zero reading that was done day 0). One of them (DP201) did not work well and was replaced on 030923 with a new transducer.

Transducer DP203 was out of order.

The measured displacements generally follow the same trend as the cable forces.

2.9 Heater power (App A, page 72–73)

The heating of both heaters started with an initially applied constant power of 900 W on 030326 and was raised to 1,500 W according to Table 2-1.

The failure in one of the heating elements (RCH2) in Heater 2 caused increasing of power with 50 W on 050629 to 050705.

The power has increased to 1,600 W in both heaters on 060609 (day 1,171).

The power in Heater 1 was raised in stages to 2,000 W (100 W/week) from 071115 to 071206 (day 1,695–1,716). This output has been implemented with and divided between two heating elements in Heater 1.

The power in Heater 2 was decreased in stages to 1,000 W (100 W / week) from 071115 to 071220 (day 1,695–1,730).

The power in Heater 1 was switched off in stages from 090817 to 090828.

The power in Heater 2 was switches off in stages from 090824 to 090828.

2.10 Temperature in the buffer (App. A, pages 74–79)

Temperature is measured in a large number of points. The plotting of results is done so that the effect of wetting and cracking can be traced, since sensors placed close to each other are collected in the same diagrams.

The highest measured temperature in the bentonite when the power has started to switch off in step on 090817 (day 2,336) was 151.2°C by sensor TB215 located in the midplane of Heater 1 at the distance 15 mm from the heater surface. The corresponding temperature on the heater surface was 154°C, which shows that the temperature drop at the slot between the heater and the bentonite ring is very small.

Temperature has also been measured (TB254, TB255 and TB256) in the sand around Heater 2 (page 82). Initially, the temperature drop was rather large in this slot (~2.5°C/cm). However, these sensors failed before day 1,000.

The increase in temperature with about one °C seen in the upper part of the buffer in the beginning of June (day ~435) is judged to be caused by the increase in tunnel air temperature that takes place in the summer (page 79).

On day ~335 three additional transducers (TB290, TB291 and TB292) placed in Ring 12 were connected to the data scanner and are reported on page 78. One of them was out of order from start.

The increase in temperature in the beginning of June 2006 (day ~1,171) depends to increasing of power with 100 W.

The increase in temperature around Heater 1 from the middle of November 2007 (day ~1,695) depends to increasing of power with 400 W.

The decrease in temperature around Heater 2 from the middle of November 2007 (day ~1,695) depends to decreasing of power with 600 W.

9 of 92 transducers were out of order when the power was switched off.

2.11 Temperature in the rock (App. A, pages 80–83)

The maximum temperature measured in the rock (73°C) is measured in the central section on the surface of the deposition hole the power has started to switch off in step on 090817(day 2,336).

The deviation from axial symmetry of the temperature measured in the rock is caused by the influence from the heating of the neighbouring Canister Retrieval Test.

On October 11 (day 930) the power in Canister Retrieval Test was switched off.

The large change in rock temperature from day 1,695 and onwards was caused by the change in the power output.

2.12 Temperature on the heater surface (App. A, pages 84–85)

The maximum temperature measured on the surface of Heater 1 was about 154°C and on the surface of Heater 2 about 90°C on 090816 when the power was switched off. There are strong temperature differences in the heaters, both radial and axial. The highest measured difference on the surface is 23°C on Heater 1 and 25°C on Heater 2.

The steady increase in temperature of Heater 1 has turned into a slow decrease. The temperature of Heater 2 has decreased since day 50.

The decreasing temperatures on the surface of Heater 2 on day 1,505 were a result of 30 litres of water injection into the sand shield.

One sensor (TH1 SE0) has stopped work day 1,234.

2.13 Temperature inside the heater (App. A, pages 86–87)

The maximum temperature measured inside Heater 1 is about 180°C and about 110°C in Heater 2 on 090816 when the power was switched off.

The very high values obtained from sensor TH2 SI3 0° before day 1,080 are not reliable.

3 Coordinate system

Measurements are done in 7 measuring sections placed on different levels (see Figure 1-1). On each level, sensors are placed in eight main directions A, AB, B, BC, C, CD, D and DA according to Figure 3-1. Direction A and C are placed in the tunnels axial direction with A headed against the end of the tunnel i.e. almost to the South (see Figure 1-1, 3-1 and 4-1). The angle α is counted anti-clockwise from direction A. The z-coordinate is counted from the bottom of the deposition hole (the cement base).

The bentonite blocks are called cylinders and rings. The cylinders are numbered C1–C4 and the rings R1–R12 respectively (see Figure 1-1).

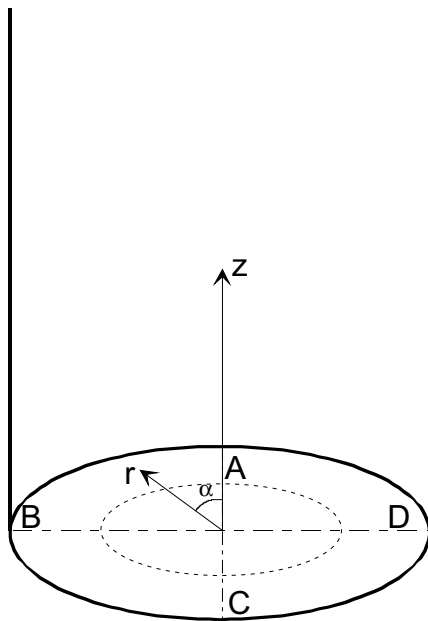


Figure 3-1. Figure describing the coordinate system used when determining the instrument positions.

4 Location of instruments

4.1 Brief description of the instruments

The different instruments that are used in the experiment are briefly described in this chapter. For additional information, see Johannesson et al. (2010).

Measurements of temperature

Buffer

Thermocouples from Pentronic have been installed for measuring temperature in the buffer. Measurements are done in 92 points in the test hole. In addition, temperature gauges are built in into the capacitive relative humidity sensors (23 sensors) as well as in the pressure gauges of vibrating wire type (37 gauges). Temperature is also measured in the psychrometers.

Heater

Temperature is measured in 11 points on the surface of the each heater. Temperature is also measured in 6 points on the inside of each heater.

Rock

Temperature in the rock and on the rock surface of the hole is measured in 40 points with thermocouples from Pentronic.

Measurement of total pressure in the buffer

Total pressure is the sum of the swelling pressure and the pore water pressure. It is measured with Geokon total pressure cells with vibrating wire transducers. 29 cells of this type have been installed.

Measurement of pore water pressure in the buffer

Pore water pressure is measured with Geokon pore pressure cells with vibrating wire transducer. 8 cells of this type have been installed.

Measurement of the water saturation process

The water saturation process is recorded by measuring the relative humidity in the pore system, which can be converted into water ratio or total suction (negative water pressure). The following techniques and devices are used:

- Vaisala relative humidity sensor of capacitive type. 29 cells of this type have been installed. The measuring range is 0–100% RH.
- Wescor psychrometers measure the dry and the wet temperature in the pore system. The measuring range is 95.5–99.6% RH corresponding to the pore water pressure –0.5 to –6MPa. 12 cells of this type have been installed.

Measurements of forces on the plug

The force on the plug caused by the swelling pressure of the bentonite is measured in 3 of the 9 anchors. The force transducers are of the type GLÖTZL.

Measurements of plug displacement

Due to straining of the anchors the swelling pressure of the bentonite will cause not only a force on the plug but also displacement of the plug. The displacement is measured in three points with transducers of the type LVDT with the range 0–50 mm.

Measurement of water flow into the sand

An artificial water pressure is applied in the outer slot, which is filled with sand. Titanium tubes equipped with filter tips are placed in the sand on two levels, 250 mm and 6,750 mm from bottom (four at each level). Water is supplied from a tank in which the water level, and thus the water inflow, is monitored with a differential pressure sensor.

4.2 Strategy for describing the position of each device

Every instrument is named with a unique name consisting of 1 letter describing the type of measurement, (T-Temperature, P-Total Pressure, U-Pore Pressure, W-Relative Humidity, C-Chemical sampling, D-Displacement and A-Artificial water), 1 letter describing where the measurement takes place (B-Buffer, H-Heater, S-Sand, R-Rock and P-plug), 1 figure denoting the deposition hole (1 is used for the CRT test and 2 is used for this experiment), and 2 figures specifying the position in the buffer according to a separate list (see Table 4-1 to 4-7). Every instrument position is described with three coordinates according to Figure 3-1. The r-coordinate is the horizontal distance from the centre of the hole and the z-coordinate is the height from the bottom of the hole (the block height is set to 500mm). The coordinate is the angle from the vertical direction A (almost South).

The position of each instrument is described in the legend in the diagrams according to the following strategy:

Buffer: Three positions according to Figure 3-1: ($z\backslash\alpha\backslash r$) meaning (z -coordinate in m. from the bottom \the angle α \the radius in m.).

The cells measuring total pressure have been installed in three different directions in order to measure the radial stress (R), the axial stress (A) and the tangential stress (T). The direction of the pressure measurement is added in Table 4-2 and in the legend for each cell.

Rock: Three positions with the following meaning: (distance in meters from the bottom\alpha according to Figure 3-1\distance in meters from the rock surface).

The bentonite blocks are called cylinders and rings. The cylinders are numbered C1–C4 and the rings R1–R12 respectively (Figure 1-1).

Heater: The denomination of the instruments in the heater differs a little from the other instruments. At first there are two letters and one figure describing the type of measurement and the place (TH for temperature and heater) and which heater (1 for lower heater and 2 for upper). Then there are again two letters describing if it is an external or internal sensor (SE or SI) and one figure describing the position on the heater (0–4 according to Figure 4-2). Finally the angle clockwise from direction A is written.

4.3 Position of each instrument in the bentonite

Measurements are done in 7 measuring sections placed on different levels (see Figure 1-1). On each level, sensors are placed in eight main directions A, AB, B, BC, C, CD, D and DA according to Figure 4-1. The bentonite blocks are called cylinders and rings. The cylinders are numbered C1–C4 and the rings R1–R12 respectively (see Figure 1-1).

An overview of the positions of the instruments is shown in Figure 1-1 and 4-1. Exact positions are described in Tables 4-1 to 4-6. These tables have been updated since the last report and the measured exact position of the transducers have been inserted.

The instruments are located in three main levels in each instrumented block, the surface of the block (only total pressure cells measuring the horizontal pressure) and 50 mm and 250 mm from the upper block surface. The thermocouples and the total pressure cells are placed in the 50 mm level for practical reasons and the other sensors in the 250 mm level.

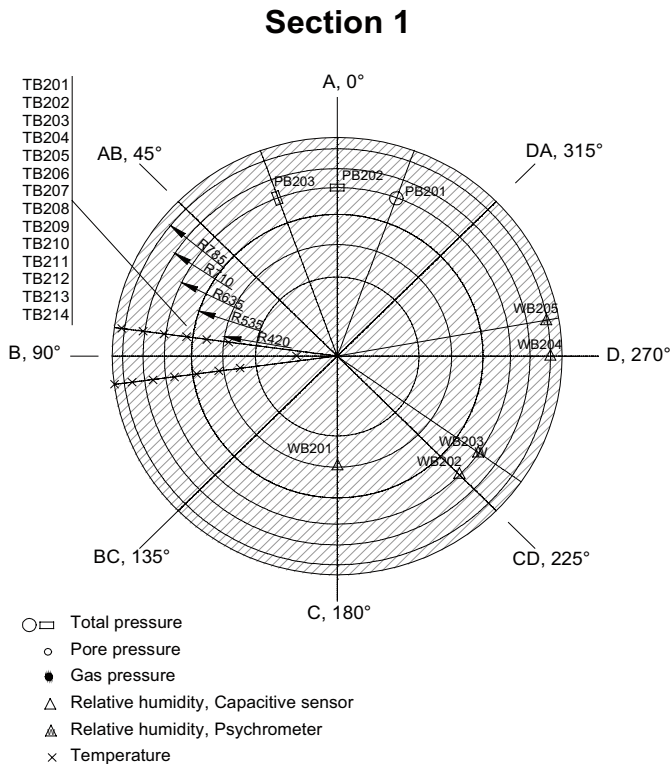


Figure 4-1. Schematic view, showing the main directions of the instrument positioning. The drawing shows the instrumentation in measuring Section 1.

Table 4-1. Numbering and position of instruments for measuring temperature (T).

Type and number	Measuring section	Block	Instrument position in block				Instrument Fabricate
			Direction	α degree	r m	Z m	
TB201	1	Cyl. 1	B	90	0.150	0.452	Pentronic
TB202	1	Cyl. 1	B	95	0.360	0.452	Pentronic
TB203	1	Cyl. 1	B	85	0.400	0.452	Pentronic
TB204	1	Cyl. 1	B	95	0.440	0.452	Pentronic
TB205	1	Cyl. 1	B	85	0.480	0.452	Pentronic
TB206	1	Cyl. 1	B	95	0.520	0.452	Pentronic
TB207	1	Cyl. 1	B	85	0.560	0.452	Pentronic
TB208	1	Cyl. 1	B	95	0.600	0.452	Pentronic
TB209	1	Cyl. 1	B	85	0.640	0.452	Pentronic
TB210	1	Cyl. 1	B	95	0.680	0.452	Pentronic
TB211	1	Cyl. 1	B	85	0.720	0.452	Pentronic
TB212	1	Cyl. 1	B	95	0.760	0.452	Pentronic
TB213	1	Cyl. 1	B	85	0.800	0.452	Pentronic
TB214	1	Cyl. 1	B	95	0.840	0.452	Pentronic
TB215	3	Ring 4	B	97.5	0.320	2.469	Pentronic
TB216	3	Ring 4	B	82.5	0.360	2.469	Pentronic
TB217	3	Ring 4	B	97.5	0.390	2.469	Pentronic
TB218	3	Ring 4	B	92.5	0.420	2.469	Pentronic
TB219	3	Ring 4	B	87.5	0.435	2.469	Pentronic
TB220	3	Ring 4	B	82.5	0.450	2.469	Pentronic
TB221	3	Ring 4	B	97.5	0.465	2.469	Pentronic
TB222	3	Ring 4	B	92.5	0.480	2.469	Pentronic
TB223	3	Ring 4	B	87.5	0.495	2.469	Pentronic
TB224	3	Ring 4	B	82.5	0.510	2.469	Pentronic
TB225	3	Ring 4	B	97.5	0.525	2.469	Pentronic
TB226	3	Ring 4	B	92.5	0.540	2.469	Pentronic
TB227	3	Ring 4	B	87.5	0.555	2.469	Pentronic
TB228	3	Ring 4	B	82.5	0.570	2.469	Pentronic
TB229	3	Ring 4	B	97.5	0.585	2.469	Pentronic
TB230	3	Ring 4	B	92.5	0.600	2.469	Pentronic
TB231	3	Ring 4	B	87.5	0.615	2.469	Pentronic
TB232	3	Ring 4	B	82.5	0.630	2.469	Pentronic
TB233	3	Ring 4	B	97.5	0.645	2.469	Pentronic
TB234	3	Ring 4	B	92.5	0.660	2.469	Pentronic
TB235	3	Ring 4	B	87.5	0.690	2.469	Pentronic
TB236	3	Ring 4	B	92.5	0.720	2.469	Pentronic
TB237	3	Ring 4	B	87.5	0.750	2.469	Pentronic
TB238	3	Ring 4	B	92.5	0.780	2.469	Pentronic
TB239	3	Ring 4	B	87.5	0.810	2.469	Pentronic
TB240	4	Cyl. 2	B	90	0.150	3.983	Pentronic
TB241	4	Cyl. 2	B	95	0.360	3.983	Pentronic
TB242	4	Cyl. 2	B	85	0.400	3.983	Pentronic
TB243	4	Cyl. 2	B	95	0.440	3.983	Pentronic
TB244	4	Cyl. 2	B	85	0.480	3.983	Pentronic
TB245	4	Cyl. 2	B	95	0.520	3.983	Pentronic

Table 4-1 cont.

Type and number	Measuring section	Block	Instrument position in block				Instrument Fabricate
			Direction	α degree	r m	Z m	
TB246	4	Cyl. 2	B	85	0.560	3.983	Pentronic
TB247	4	Cyl. 2	B	95	0.600	3.983	Pentronic
TB248	4	Cyl. 2	B	85	0.640	3.983	Pentronic
TB249	4	Cyl. 2	B	95	0.680	3.983	Pentronic
TB250	4	Cyl. 2	B	85	0.720	3.983	Pentronic
TB251	4	Cyl. 2	B	95	0.760	3.983	Pentronic
TB252	4	Cyl. 2	B	85	0.800	3.983	Pentronic
TB253	4	Cyl. 2	B	95	0.825	3.983	Pentronic
TB254	6	Ring 10	B	90	0.343	6.056	Pentronic
TB255	6	Ring 10	B	90	0.400	6.056	Pentronic
TB256	6	Ring 10	B	90	0.463	6.056	Pentronic
TB257	6	Ring 10	B	97.5	0.540	6.006	Pentronic
TB258	6	Ring 10	B	92.5	0.555	6.006	Pentronic
TB259	6	Ring 10	B	87.5	0.570	6.006	Pentronic
TB260	6	Ring 10	B	82.5	0.585	6.006	Pentronic
TB261	6	Ring 10	B	97.5	0.600	6.006	Pentronic
TB262	6	Ring 10	B	92.5	0.615	6.006	Pentronic
TB263	6	Ring 10	B	87.5	0.630	6.006	Pentronic
TB264	6	Ring 10	B	82.5	0.645	6.006	Pentronic
TB265	6	Ring 10	B	97.5	0.660	6.006	Pentronic
TB266	6	Ring 10	B	92.5	0.675	6.006	Pentronic
TB267	6	Ring 10	B	87.5	0.690	6.006	Pentronic
TB268	6	Ring 10	B	82.5	0.705	6.006	Pentronic
TB269	6	Ring 10	B	97.5	0.720	6.006	Pentronic
TB270	6	Ring 10	B	92.5	0.735	6.006	Pentronic
TB271	6	Ring 10	B	87.5	0.750	6.006	Pentronic
TB272	6	Ring 10	B	82.5	0.765	6.006	Pentronic
TB273	6	Ring 10	B	97.5	0.780	6.006	Pentronic
TB274	6	Ring 10	B	92.5	0.795	6.006	Pentronic
TB275	6	Ring 10	B	87.5	0.810	6.006	Pentronic
TB276	7	Cyl. 3	B	90	0.150	7.524	Pentronic
TB277	7	Cyl. 3	B	95	0.360	7.524	Pentronic
TB278	7	Cyl. 3	B	85	0.400	7.524	Pentronic
TB279	7	Cyl. 3	B	95	0.440	7.524	Pentronic
TB280	7	Cyl. 3	B	85	0.480	7.524	Pentronic
TB281	7	Cyl. 3	B	95	0.520	7.524	Pentronic
TB282	7	Cyl. 3	B	85	0.560	7.524	Pentronic
TB283	7	Cyl. 3	B	95	0.600	7.524	Pentronic
TB284	7	Cyl. 3	B	85	0.640	7.524	Pentronic
TB285	7	Cyl. 3	B	95	0.680	7.524	Pentronic
TB286	7	Cyl. 3	B	85	0.720	7.524	Pentronic
TB287	7	Cyl. 3	B	95	0.760	7.524	Pentronic
TB288	7	Cyl. 3	B	85	0.800	7.524	Pentronic
TB289	7	Cyl. 3	B	95	0.825	7.524	Pentronic
TB290		Ring 12	B	90	0.360	6.881	Pentronic
TB291		Ring 12	B	90	0.420	6.881	Pentronic
TB292		Ring 12	B	90	0.480	6.881	Pentronic

Table 4-2. Numbering and position of instruments measuring total pressure (P).

Type and number	Measuring section	Block	Instrument position in block				Instrument Fabricate	Direction of pressure measurement
			Direction	α degree	r m	Z m		
PB201	1	Cyl. 1	A	340	0.635	0.502	Geokon	Axial
PB202	1	Cyl. 1	A	0	0.635	0.452	Geokon	Radial
PB203	1	Cyl. 1	A	20	0.635	0.452	Geokon	Tangential
PB204	2	R3	D	250	0.420	1.968	Geokon	Radial
PB205	2	R3	D	290	0.420	2.018	Geokon	Axial
PB206	2	R3	A	8	0.535	1.968	Geokon	Radial
PB207	2	R3	A	20	0.535	1.968	Geokon	Tangential
PB208	2	R3	AB	45	0.585	2.018	Geokon	Axial
PB209	2	R3	B	100	0.635	1.968	Geokon	Tangential
PB210	2	R3	C	170	0.710	1.968	Geokon	Tangential
PB211	2	R3	C	180	0.710	1.968	Geokon	Radial
PB212	2	R3	D	260	0.748	2.018	Geokon	Axial
PB213	2	R3	D	270	0.875	1.950	Geokon	Radial on rock
PB214	4	Cyl. 2	A	340	0.635	4.033	Geokon	Axial
PB215	4	Cyl. 2	A	0	0.635	3.983	Geokon	Radial
PB216	4	Cyl. 2	A	20	0.635	3.983	Geokon	Tangential
PB217	5	Ring 9	D	270	0.535	5.319	Geokon	Radial, against sand
PB218	5	Ring 9	A	340	0.635	5.554	Geokon	Axial
PB219	5	Ring 9	A	0	0.635	5.504	Geokon	Radial
PB220	5	Ring 9	A	20	0.635	5.504	Geokon	Tangential
PB221	5	Ring 9	B	70	0.710	5.554	Geokon	Axial
PB222	5	Ring 9	B	110	0.710	5.504	Geokon	Radial
PB223	5	Ring 9	C	160	0.745	5.554	Geokon	Axial
PB224	5	Ring 9	C	180	0.770	5.504	Geokon	Radial
PB225	5	Ring 9	C	200	0.740	5.504	Geokon	Tangential
PB226	5	Ring 9	D	270	0.875	5.450	Geokon	Radial on rock
PB227	7	Cyl. 3	A	340	0.635	7.574	Geokon	Axial
PB228	7	Cyl. 3	A	0	0.635	7.524	Geokon	Radial
PB229	7	Cyl. 3	A	20	0.635	7.524	Geokon	Tangential
PB230	2	R3	C	180	0.315	1.968	DBE	Radial
PB231	5	R9	C	180	0.535	5.504	DBE	Radial

Table 4-3. Numbering and position of instruments measuring pore pressure (U).

Type and number	Measuring section	Block	Instrument position in block				Instrument Fabricate	Remark
			Direction	α degree	r m	Z m		
UB201	2	Ring 3	D	270	0.420	1.768	Geokon	
UB202	2	Ring 3	A	350	0.535	1.768	Geokon	
UB203	2	Ring 3	B	90	0.635	1.768	Geokon	
UB204	2	Ring 3	D	280	0.785	1.768	Geokon	
US205	5	Ring 9	D	270	0.510	5.304	Geokon	In sand
UB206	5	Ring 9	DA	315	0.635	5.304	Geokon	
UB207	5	Ring 9	B	90	0.710	5.304	Geokon	
UB208	5	Ring 9	CD	225	0.785	5.304	Geokon	
UB209	2	Ring 3	C	200	0.315	1.968	DBE	
UB210	5	Ring 9	C	150	0.510	5.304	DBE	

Table 4-4. Numbering and position of instruments measuring water content (W).

Type and number	Measuring section	Block	Instrument position in block				Instrument Fabricate	Remark
			Direction	α degree	r m	Z m		
WB201	1	Cyl.1	C	180	0.420	0.252	Rotronic	
WB202	1	Cyl.1	CD	225	0.635	0.252	Vaisala	
WB203	1	Cyl.1	CD	235	0.635	0.252	Wescor	
WB204	1	Cyl.1	D	270	0.785	0.252	Rotronic	
WB205	1	Cyl.1	D	280	0.785	0.252	Wescor	
WB206	3	Ring 4	BC	135	0.360	2.269	Vaisala	
WB207	3	Ring 4	C	180	0.420	2.269	Rotronic	
WB208	3	Ring 4	CD	225	0.485	2.269	Vaisala	
WB209	3	Ring 4	D	270	0.560	2.269	Rotronic	
WB210	3	Ring 4	DA	315	0.635	2.269	Vaisala	
WB211	3	Ring 4	DA	325	0.635	2.269	Wescor	
WB212	3	Ring 4	A	0	0.710	2.269	Rotronic	
WB213	3	Ring 4	A	10	0.710	2.269	Wescor	
WB214	3	Ring 4	AB	45	0.785	2.269	Vaisala	
WB215	3	Ring 4	AB	55	0.785	2.269	Wescor	
WB216	4	Cyl.2	C	180	0.420	3.783	Rotronic	
WB217	4	Cyl.2	CD	225	0.635	3.783	Vaisala	
WB218	4	Cyl.2	CD	235	0.635	3.783	Wescor	
WB219	4	Cyl.2	D	270	0.785	3.783	Rotronic	
WB220	4	Cyl.2	D	280	0.785	3.783	Wescor	
WS221	5	Ring 9	BC	135	0.525	5.304	Vaisala	In sand
WS222	6	Ring 10	BC	135	0.525	5.806	Vaisala	In sand
WB223	6	Ring 10	C	180	0.585	5.806	Rotronic	
WB224	6	Ring 10	CD	225	0.635	5.806	Vaisala	
WB225	6	Ring 10	D	270	0.685	5.806	Rotronic	
WB226	6	Ring 10	D	280	0.685	5.806	Wescor	
WB227	6	Ring 10	DA	315	0.735	5.806	Vaisala	
WB228	6	Ring 10	DA	325	0.735	5.806	Wescor	
WB229	6	Ring 10	A	0	0.785	5.806	Rotronic	
WB230	6	Ring 10	A	10	0.785	5.806	Wescor	
WB231	7	Cyl.3	C	180	0.420	7.374	Rotronic	
WB232	7	Cyl.3	CD	225	0.635	7.374	Vaisala	
WB233	7	Cyl.3	CD	235	0.635	7.374	Wescor	
WB234	7	Cyl.3	D	270	0.785	7.374	Rotronic	
WB235	7	Cyl.3	D	280	0.785	7.374	Wescor	

4.4 Instruments in the rock

Temperature measurements

40 thermocouples are located in ten boreholes in the rock (see Figure 1-1). The depth of each borehole is 1.5 m. In each borehole 4 thermocouples are placed at different distances from the rock surface. Observe that the coordinate system does not count the radius but the radial distance from the rock surface of the deposition hole. The position of each instrument is described in Table 4-5.

Table 4-5. Numbering and positions of thermocouples in the rock.

Mark	Level m	Direction degree	Distance from rock surface m	Instrument Fabricate
TR201	0	Center	0.000	Pentronic
TR202	0	Center	0.375	Pentronic
TR203	0	Center	0.750	Pentronic
TR204	0	Center	1.500	Pentronic
TR205	0.61	10°	0.000	Pentronic
TR206	0.61	10°	0.375	Pentronic
TR207	0.61	10°	0.750	Pentronic
TR208	0.61	10°	1.500	Pentronic
TR209	0.61	80°	0.000	Pentronic
TR210	0.61	80°	0.375	Pentronic
TR211	0.61	80°	0.750	Pentronic
TR212	0.61	80°	1.500	Pentronic
TR213	0.61	170°	0.000	Pentronic
TR214	0.61	170°	0.375	Pentronic
TR215	0.61	170°	0.750	Pentronic
TR216	0.61	170°	1.500	Pentronic
TR217	3.01	10°	0.000	Pentronic
TR218	3.01	10°	0.375	Pentronic
TR219	3.01	10°	0.750	Pentronic
TR220	3.01	10°	1.500	Pentronic
TR221	3.01	80°	0.000	Pentronic
TR222	3.01	80°	0.375	Pentronic
TR223	3.01	80°	0.750	Pentronic
TR224	3.01	80°	1.500	Pentronic
TR225	3.01	170°	0.000	Pentronic
TR226	3.01	170°	0.375	Pentronic
TR227	3.01	170°	0.750	Pentronic
TR228	3.01	170°	1.500	Pentronic
TR229	5.41	10°	0.000	Pentronic
TR230	5.41	10°	0.375	Pentronic
TR231	5.41	10°	0.750	Pentronic
TR232	5.41	10°	1.500	Pentronic
TR233	5.41	80°	0.000	Pentronic
TR234	5.41	80°	0.375	Pentronic
TR235	5.41	80°	0.750	Pentronic
TR236	5.41	80°	1.500	Pentronic
TR237	5.41	170°	0.000	Pentronic
TR238	5.41	170°	0.375	Pentronic
TR239	5.41	170°	0.750	Pentronic
TR240	5.41	170°	1.500	Pentronic

4.5 Instruments in the heaters

Temperature is measured both on the heater surface and inside the heater (García-Siñeriz and Fuentes-Cantillana 2002). Eleven thermocouples are installed on each heaters surface. Three groups of three thermocouples are installed 100 mm from each heater end, and in the middle of the heater, with a distribution of 120°. Two additional thermocouples are installed in the centre of the bottom lid and the top cover. Temperature inside the heater insert is measured at 6 points with thermocouples.

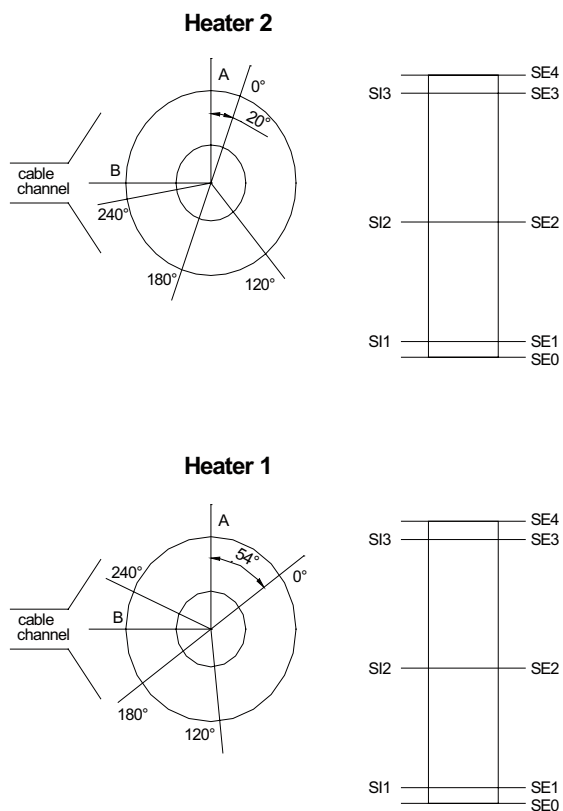
Figure 4-2 shows how these thermocouples are placed (see also section 4.2). Table 4-6 and 4-7 show the positions.

Table 4-6. Numbering and position of instruments for measuring the temperature on the heaters surface (T).

Type and number	Heater	Instruments coordinates				Instrument Fabricate	Remark
		Position	α degree	r m	Z m		
TH1 SE0	1	Bottom	0	0.000	0.500		
TH1 SE1 0°	1	Lower sec.	0	0.305	0.600		
TH1 SE1 240°	1	Lower sec.	240	0.305	0.600		
TH1 SE1 120°	1	Lower sec.	120	0.305	0.600		
TH1 SE2 0°	1	Middle sec.	0	0.305	2.000		
TH1 SE2 240°	1	Middle sec.	240	0.305	2.000		
TH1 SE2 120°	1	Middle sec.	120	0.305	2.000		
TH1 SE3 0°	1	Upper sec.	0	0.305	3.400		
TH1 SE3 240°	1	Upper sec.	240	0.305	3.400		
TH1 SE3 120°	1	Upper sec.	120	0.305	3.400		
TH1 SE4	1	Top	0	0.000	3.500		
TH2 SE0	2	Bottom	0	0.000	4.000		
TH2 SE1 0°	2	Lower sec.	0	0.305	4.100		
TH2 SE1 240°	2	Lower sec.	240	0.305	4.100		
TH2 SE1 120°	2	Lower sec.	120	0.305	4.100		
TH2 SE2 0°	2	Middle sec.	0	0.305	5.500		
TH2 SE2 240°	2	Middle sec.	240	0.305	5.500		
TH2 SE2 120°	2	Middle sec.	120	0.305	5.500		
TH2 SE3 0°	2	Upper sec.	0	0.305	6.900		
TH2 SE3 240°	2	Upper sec.	240	0.305	6.900		
TH2 SE3 120°	2	Upper sec.	120	0.305	6.900		
TH2 SE4	2	Top	0	0.000	7.000		

Table 4-7. Numbering and position of instruments for measuring the temperature inside the heaters (T).

Type and number	Heater	Instruments coordinates			Instrument Fabricate	Remark
		Position	α degree	Z m		
TH1 SI1 0°	1	Lower sec.	0	0.60		
TH1 SI1 180°	1	Lower sec.	180	0.60		
TH1 SI2 0°	1	Middle sec.	0	2.00		
TH1 SI2 180°	1	Middle sec.	180	2.00		
TH1 SI3 0°	1	Upper sec.	0	3.40		
TH1 SI3 180°	1	Upper sec.	180	3.40		
TH2 SI1 0°	2	Lower sec.	0	0.60		
TH2 SI1 180°	2	Lower sec.	180	0.60		
TH2 SI2 0°	2	Middle sec.	0	2.00		
TH2 SI2 180°	2	Middle sec.	180	2.00		
TH2 SI3 0°	2	Upper sec.	0	3.40		
TH2 SI3 180°	2	Upper sec.	180	3.40		



Figur 4-2. Location of thermocouples inside (SI) and on (SE) the heaters.

4.6 Instruments on the plug

Three force transducers and three displacement transducers have been placed on the plug to measure the force of the anchors and the displacement of the plug. The location of these transducers can be described in relation to Figure 4-3, which shows a schematic view of the plug with the slots, rods and cables.

The rods are numbered 1–9 anti-clockwise and number 1 is the southern rod 18° from direction A. The force transducers are placed on rods 3, 6, and 9. The displacement transducers are placed between the rods on the steel ring in the periphery of the plug. They are fixed on the rock surface and measure thus the displacement relative to the rock.

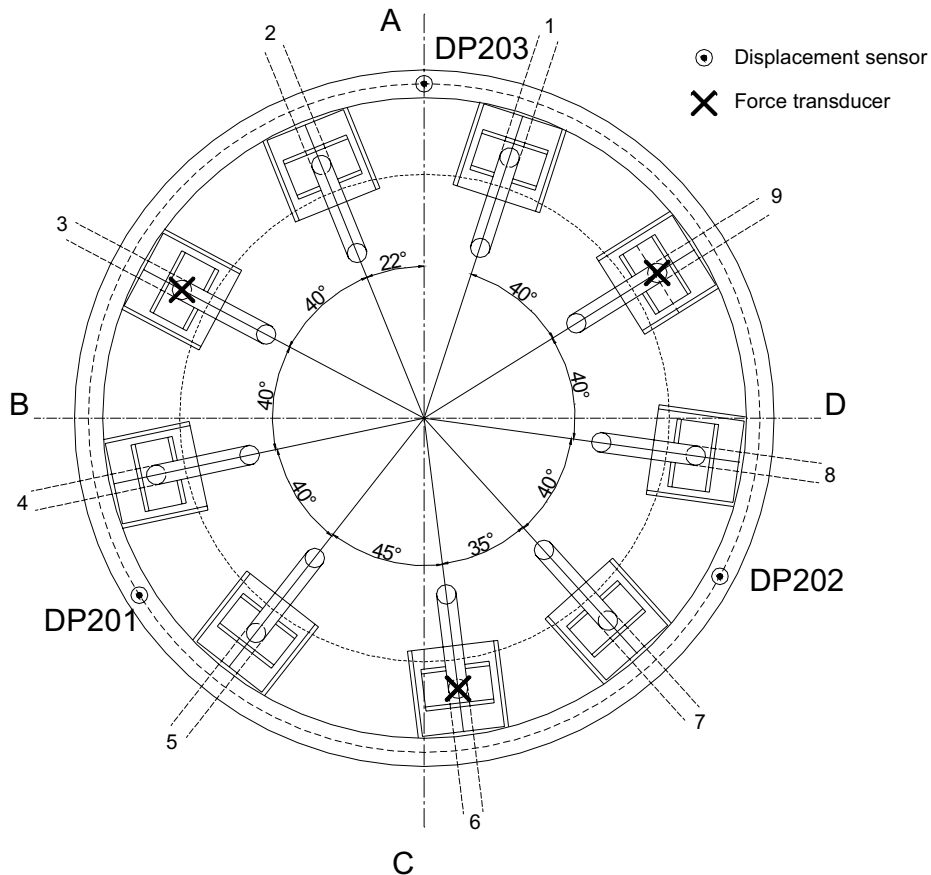


Figure 4-3. Schematic view showing the positions of the rods and the displacement and force transducers on the retaining plug.

5 Discussion of results

5.1 General

The aim of this chapter is two-parted: (i) to give an updated interpretation of the project as a whole; and (ii) to highlight the latest developments. More detailed discussions of earlier results can be found in previous data reports.

During the course of the dismantling operation a number of sensors have been retrieved and subsequently tested at different operational conditions (see Appendix B). Thermocouples were tested *in situ* in the deposition hole at two temperatures. Three types of pressure sensors (Druck; and Geocon, total and pore pressure sensors) were exposed to different pressures levels, whereas a few capacitive relative humidity sensors (Rotronic and Vaisala) were exposed to different RH-climates. These tests generally showed good results for the thermocouples, the Geokon pore pressure sensors and the Druck pressure sensors. In contrast, the Geokon total pressure sensors and the capacitive relative humidity sensors in general exhibited a function outside the stated specifications.

The results for the thermocouples, the Druck sensors and the Geocon pore pressure sensors clearly show that the data from these sensors are highly credible. Moreover, even if most of the Geocon total pressure sensors only were graded as “under specification”, which in most cases was due to a linear error higher than 5%, this grade appears to be slightly pessimistic, since 5% is virtually negligible for a typical swelling pressure of 8 MPa. The data from the total pressure sensors therefore also appears to be quite credible.

The least accurate among the investigated sensors were the capacitive RH-sensors. This should not discredit the data from the initial phase, considering the subsequent exposure of heat and water pressure on these sensors.

5.2 Total inflow of water

The total injected water volume is shown in (App. A\page 67) and had reached 4.2 m³ at the termination of the water injection on August 16, 2009. Table 5-1 shows the pore space available at the beginning of the test. The calculated available pore volume has thereby been exceeded with 1.5 m³. This discrepancy appears to be caused by a water leakage, possibly into the rock. This has previously been elaborated by Goudarzi et al. (2006).

The inflow has varied significantly during the test period. During the first 75 days the inflow was about 15 l/d, while it dropped to about 1.3 l/d during the subsequent 250 days. On average during the period from January 1, 2008 to the termination of the water injection the inflow was 0.7 l/d.

Three major events can be noticed in the applied scheme for pressurization (Table 5-2):

- During the first 377 days, the sand filter was only pressurized through the lower injection points, while the upper were open to the atmosphere. After this day, upper injection points have also been pressurized while none of the injection points has been open to the atmosphere.
- The second event was the installation of equipment for measuring pressure at each injection point on October 8, 2004 (day 562) (see Figure 5-1). Since then, at least one out of eight injection points have been closed and used for monitoring of the actual pressure in the sand filter.
- The third event was the change of water quality on April 17, 2007. The background for this was that the injection points in the sand filter have exhibited a high flow resistance during the operation phase of the test. In order to reduce this resistance, the formation water used earlier was replaced by de-ionized water. The effect of this was noticed almost immediately. Later on (on August 13, 2007) the small tank used at that time was replaced by a larger tank which enabled a higher inflow without the need of frequent refilling.

Table 5-1. TBT Pore space.

	Available at test start [m ³]
Sand filter	0.77
Pellets filling	0.24
Bentonite	1.08
Heater/bentonite clearance	0.06
Sand shield	0.55
Total	2.70

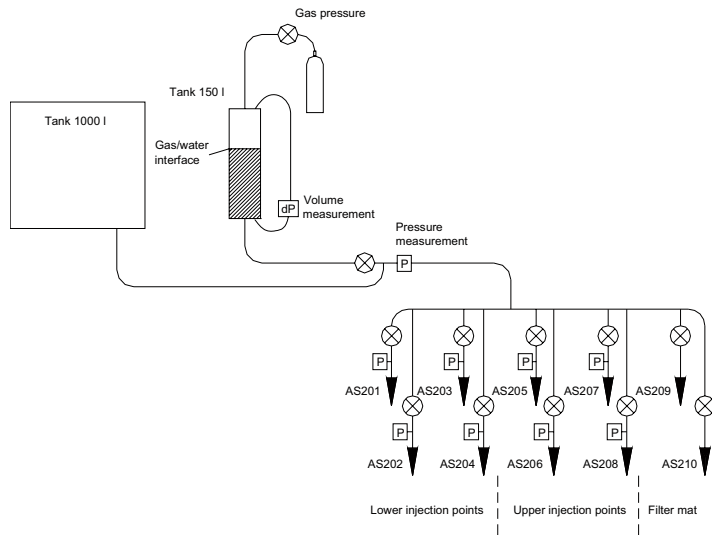


Figure 5-1. Schematic view of injection system.

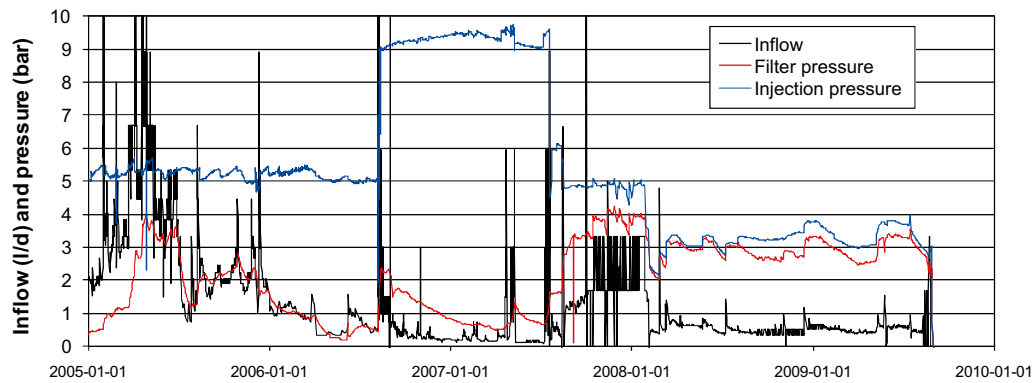


Figure 5-2. Development of relative pressures (injection and in sand filter) and inflow since the second hydraulic test.

The injection pressure was reduced at the end of January 2008 from 5 bar to 3–3.5 bar (see Table 5-2 and Table 5-3). The reason for this was the observed leakage in the middle of January 2008. This leakage was however found to originate from the shield hydration (see below). Due to this event, the pressurization of the filter mat was temporarily turned off (from February 1 to April 1). After this, the injection pressure was kept fairly constant at a level between 3 and 4 bar up till the termination of the water injection.

Hydration of the sand shield

In this activity, the sand shield around the upper heater was injected with water. The aim of this was to facilitate a number of hydraulic tests and gas injection tests through the upper buffer package. The activity ended in the beginning of April 2008 and spanned thereby over almost a whole year. In order to facilitate an overview of this extensive activity, it was reported in full in a previous data report (Goudarzi et al. 2008).

5.3 Temperatures

Temperatures are monitored by use of thermocouples in three cylinders (C1, C2 and C3) and two rings (R4 and R10), cf. Figure 1-1. In addition, temperature readings are provided by the capacitance-type relative humidity (RH) sensors. In general, the temperature results exhibit consistent trends up to maximum values after about 200 days (App. A\pages 74–79). A few exceptions have occurred for inner parts in Cyl 2 and the inner sand shield at Ring 10, where the maximum temperatures were reached after only about 40 and 60 days, respectively (App. A\pages 76–77).

The CRT experiment was located 6 m from the TBT experiment. This experiment was initiated approximately 880 days before the start of the TBT experiment and has therefore contributed with a certain heat flux. The CRT was terminated in October 2005. In order to compensate for this loss, the power output from the TBT heaters was increased from 1,500 to 1,600 W on June 9, 2006.

The power output from the heaters was changed during the last two months of 2007. The power from the lower heater was increased from 1,600 to 2,000 W, while the output from the upper heater was decreased from 1,600 W to 1,000 W. All changes were made in weekly steps of 100 W. This change altered the thermal conditions in the experiment, and at the end 2007 the temperature on the mid-section of the lower heater was 158°C while the corresponding value for the upper heater was 89°C. Slightly lower temperatures prevailed until August 16 2009, when the mid-section temperatures on the lower and the upper heaters were 152°C and 86°C, respectively (Figure 5-3).

Table 5-2. Injection point pressurization scheme (values are relative pressures). The actual water pressure in the sand filter is only measured at those points that are closed.

Intervals	Lower injection points				Upper injection points				Filter mat		p (bar)
	201	202	203	204	205	206	207	208	209	210	
030326–040406 <i>Day 0–377</i>	○	○	○	○	⊕	⊕	⊕	⊕	⊗	⊗	7
040406–040615 <i>Day 377–447</i>	○	○	○	○	○	○	○	○	⊗	⊗	0
040615–040616 <i>Day 447–448</i>	Hydraulic test I										
040616–041008 <i>Day 448–562</i>	○	○	○	○	○	○	○	○	⊗	⊗	1.5
041008–041014 <i>Day 562–568</i>	Hydraulic test II										
041014–041110 <i>Day 568–595</i>	⊗	⊗	⊗	⊗	○	⊗	○	⊗	⊗	⊗	5
041110–050728 <i>Day 595–856</i>	○	○	⊗	○	○	○	⊗	○	⊗	⊗	5
050728–051209 <i>Day 856–989</i>	○	⊗	○	○	○	⊗	○	○	⊗	⊗	5
051209–051212 <i>Day 989–992</i>	○	⊗	○	○	○	⊗	○	○	○	⊗	5
051212–060517 <i>Day 992–1,148</i>	○	⊗	○	○	○	⊗	○	○	○	○	5
060517–060614 <i>Day 1,148–1,176</i>	Back flushing of injection points										
060614–060807 <i>Day 1,176–1,230</i>	○	○	⊗	○	○	○	○	○	○	○	5
060807–060811 <i>Day 1,230–1,234</i>	Increase of injection pressure										
060811–070417 <i>Day 1,234–1,483</i>	○	○	⊗	○	○	○	○	○	○	○	9
070417 <i>Day 1,483</i>	Change in water quality										
070417–070423 <i>Day 1,483–1,489</i>	○	○	⊗	○	○	○	○	○	○	○	9
070423–070509 <i>Day 1,489–1,505</i>	○	○	⊗	○	○	○	⊗	○	○	○	9
070509–070716 <i>Day 1,505–1,573</i>	○	○	⊗	○	○	⊗	⊗	○	○	○	9
070717–070723 <i>Day 1,574–1,580</i>	○	○	⊗	○	○	⊗	⊗	○	○	○	5
070724–070812 <i>Day 1,581–1,600</i>	○	○	⊗	○	○	⊗	⊗	○	○	○	6
070813–070815 <i>Day 1,601–1,603</i>	○	○	⊗	○	○	○	○	⊗	○	○	5.5
070816–070905 <i>Day 1,604–1,624</i>	○	○	⊗	○	○	○	○	⊗	○	○	5
070906–080128 <i>Day 1,625–1,769</i>	○	○	⊗	○	○	○	⊗	○	○	○	5

○ = Open and pressurized.
 ⊕ = Open to atmosphere.
 ⊗ = Closed.

Table 5-3. Injection point pressurization scheme (values are relative pressures). The actual water pressure in the sand filter is only measured at those points that are closed.

Intervals	Lower injection points				Upper injection points				Filter mat		P (bar)
	201	202	203	204	205	206	207	208	209	210	
080129–080201 Day 1,770–1,773	○	○	⊗	○	○	○	⊗	○	○	○	3.5
080202–080204 Day 1,774–1,776	○	○	⊗	○	○	○	⊗	○	⊗	⊗	3.5
080205–080225 Day 1,777–1,797	○	○	⊗	○	○	○	⊗	○	⊗	⊗	2
080226–080310 Day 1,798–1,811	○	○	⊗	○	○	○	⊗	○	⊗	⊗	3
080311–080401 Day 1,812–1,833	○	○	⊗	○	○	○	⊗	○	⊗	⊗	3.5
080402–090828 Day 1,834–2,347	○	○	⊗	○	○	○	⊗	○	○	○	3–4

○ = Open and pressurized.
 ⊕ = Open to atmosphere.
 ⊗ = Closed.

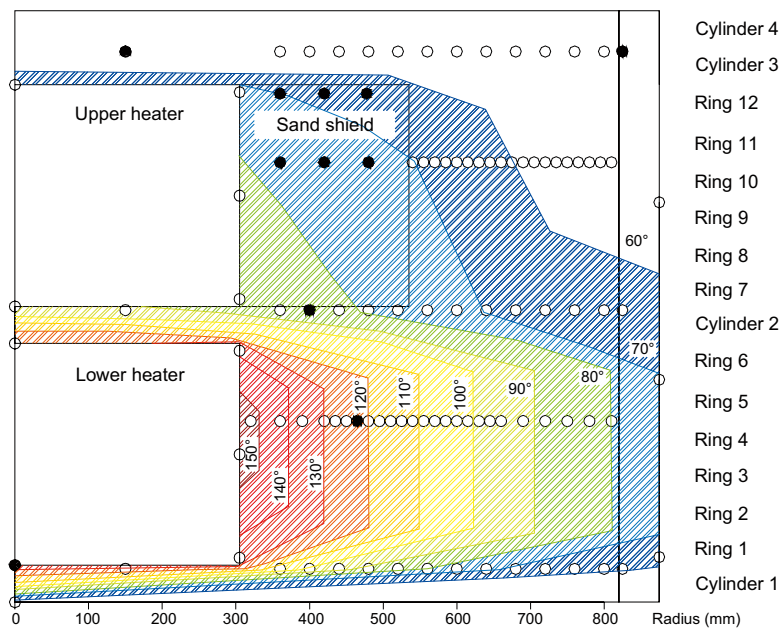


Figure 5-3. Temperature distribution on August 16, 2009. Rings indicate sensor positions. Filled rings indicate sensors out of order.

It can be noted that the hydration of the sand shield influenced the conditions around the upper heater and this is reflected by some of the temperature data. The temperatures on the upper heater (App. A\page 85) tended to decrease whereas the temperatures in Ring 10 tended to increase (App. A\page 77). This change can be explained as an increased heat transport through the sand shield.

The power output from the heaters was terminated in steps during the period from August 17 to August 28. The temperatures decreased rapidly after this event and reached below 30°C within two months after the termination.

Temperature profiles and thermal conductivities

Temperature profiles in Ring 4 and Ring 10 are shown for different times in Figure 5-4. The effect of the change in power output is very distinct, with a higher temperature level in Ring 4 and a lower level in Ring 10 (especially in the sand shield). The latest point (day 2,335) corresponds to August 16 2009.

Figure 5-5 illustrates the evolution of the apparent thermal conductivity in Ring 4. These results are based on the slopes of temperature-distance curves derived from thermocouple readings in Ring 4, and on the assumption that the heat flux at mid-height can be approximated to be strictly radial. The thermal conditions after the change in power output at the end of 2007 were very different than the preceding conditions. The evaluated conductivity values for the point after this event were therefore calibrated so that the conductivity at 155 mm from the heater surface was the same as the previous one. In general, these graphs should be interpreted with some caution: some of the changes may be due to variation of the mid-height heat flux, and some may be due to dislocation of individual sensors.

It can be noted that the innermost point, at 35 mm from the heater surface, dropped immediately after test start, but has thereafter increased steadily. In contrast, a point at 155 mm from the heater appears to have undergone a rapid increase in the beginning and has thereafter remained fairly constant.

5.4 Relative humidity/suction

Recorded RH values and suctions indicate that moisture contents generally increase: RH from 72 to maximum 100% (App. A\pages 59–64); suction between 6 and 1 MPa (App. A\pages 54–58).

A significant exception was the suction *increase* in Ring 10 at radius 785 and 735 mm after day 225 (App. A\page 57). Although this increase correlated with a general decrease in stresses in parts of Ring 9, it was most likely caused by a shortage in water supply, resulting in a localized desiccation cycle to occur. The trend was also reversed when water injection through the upper tubes was introduced (see Section 5.2), which supports the water supply explanation for these observations.

The hydration of the buffer, as recorded by the RH-sensors, is illustrated in Figure 5-6. Occasions when capacitive sensor signals showing $RH \approx 100\%$ (Vaisala and Rotronic), and all *active* signals from psychrometers, corresponding to $RH > 95\%$ (Wescor), are compiled. These occasions are taken as indications of *vapor* saturation rather than of *buffer* saturation. The reason for this is that the rapid evolution of the RH-sensors is contrasted by the slow response of the pore pressure sensors. The current understanding is that the process of reaching full saturation is slow. At the latter phase of the experiment, all operational capacitive RH sensors indicated saturated vapor while there was not any psychrometers yielding any signals.

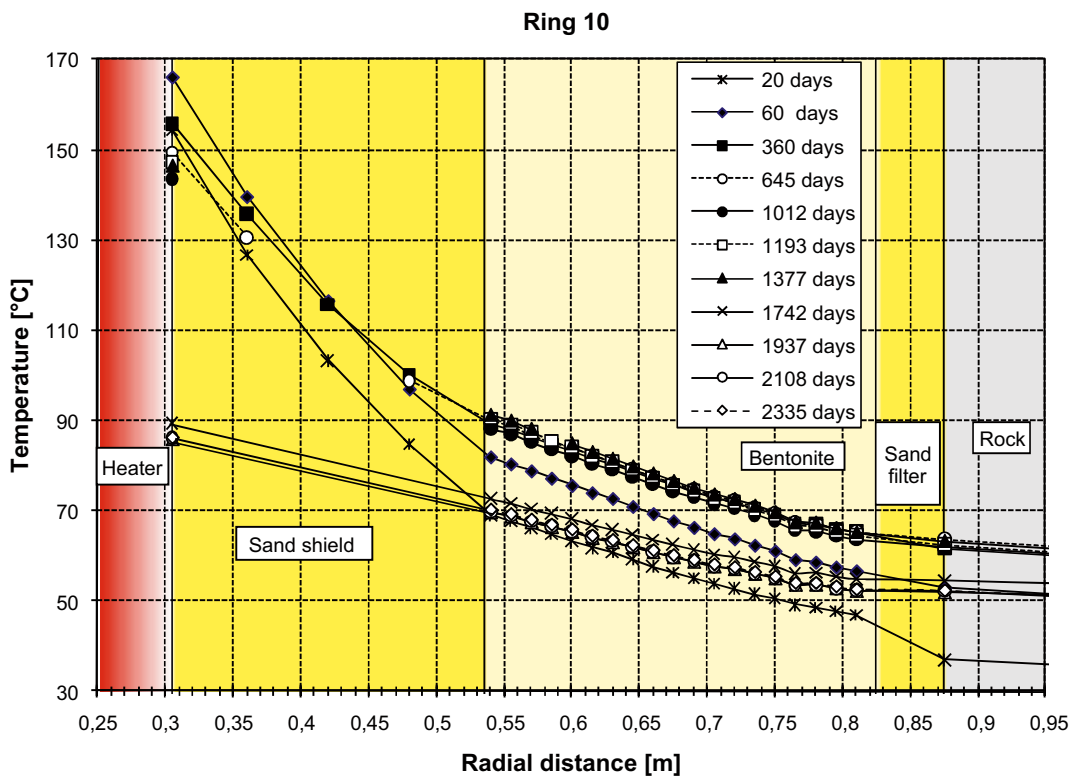
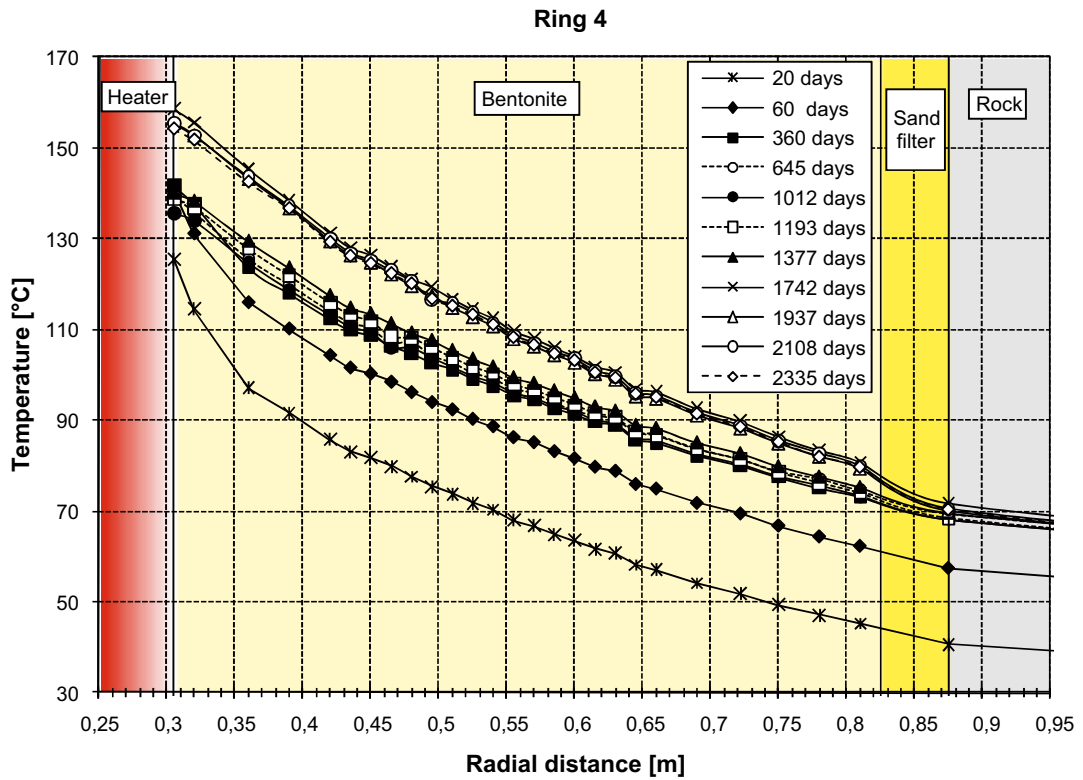


Figure 5-4. Temperatures measured at mid-height of Heater 1 (Ring 4) and Heater 2 (Ring 10).

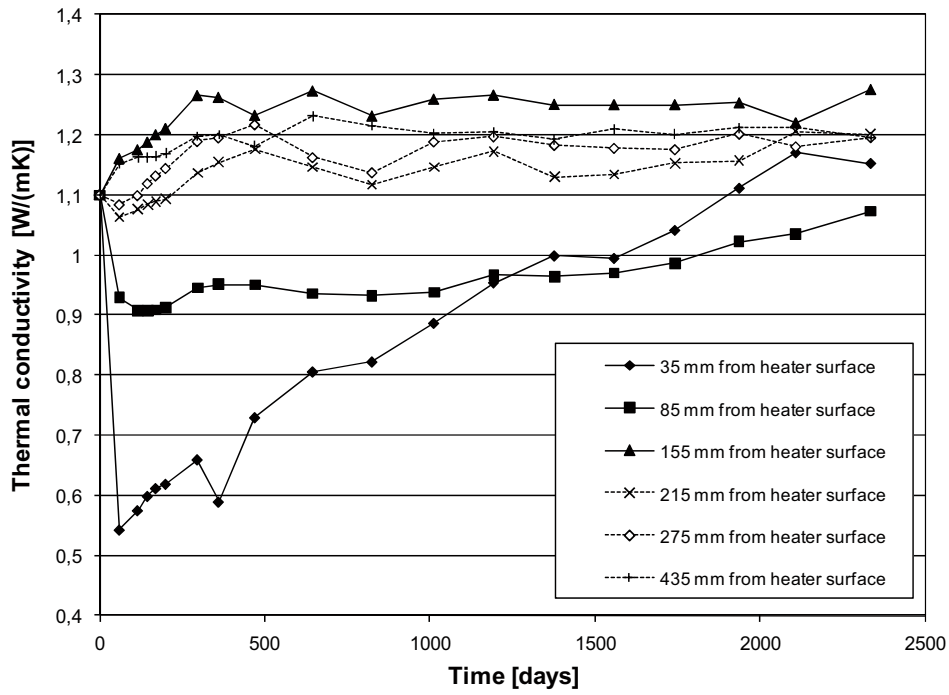


Figure 5-5. Thermal conductivity development in Ring 4.

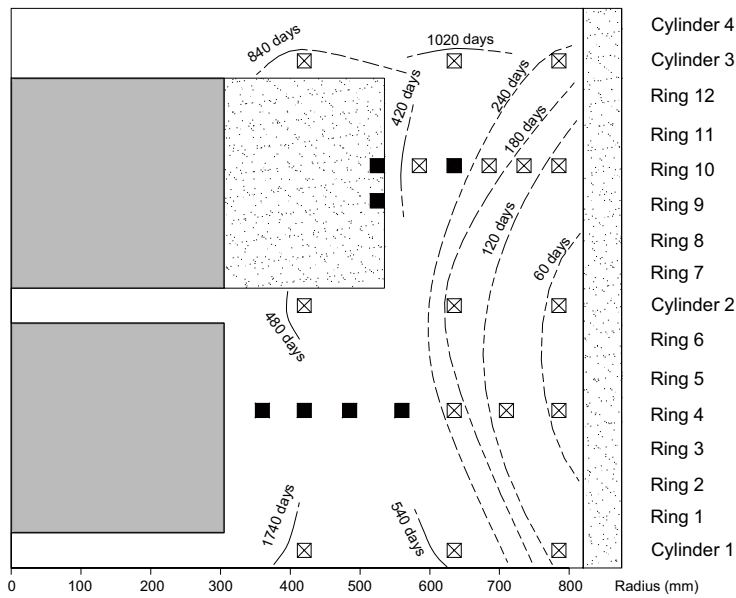


Figure 5-6. Occurrences of vapour saturation. Boxes are sensor positions. Ticked boxes indicate saturation. Filled boxes indicate sensors that failed prior to vapour saturation.

5.5 Pore pressure

Ideally, pore pressure sensors should give a zero signal as long as the condition isn't totally saturated. The first build-up of pore pressure was noticed at the outermost sensor in Ring 9 in the beginning of 2005. This coincided with the increase of filter pressure at that time. The outermost sensor in Ring 3 as well as the other sensors in Ring 9 (in the bentonite, but not the sand shield) responded within 200 days afterwards. The data from the responding sensors appeared to be correlated with the pressure in the sand filter. The absolute level of the sensors was however higher than the sand filter pressure, which can put the accuracy of the pore pressure sensors into question.

The shield hydration and the change in power output have both influenced the pore pressure. The shield hydration led to a temporary reduction of the pore pressure in the bentonite in Ring 9 (in the sand shield it increased). The power increase from Heater 1 led to the response of all sensors in Ring 3. All the pore pressure sensors, except the UB205 sensor in the sand shield and the UB201 sensor in Ring 3, recovered however later on (App. A\pages 65–66). The unexpected trend displayed by the UB201 sensor during the autumn of 2008 is described in the next section.

The termination of the heaters (and the water injection) led to a complete loss of pore pressure in Ring 9. The outermost sensor in Ring 3 (UB201) appears however to have recovered after this event and displayed a high value (0.3 MPa) during the dismantling operation. This behavior appears to be questionable since the filter was non-pressurized at the time and this indicates that the sensor had malfunctioned.

5.6 Total pressure

Results from pressure monitoring are shown in App. A\pages 45–53. The total pressure in virtually all blocks (Cylinder 3 excepted) has generally displayed a fairly rapid buildup and had largely stabilized in the beginning of 2007 (day ~1,500) before the beginning of the shield hydration and the power change.

The hydration of the sand shield resulted in a decrease in total pressure and pore pressure in Ring 9. This was especially apparent during the first hydration attempts in the middle of 2007, but also at the end of that year (App. A\pages 50–52 and page 66). This appears to be an effect of swelling of the buffer into the sand shield.

The change in power output at the end of 2007 also influenced the total pressures. The total pressures around the lower heater (Ring 3) first displayed a minor increase, after which they decreased slightly more than the initial increase. The cause of the general pressure decrease in Ring 9 observed at the end of 2007 is difficult to identify, since the decrease in power output coincided with the shield hydration. A few months after these events the pressures appear to have recovered to their original levels. A comparison of axial pressures and cable forces is shown in Figure 5-8.

The pressures, as recorded by the two innermost pressure sensors in Ring 3 around the lower heater, decreased significantly during August and September 2008. The total pressure (PB204) decreased from approximately 7 to 4 MPa (App. A\page 46), while the pore pressure (UB201) decreased from approximately 1 to 0.3 bar (App. A\page 65). This pressure decrease had not recovered at the end of 2008. The total pressure (PB204) had recovered up to approximately 5 MPa before the termination of the heaters (see Figure 5-7) whereas the pore pressure (UB201) never recovered.

The termination of the heaters in August 2009 led to a significant reduction of the total pressure, in some locations with more than 50%. A corresponding drop, although much less extensive, was noticed in the cable forces (Figure 5-8) as well as the displacement of the plug (App. A\page 71). After this drop, the pressure at several locations recovered with a few MPa until the dismantling operation began with the unloading of the cables. This final drop was quite immediate in the upper part (i.e. Cylinder 3), whereas pressures remained in the lower part for a few months during the dismantling operation.

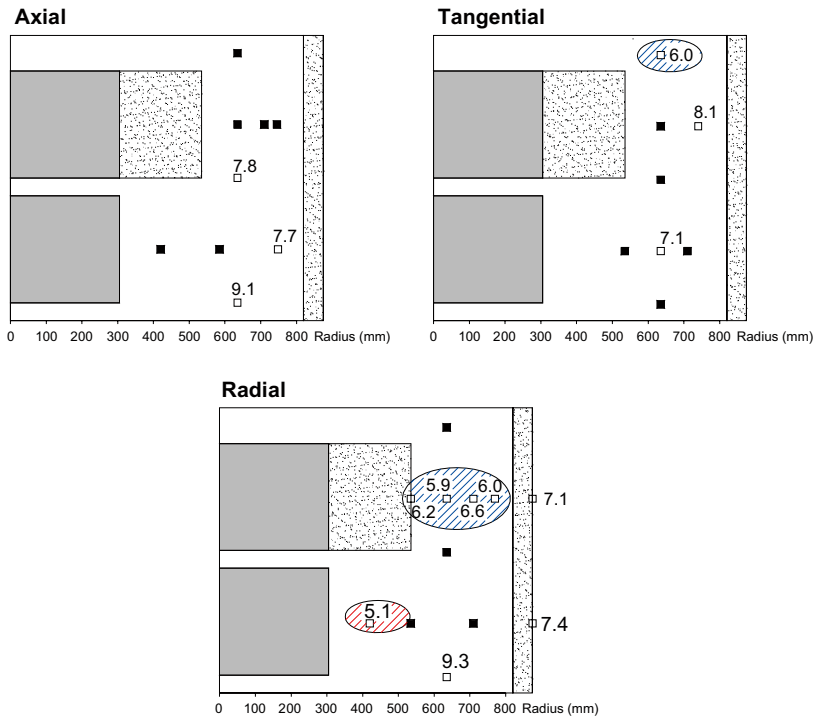


Figure 5-7. Total pressure distribution on August 16, 2009. Values in MPa. Boxes are sensor positions. Filled boxes indicate sensors out of order. Levels below 7 MPa marked blue. Significant reduction during autumn 2008 marked red.

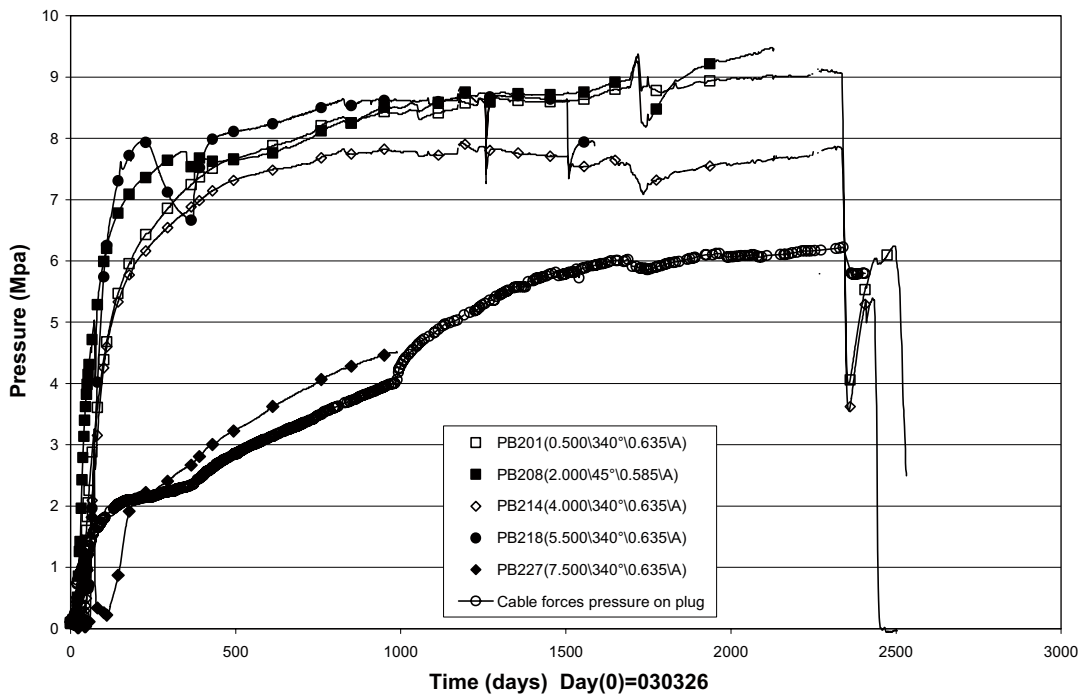


Figure 5-8. Axial pressure measured in different sections. Cable forces are shown as pressures, assuming an even distribution over the rock hole area (2.4 m^2).

References

SKB's (Svensk Kärnbränslehantering AB) publications can be found at www.skb.se/publications.

García-Siñeriz J L, Fuentes-Cantillana J L, 2002. Äspö Hard Rock Laboratory. Temperature Buffer Test. Feasibility study for the heating system at the TBT test carried out at the Äspö HRL in Sweden. SKB IPR-03-18, Svensk Kärnbränslehantering AB.

Goudarzi R, Åkesson M, Hökmark H, 2006. Äspö Hard Rock Laboratory. Temperature Buffer Test. Sensors data report (period 030326–060701). Report No:8. SKB IPR-06-27, Svensk Kärnbränslehantering AB.

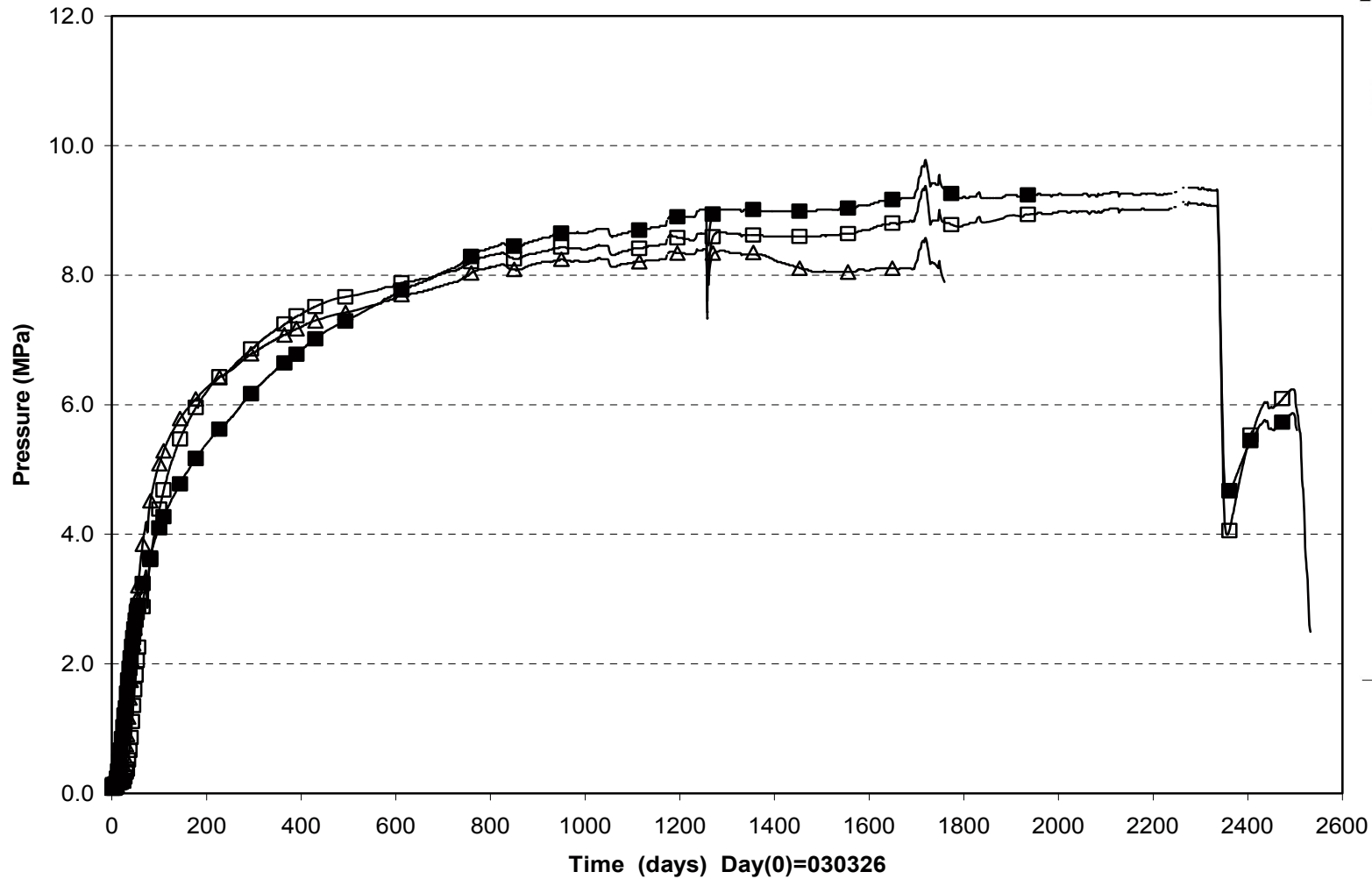
Goudarzi R, Åkesson M, Hökmark H, 2008. Äspö Hard Rock Laboratory. Temperature Buffer Test. Sensors data report (period 030326–080101). Report No:11. SKB IPR-08-16, Svensk Kärnbränslehantering AB.

Johannesson L-E, Sandén T, Åkesson M, Bárcena I, García-Siñeriz J L, 2010. Temperature Buffer Test. Installation of buffer, heaters and instruments in the deposition hole. SKB P-12-02. Svensk Kärnbränslehantering AB.

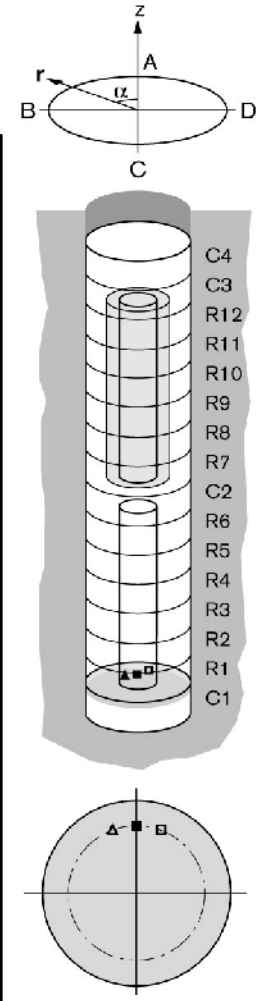
Appendix A

Measured data

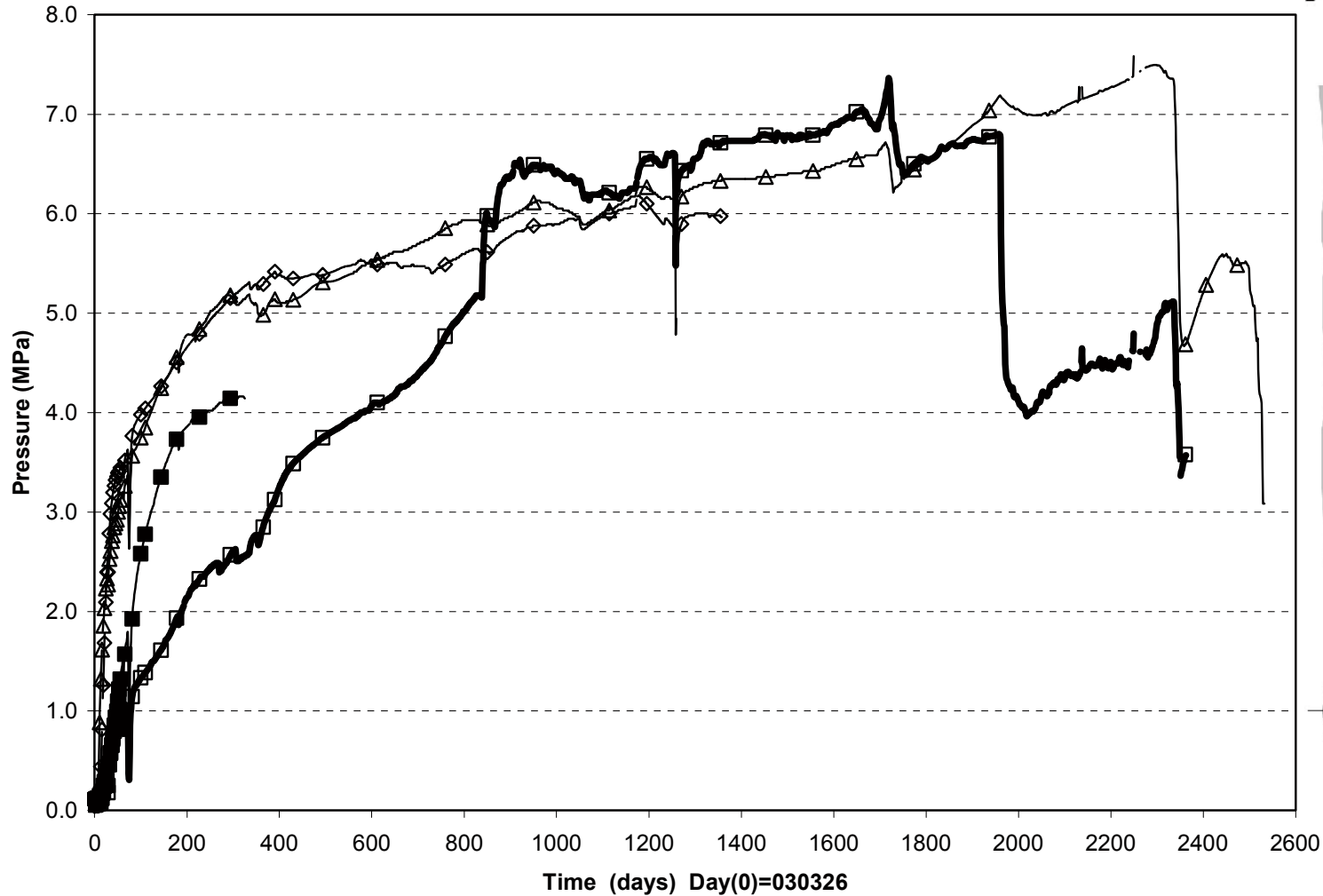
Total pressure/Cyl.1 (030326-100301)
Geokon



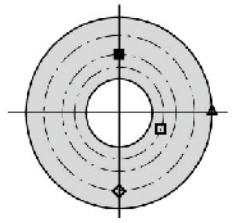
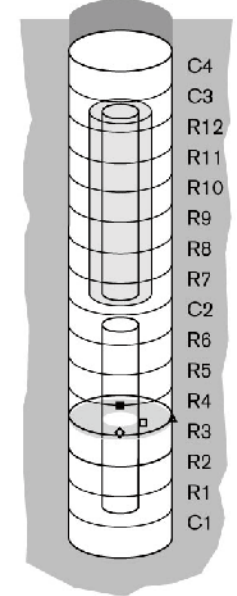
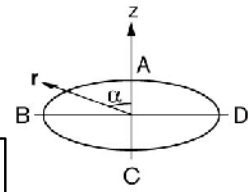
□ PB201(0.500\340°\0.635\A) ■ PB202(0.450\0°\0.635\R) △ PB203(0.450\20°\0.635\T)



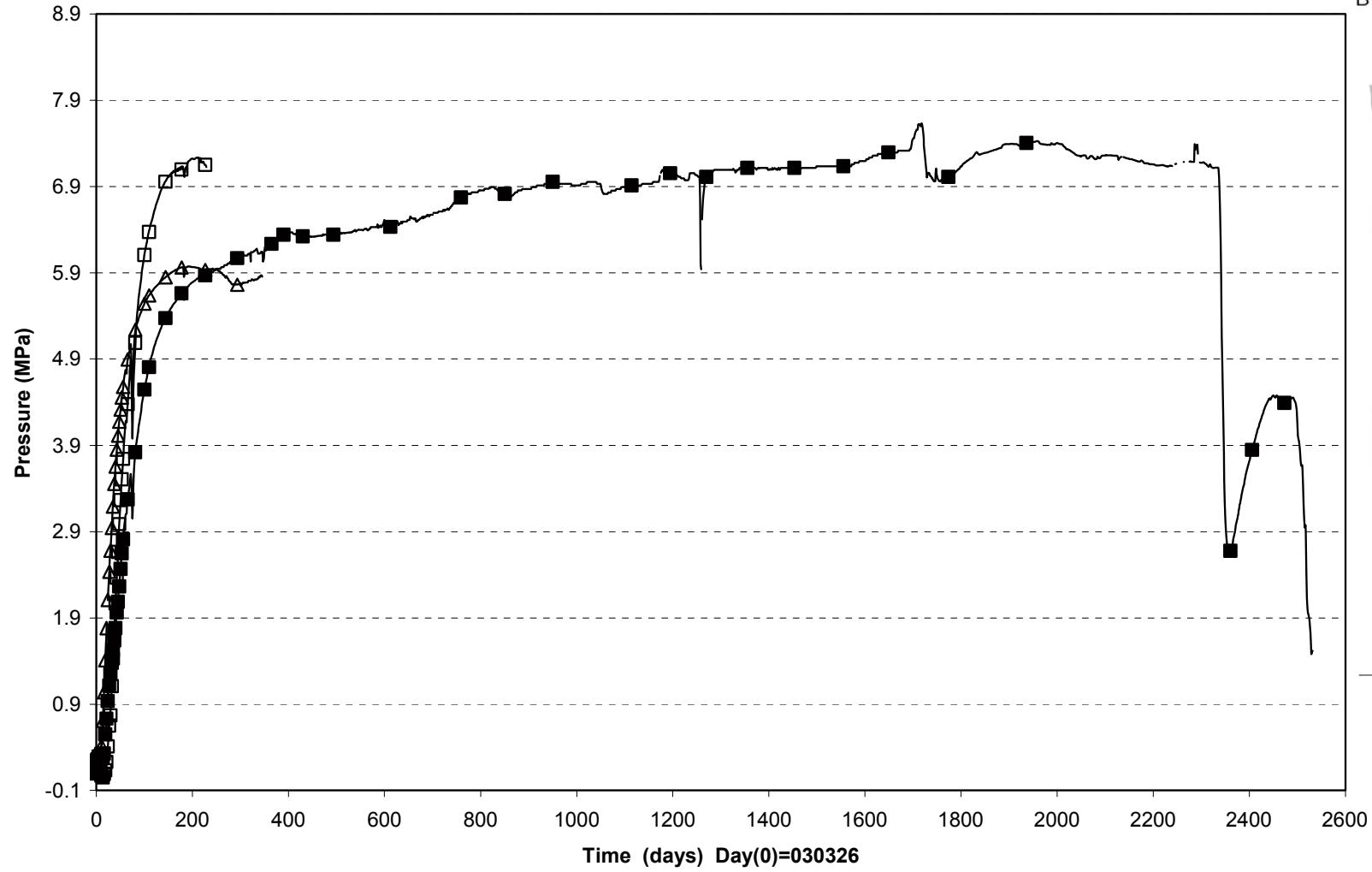
Total pressure/Ring 3 (030326-100301) Geokon



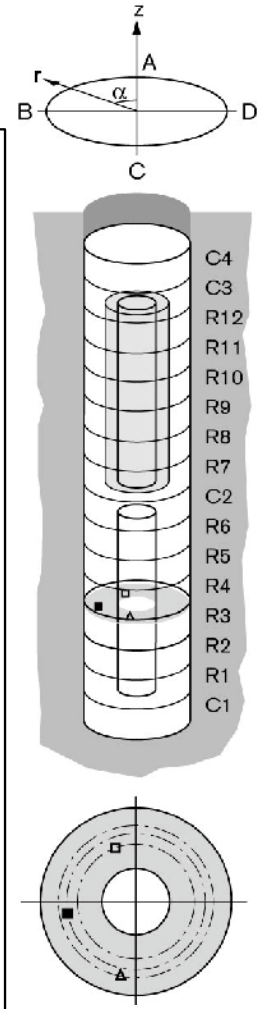
□ PB204(1.950\250°\0.420\R) ■ PB206(1.950\8°\0.535\R) ◇ PB211(1.950\180°\0.710\R) △ PB213(1.950\270°\0.875\R)



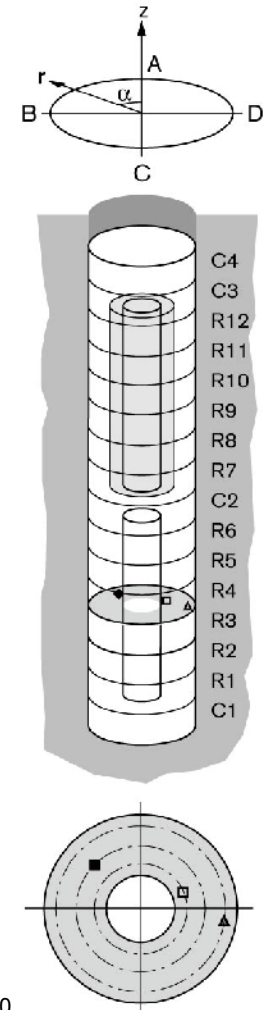
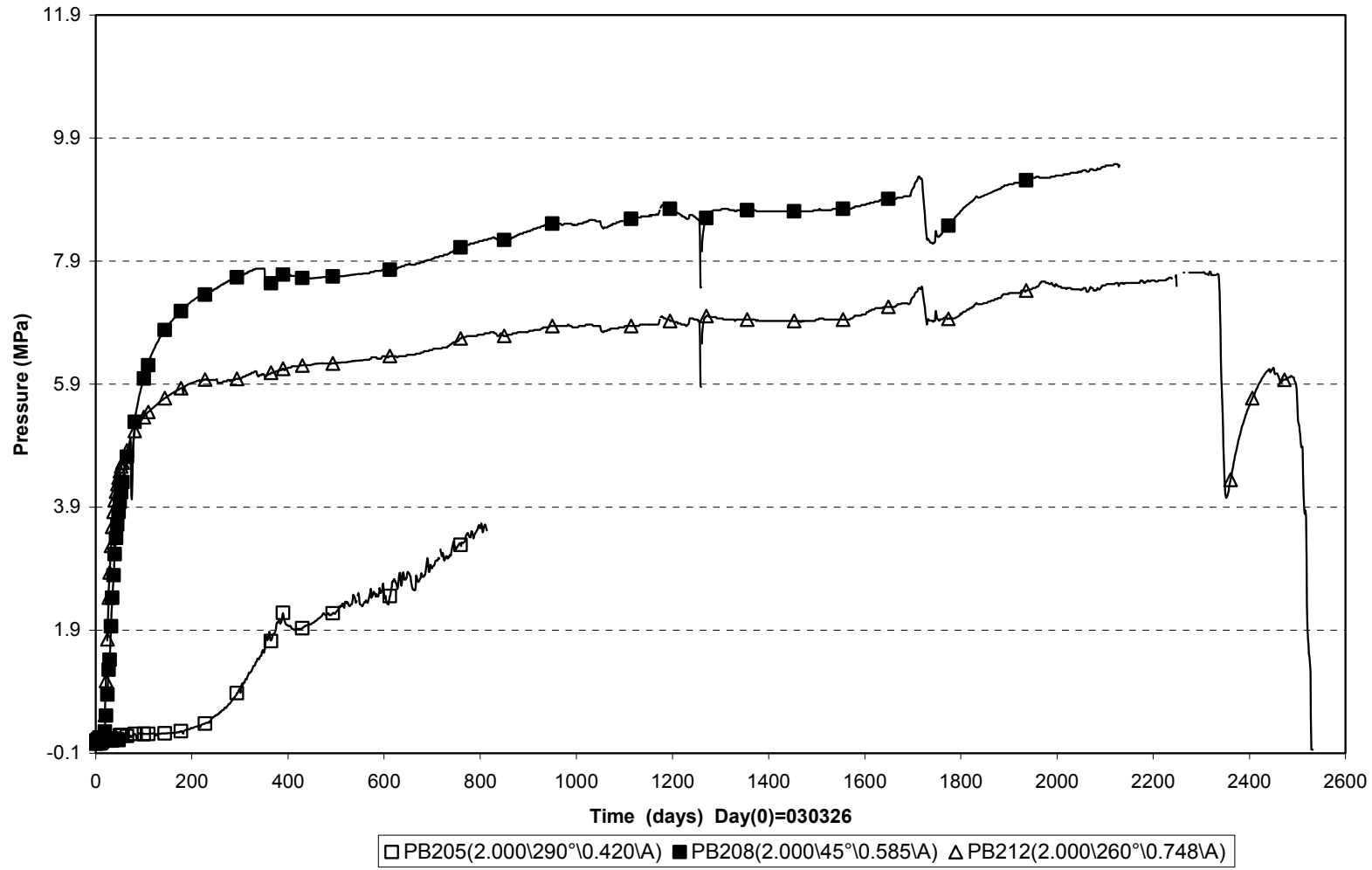
Total pressure/R3 (030326-100301) Geokon



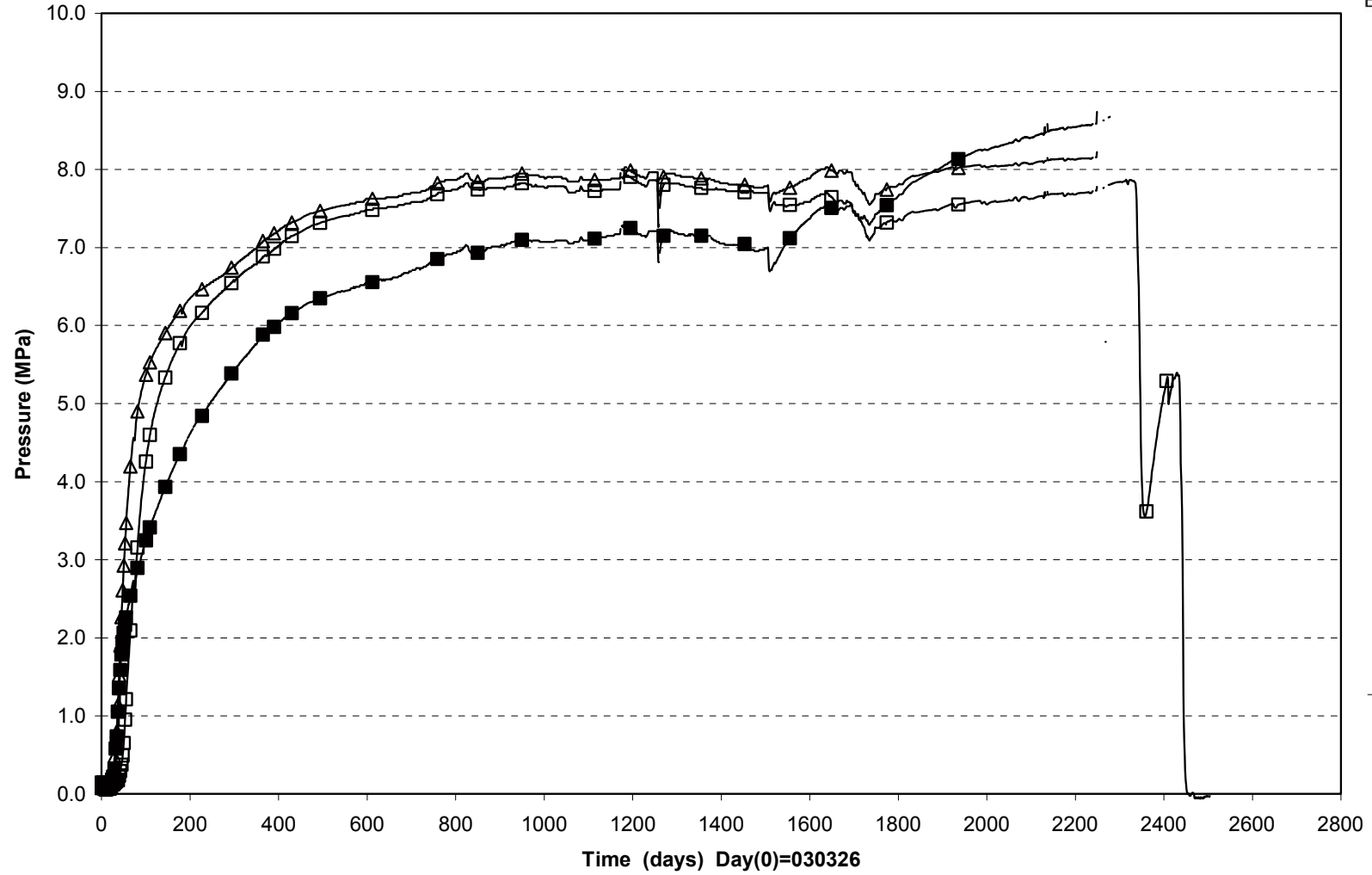
□ PB207(1.950\20°\0.535\T) ■ PB209(1.950\100°\0.635\T) △ PB210(1.950\170°\0.710\T)



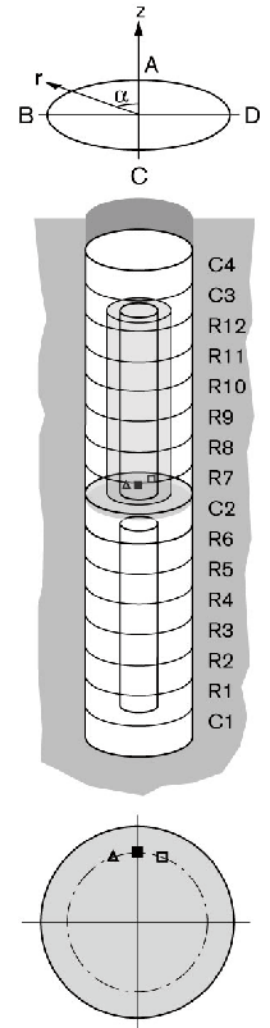
Total pressure/R3 (030326-100301) Geokon



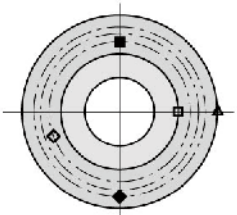
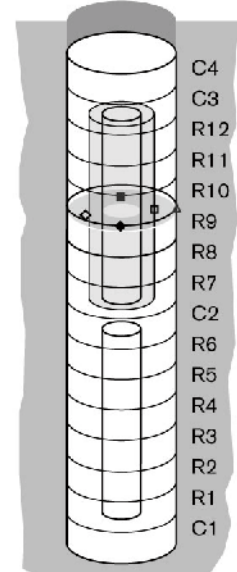
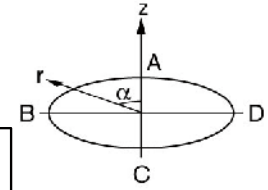
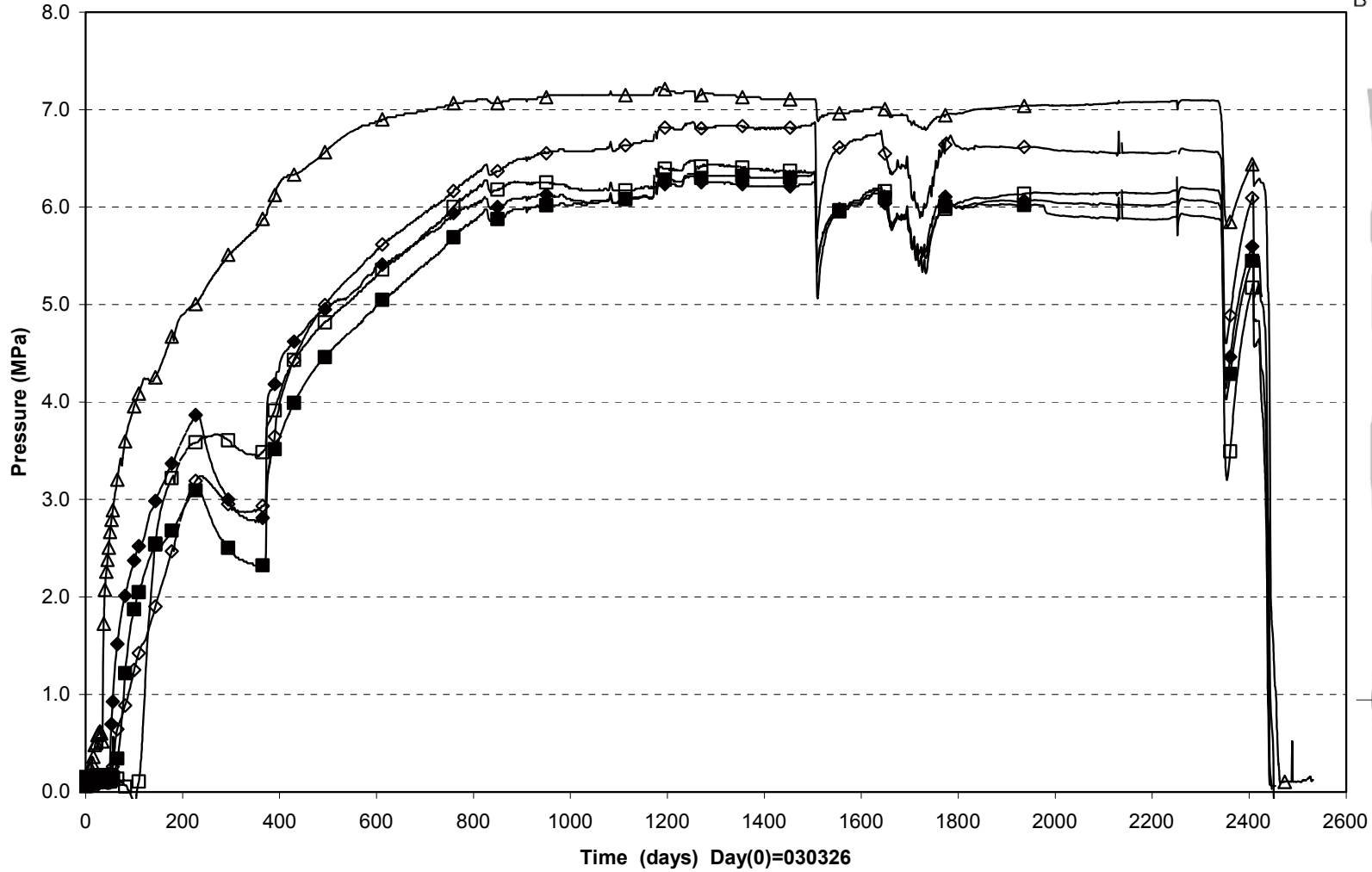
Total pressure/Cyl.2 (030326-100301) Geokon



□ PB214(4.000\340°\0.635\A) ■ PB215(3.950\0°\0.635\R) △ PB216(3.950\20°\0.635\T)

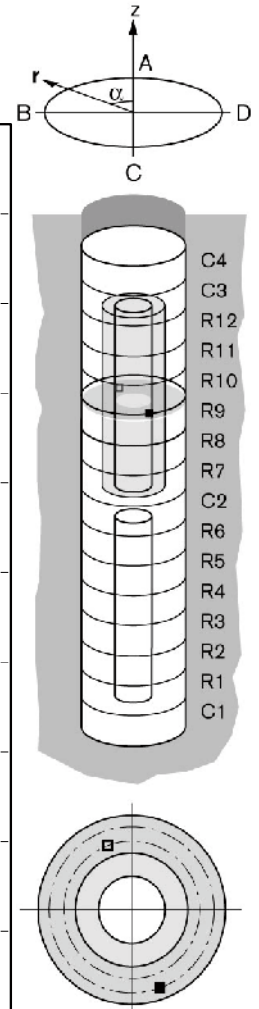
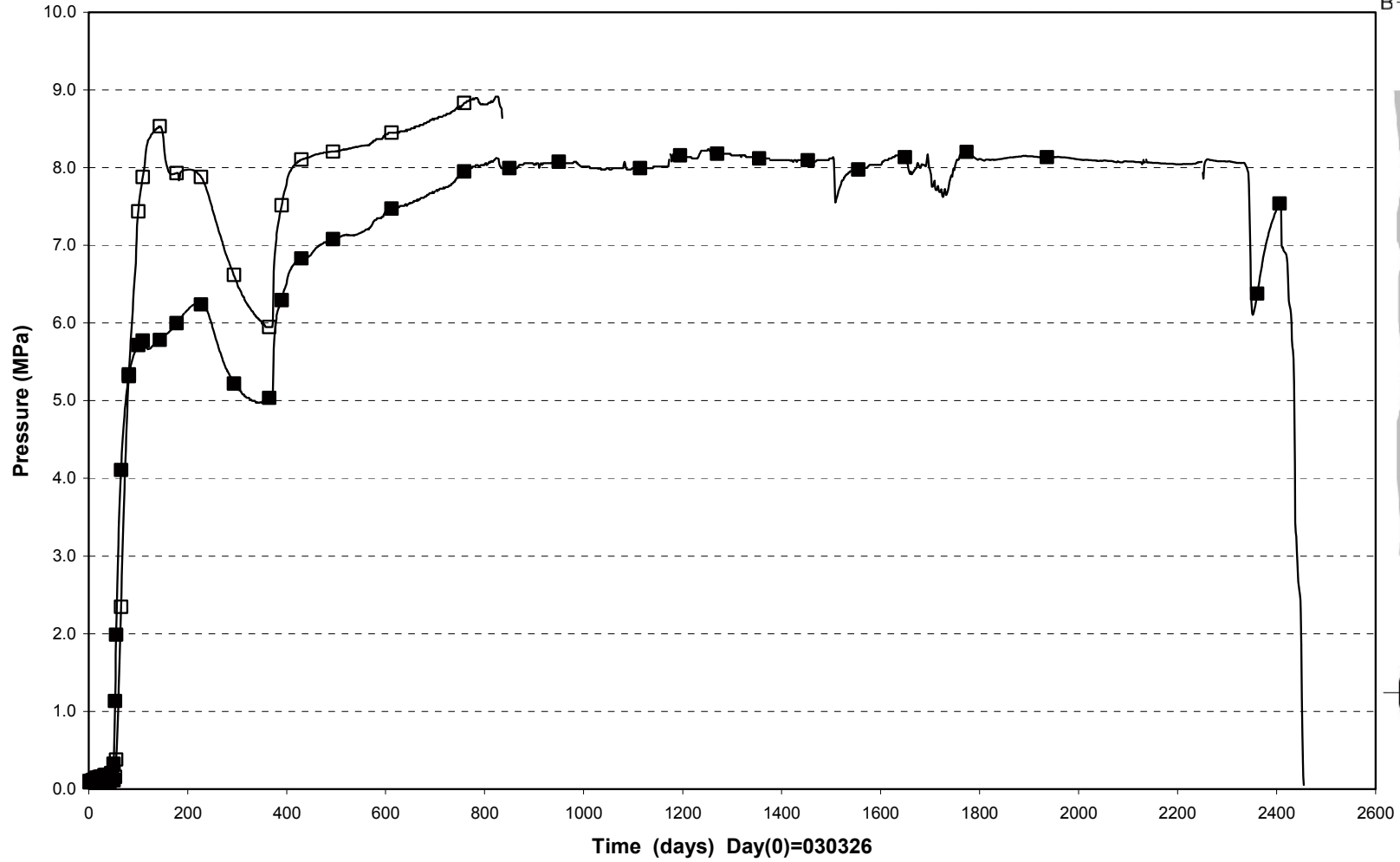


Total pressure/Ring 9 (090816-100301) Geokon



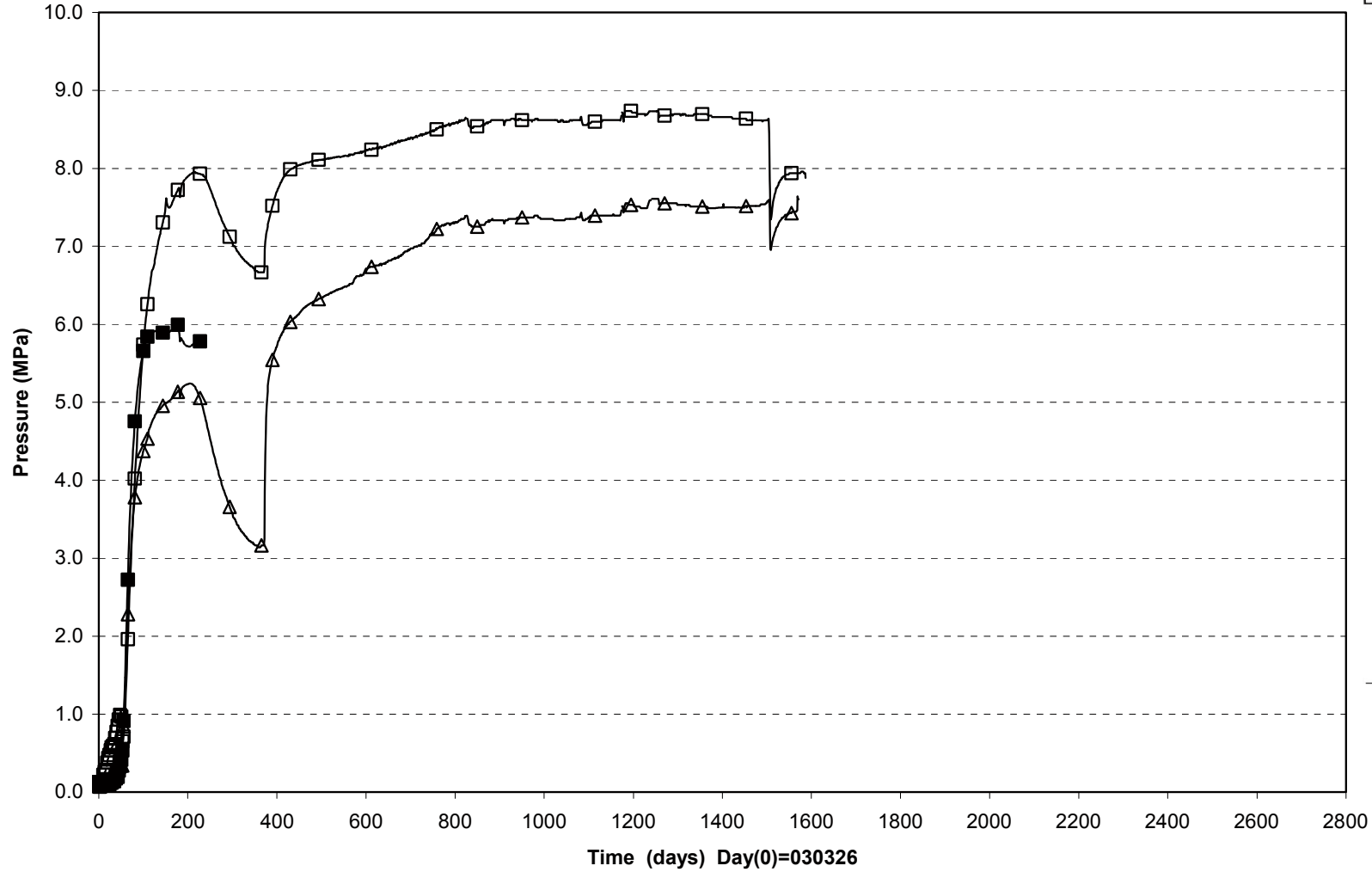
□ PB217(5.450\270°\0.535\R) ■ PB219(5.450\0°\0.635\R) ◇ PB222(5.450\110°\0.710\R) ◆ PB224(5.450\180°\0.770\R) △ PB226(5.450\270°\0.875\R)

Total pressure/Ring 9 (090816-100301) Geokon

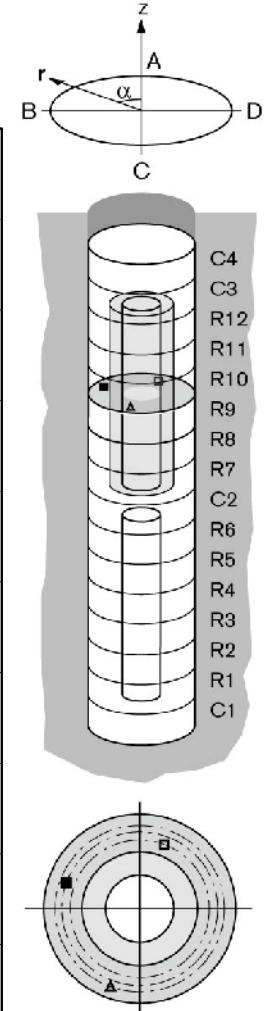


□ PB220(5.450\20°\0.635\T) ■ PB225(5.450\200°\0.740\T)

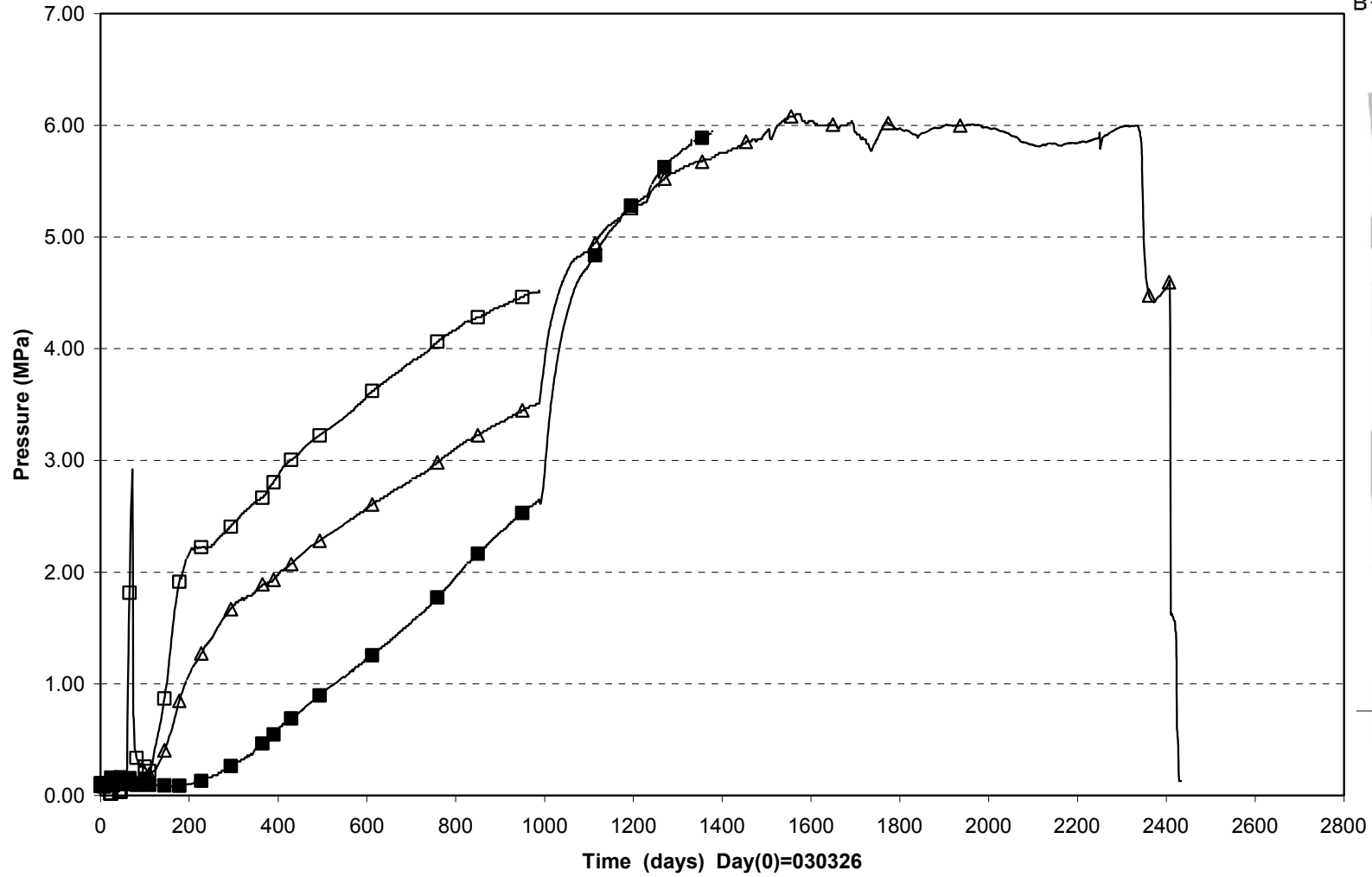
Total pressure/R9 (030326-100301) Geokon



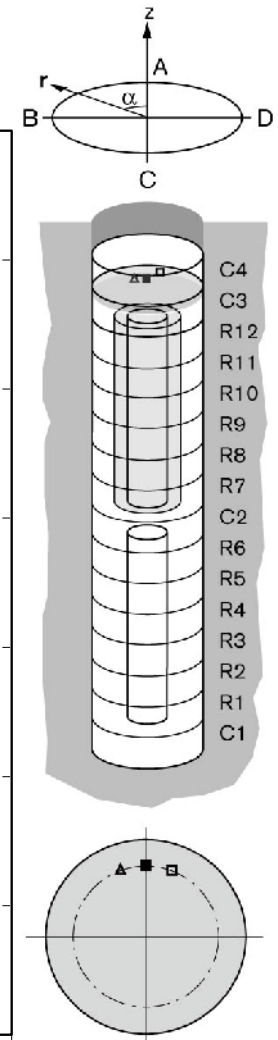
□ PB218(5.500\340°\0.635\A) ■ PB221(5.500\70°\0.710\A) △ PB223(5.500\160°\0.745\A)



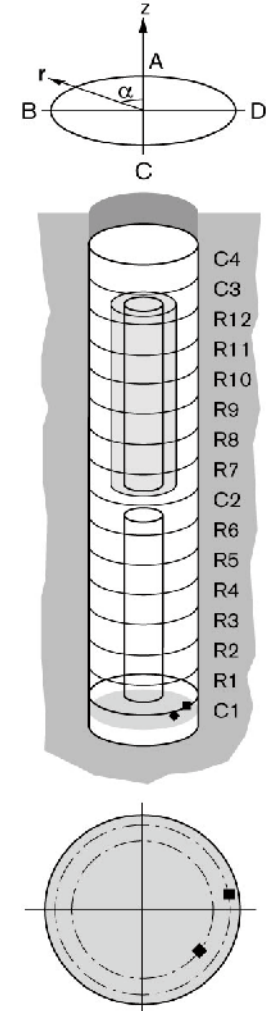
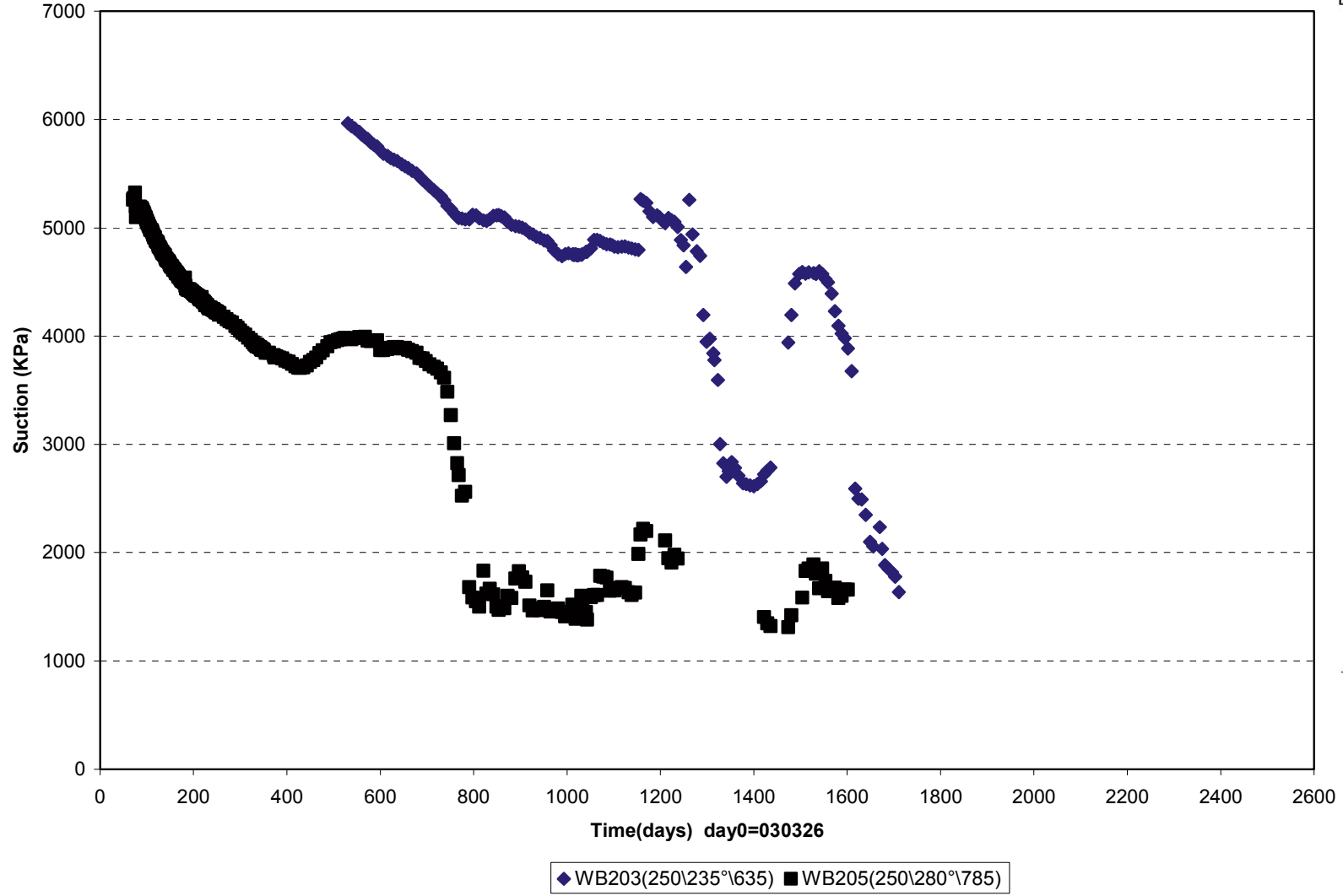
Total pressure/Cyl.3 (030326-100301) Geokon



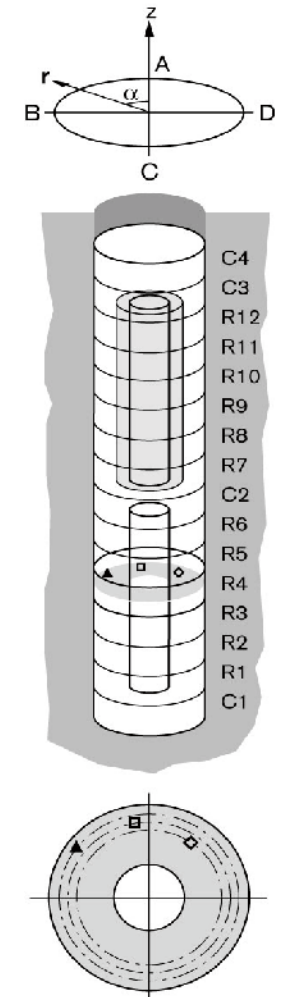
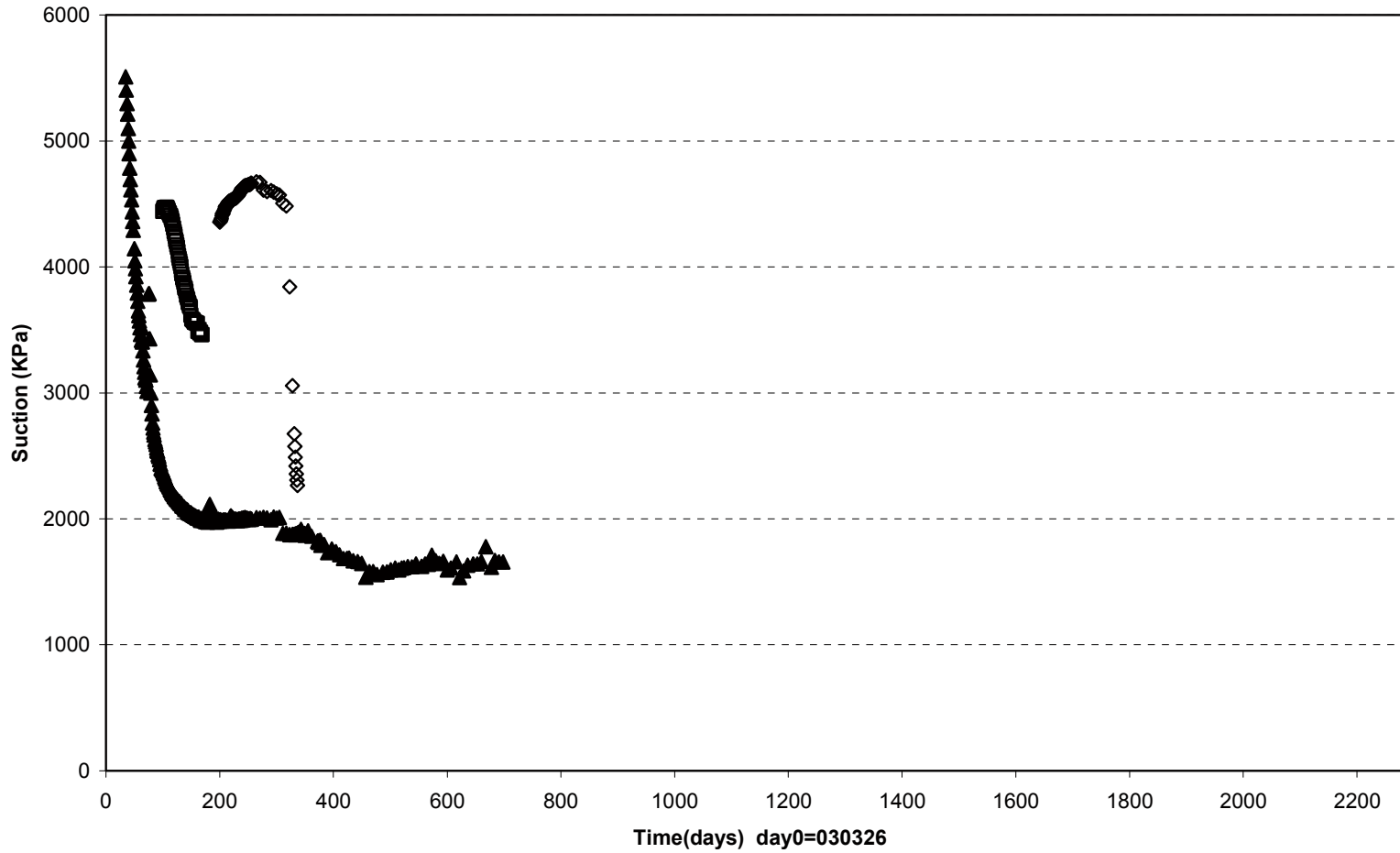
□ PB227(7.500\340°\0.635\A) ■ PB228(7.450\0°\0.635\R) △ PB229(7.450\20°\0.635\T)



TBT\ Cyl.1 (030326-100301) Suction - Wescor

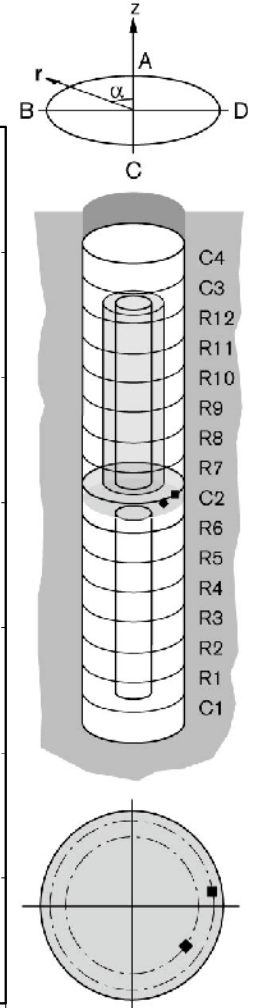
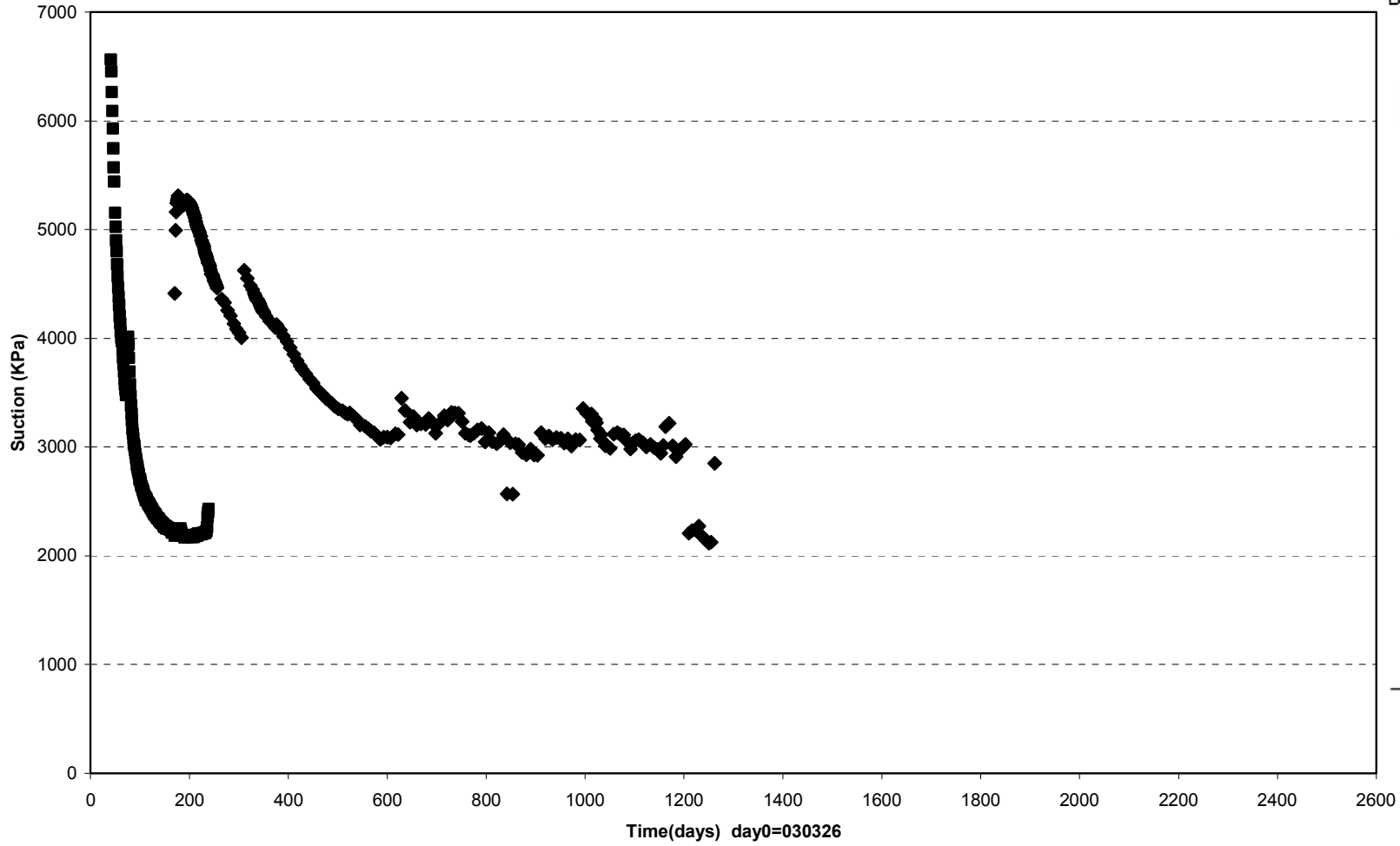


TBT\ Ring 4 (030326-100301) Suction - Wescor



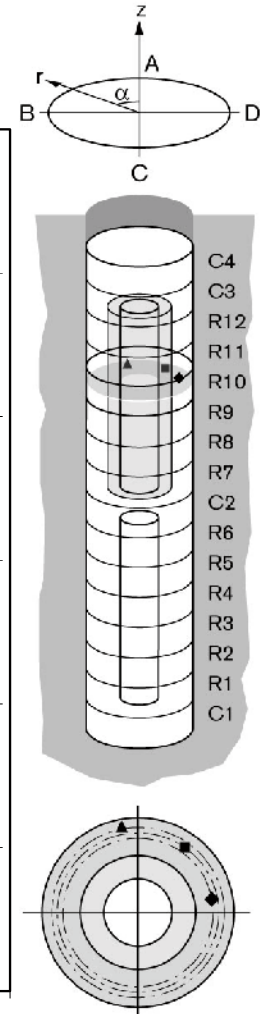
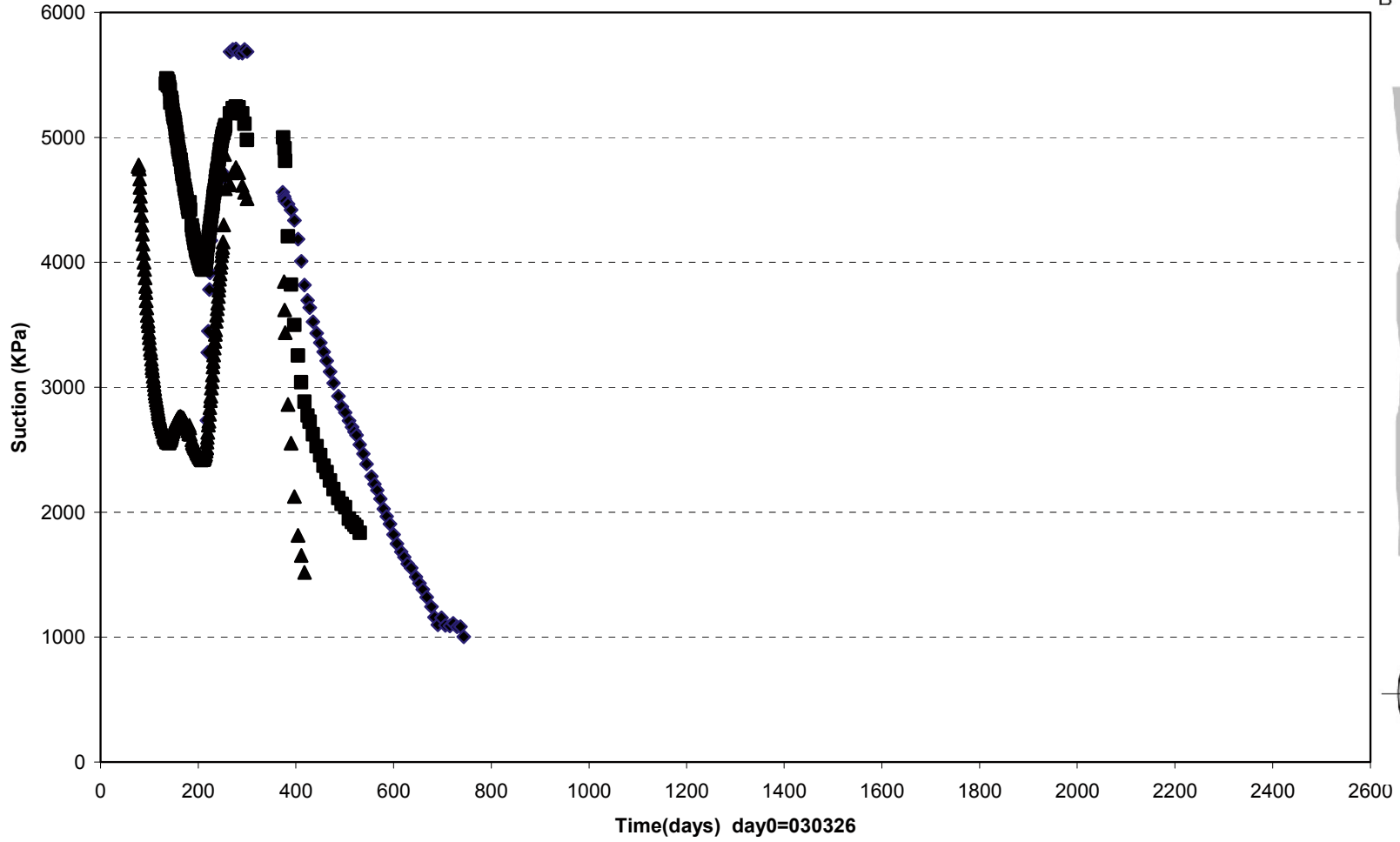
◇ WB211(2250\325°\635) □ WB213(2250\10°\710) ▲ WB215(2250\55°\785)

TBT\ Cyl.2 (030326-100301) Suction - Wescor



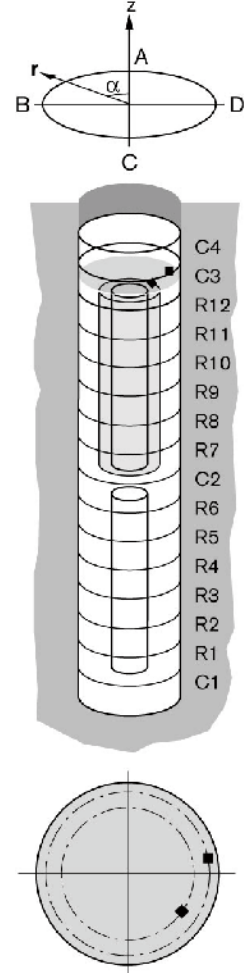
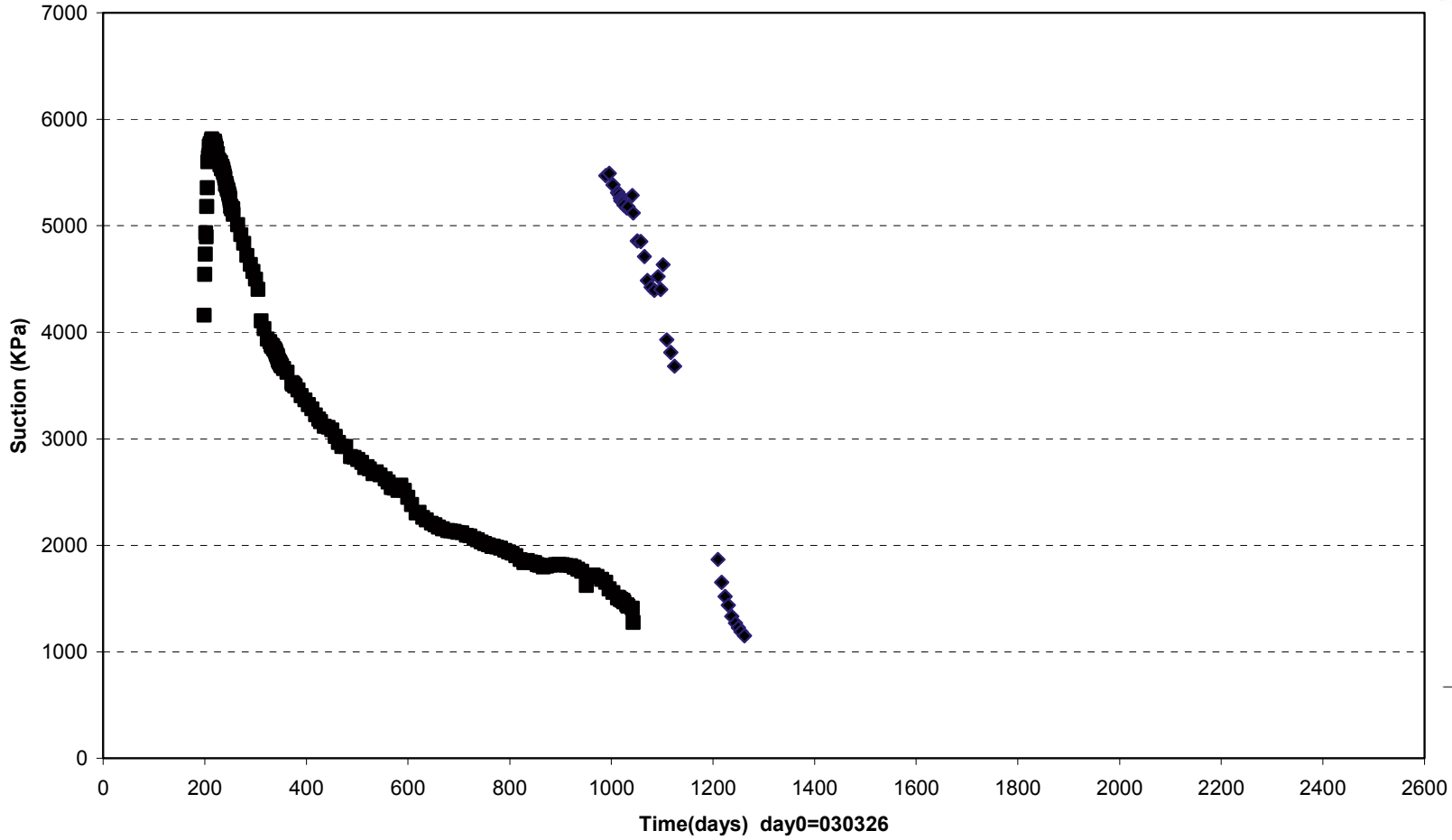
◆ WB218(3750\235°\635) ■ WB220(3750\280°\785)

TBT\ Ring 10 (030326-100301) Suction - Wescor



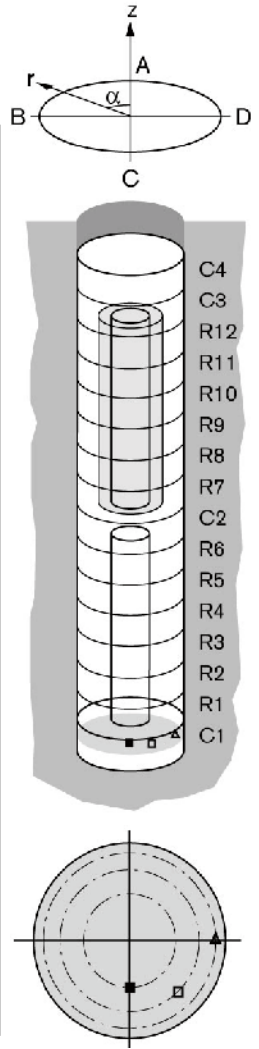
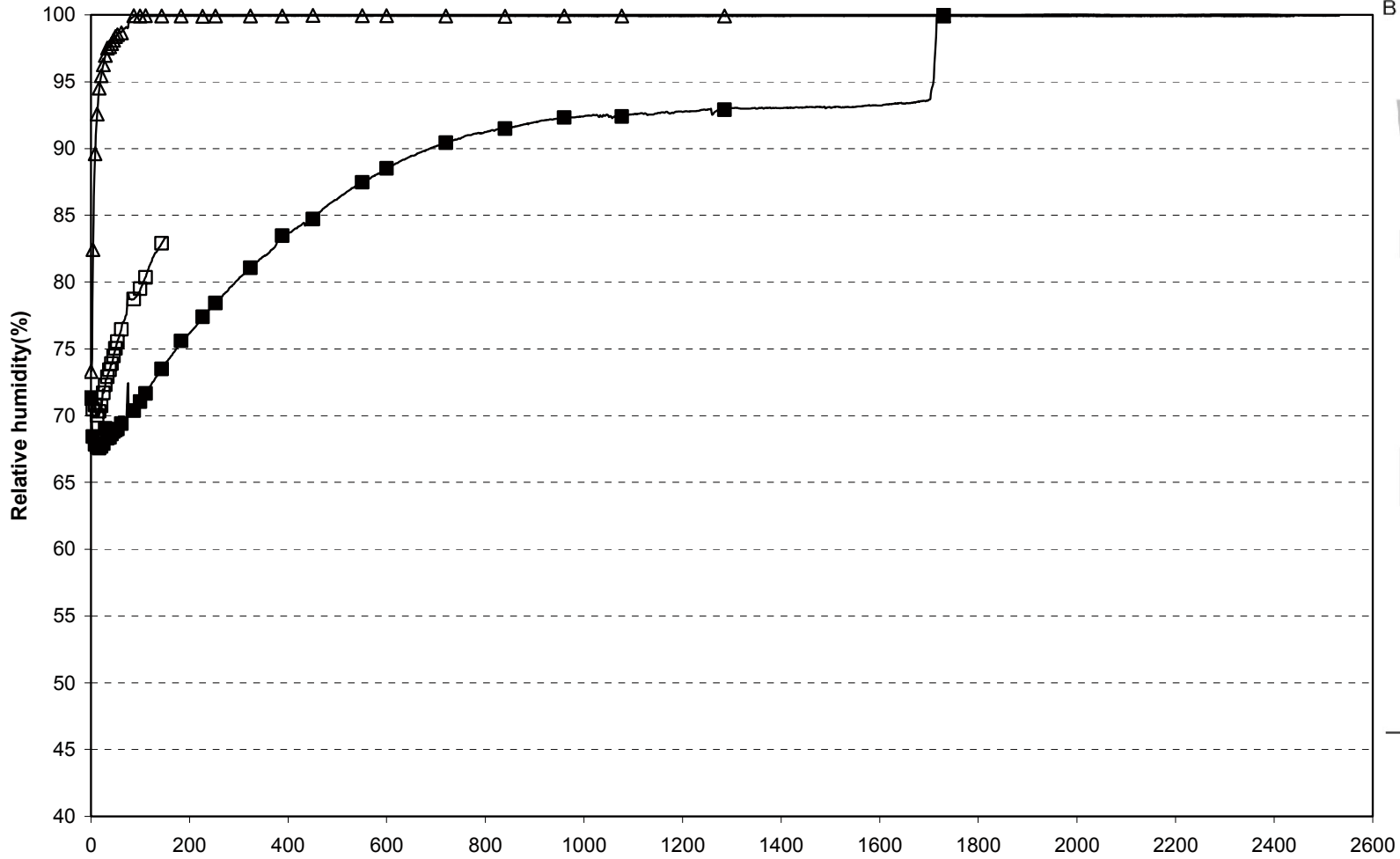
◆ WB226(5750\280°\685) ■ WB228(5750\325°\735) ▲ WB230(5750\10°\785)

TBT\ Cyl.3 (030326-100301) Suction - Wescor



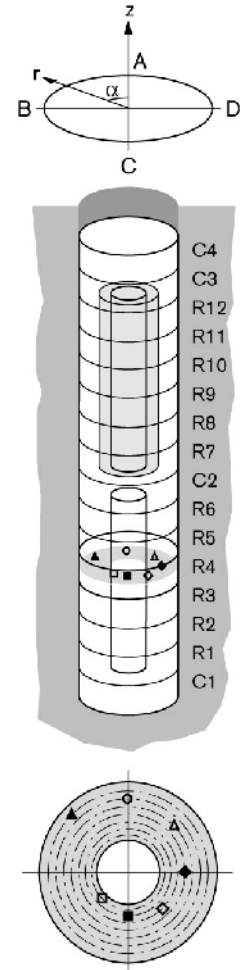
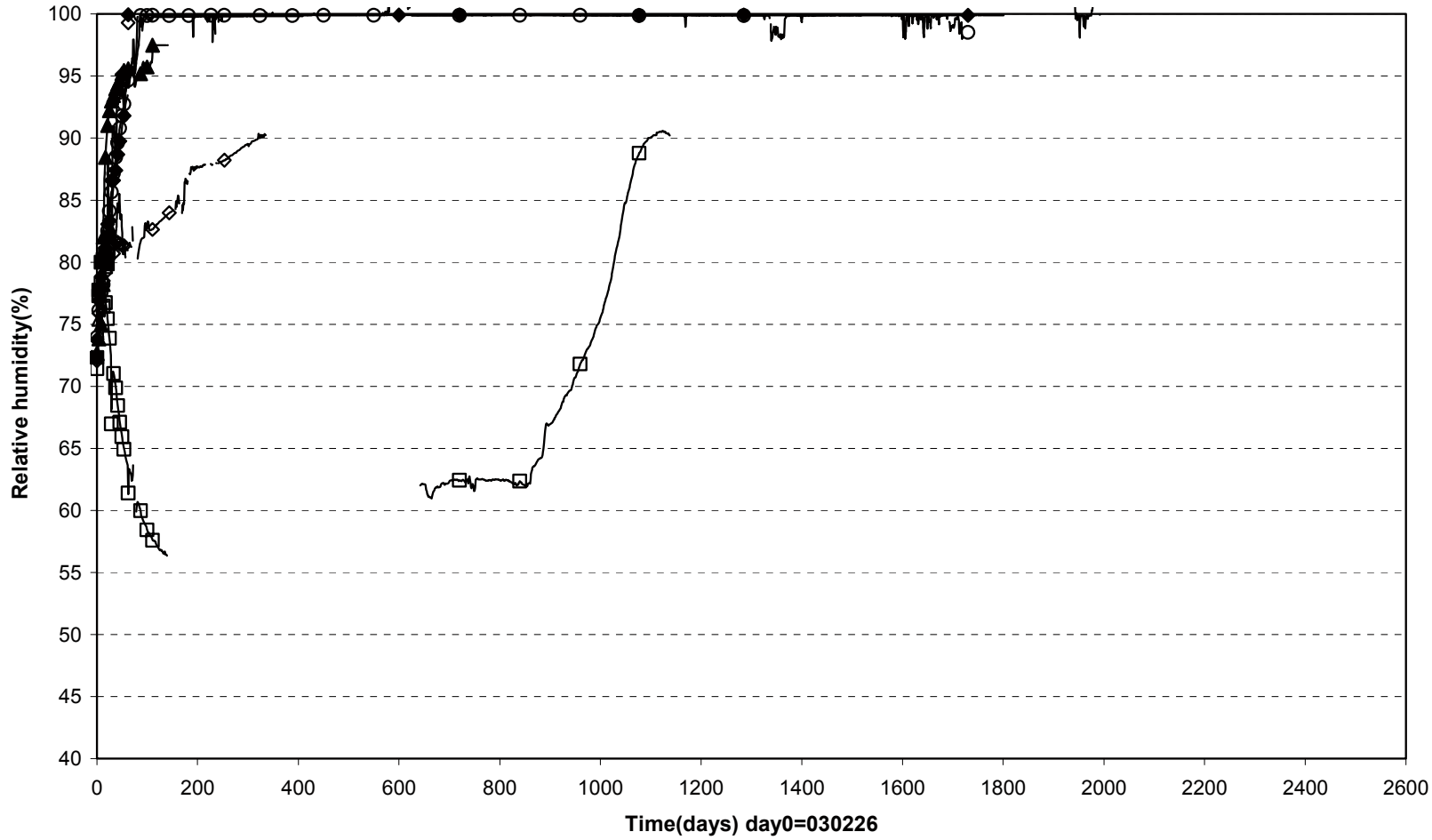
◆ WB233(7250\235°\635) ■ WB235(7250\280°\785)

TBT\Cyl.1 (030326-100301) Relative humidity - Vaisala & Rotronic

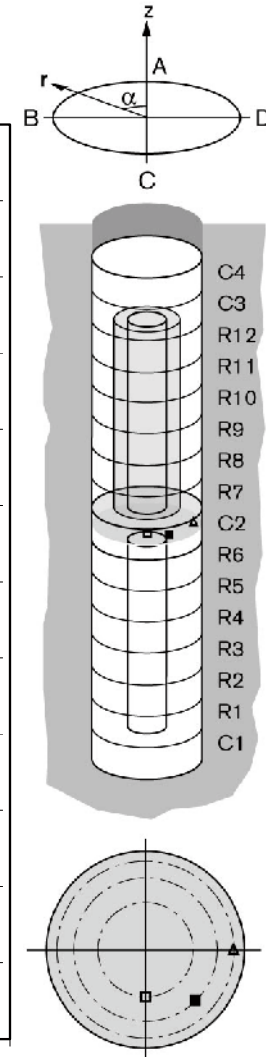
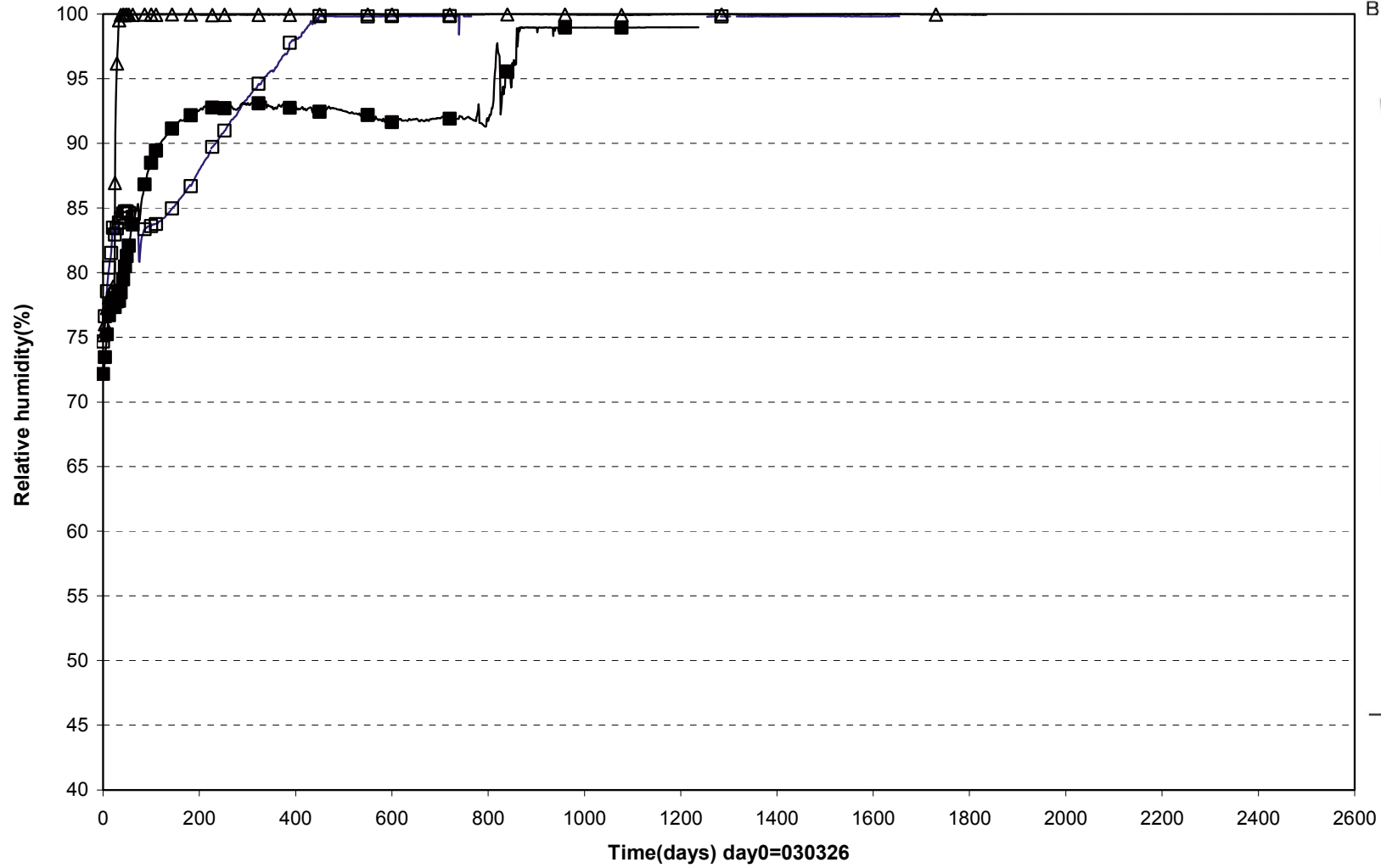


■ WB201(250\180°\420) □ WB202(250\225°\635) △ WB204(250\270°\785)

TBT\ Ring 4 (030326-100301) Relative humidity - Vaisala & Rotronic

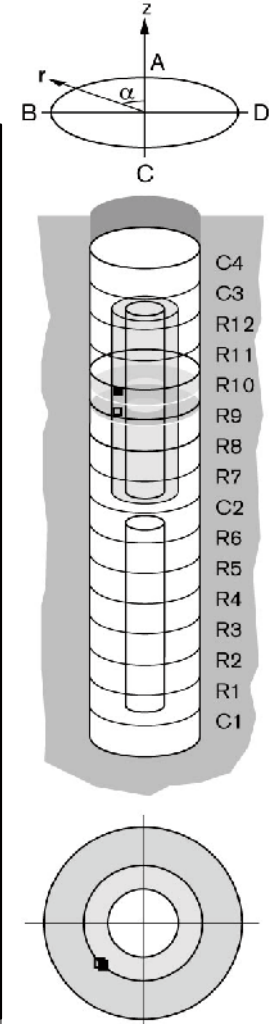
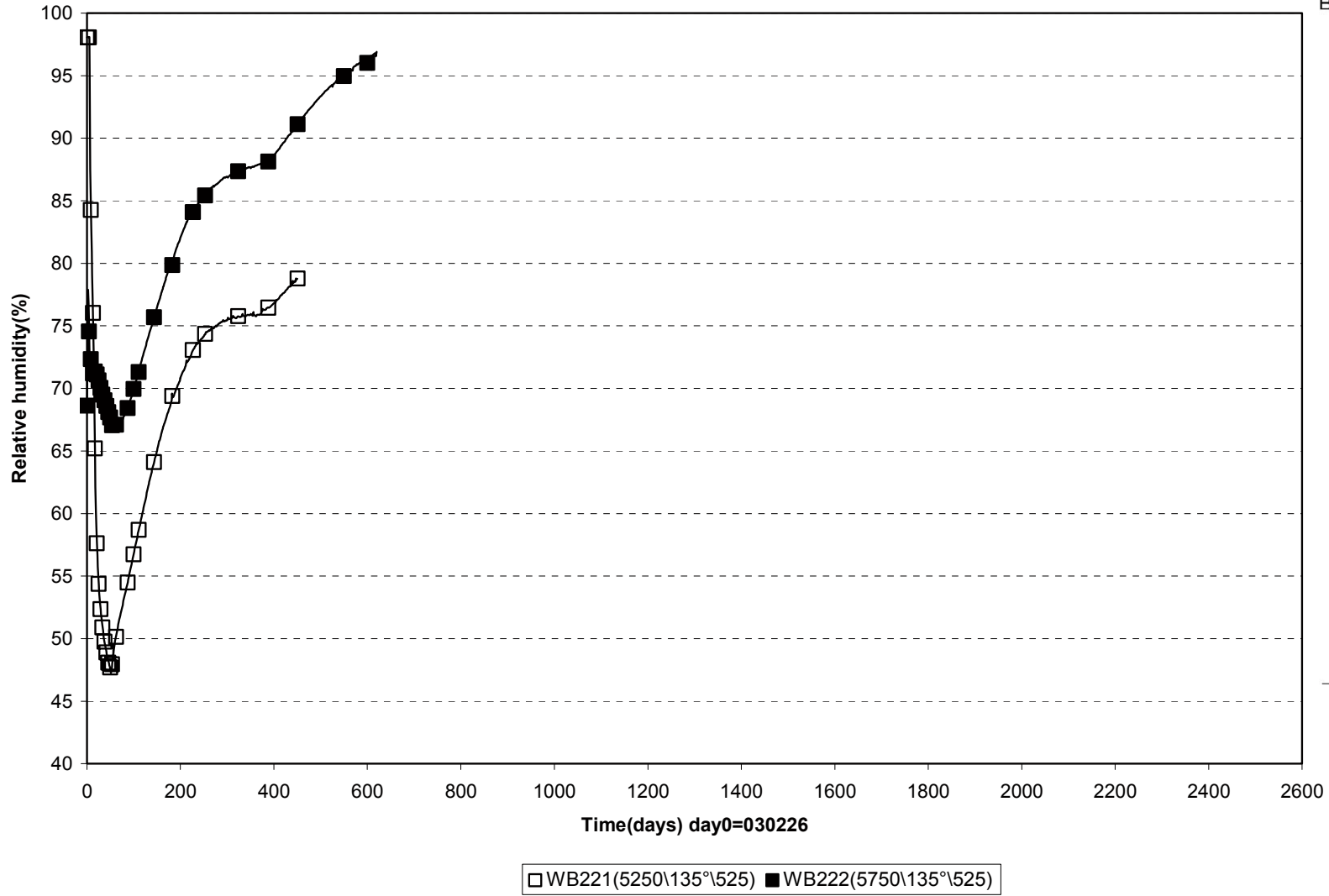


TBT\Cyl.2 (030326-100301)
Relative humidity - Vaisala & Rotronic

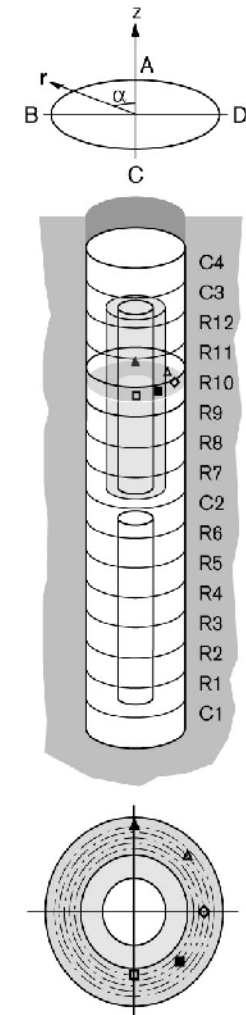
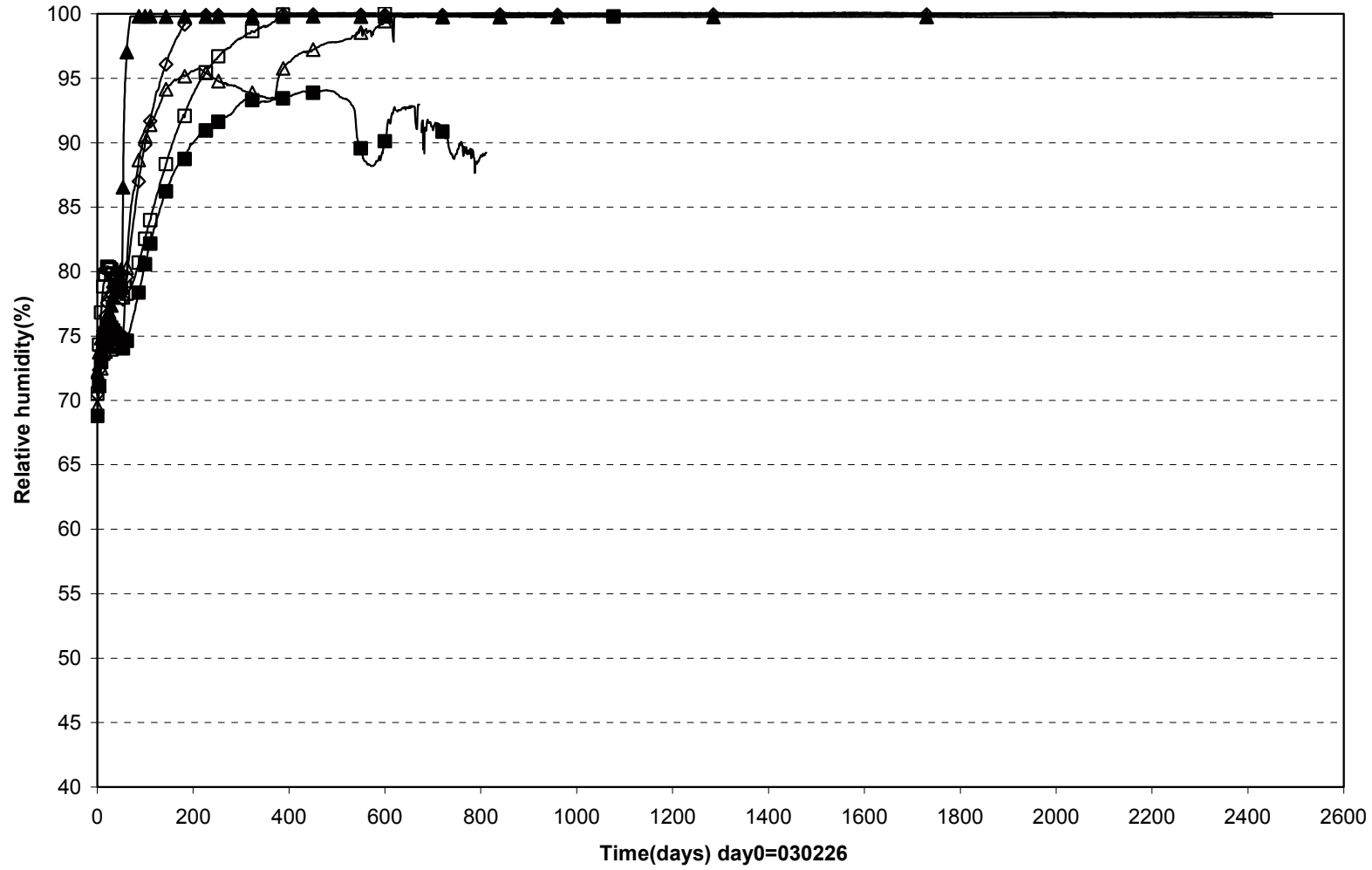


□ WB216(3750\180°\420) ■ WB217(3750\225°\635) △ WB219(3750\270°\785)

TBT\ Ring 9-10 (030326-100301)
Relative humidity - Vaisala & Rotronic

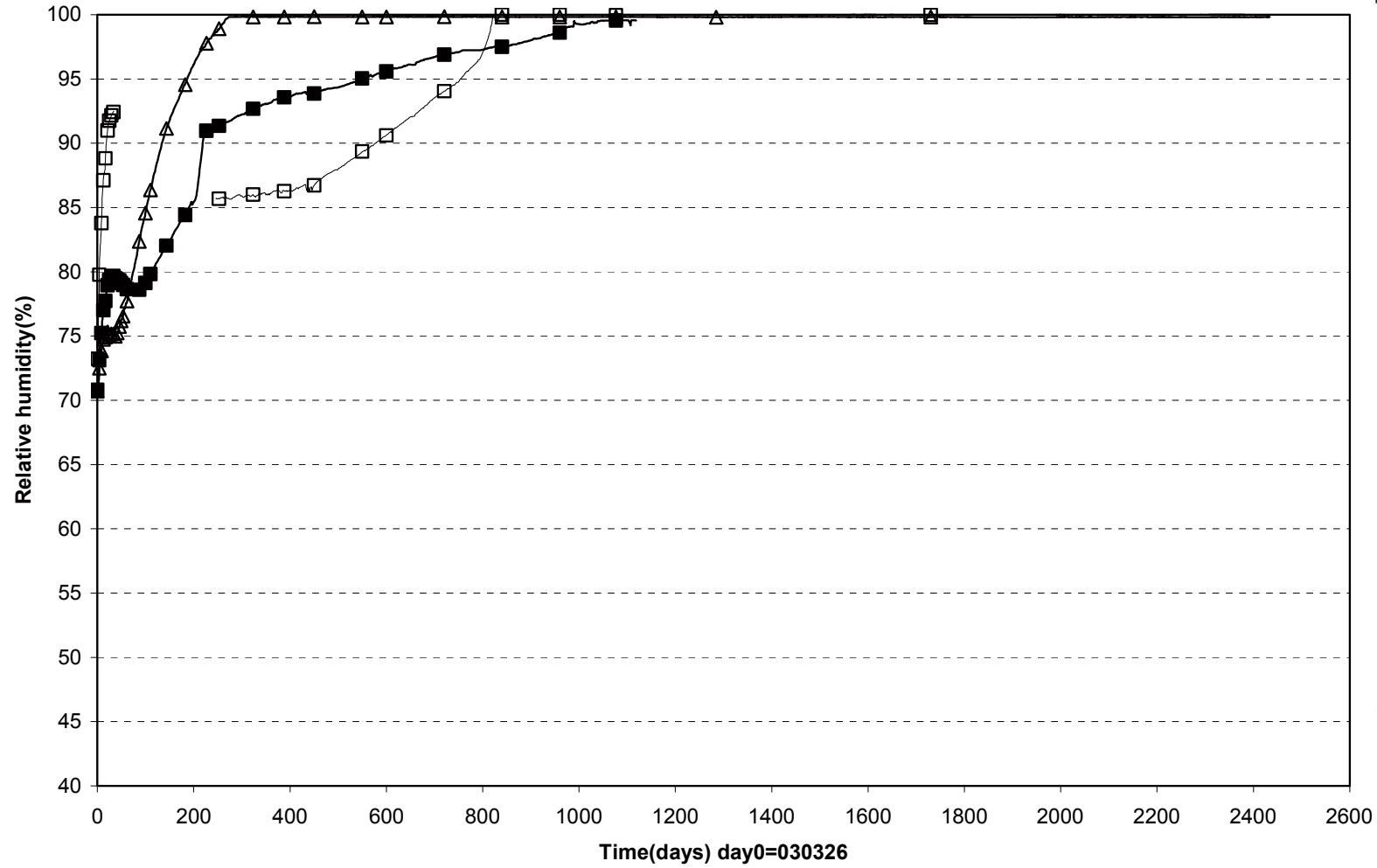


TBT\ Ring 10 (030326-100301) Relative humidity - Vaisala & Rotronic

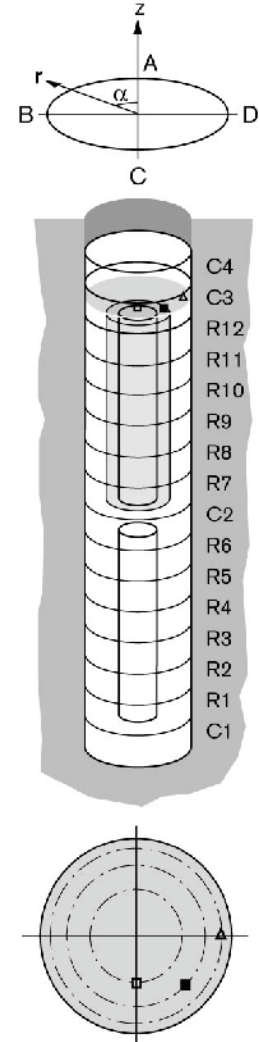


□ WB223(5750\180°\585) ■ WB224(5750\225°\635) ◇ WB225(5750\270°\685) △ WB227(5750\315°\735) ▲ WB229(5750\0°\785)

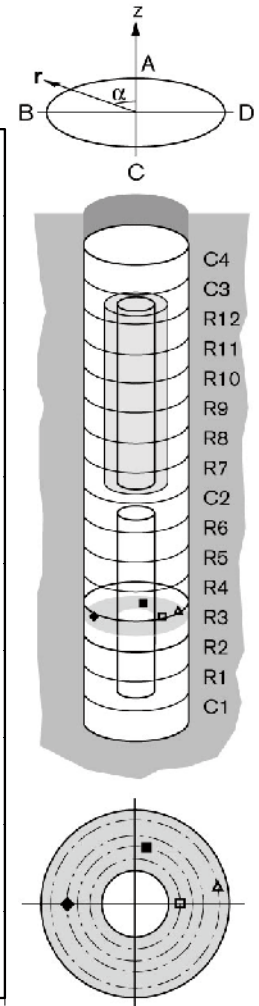
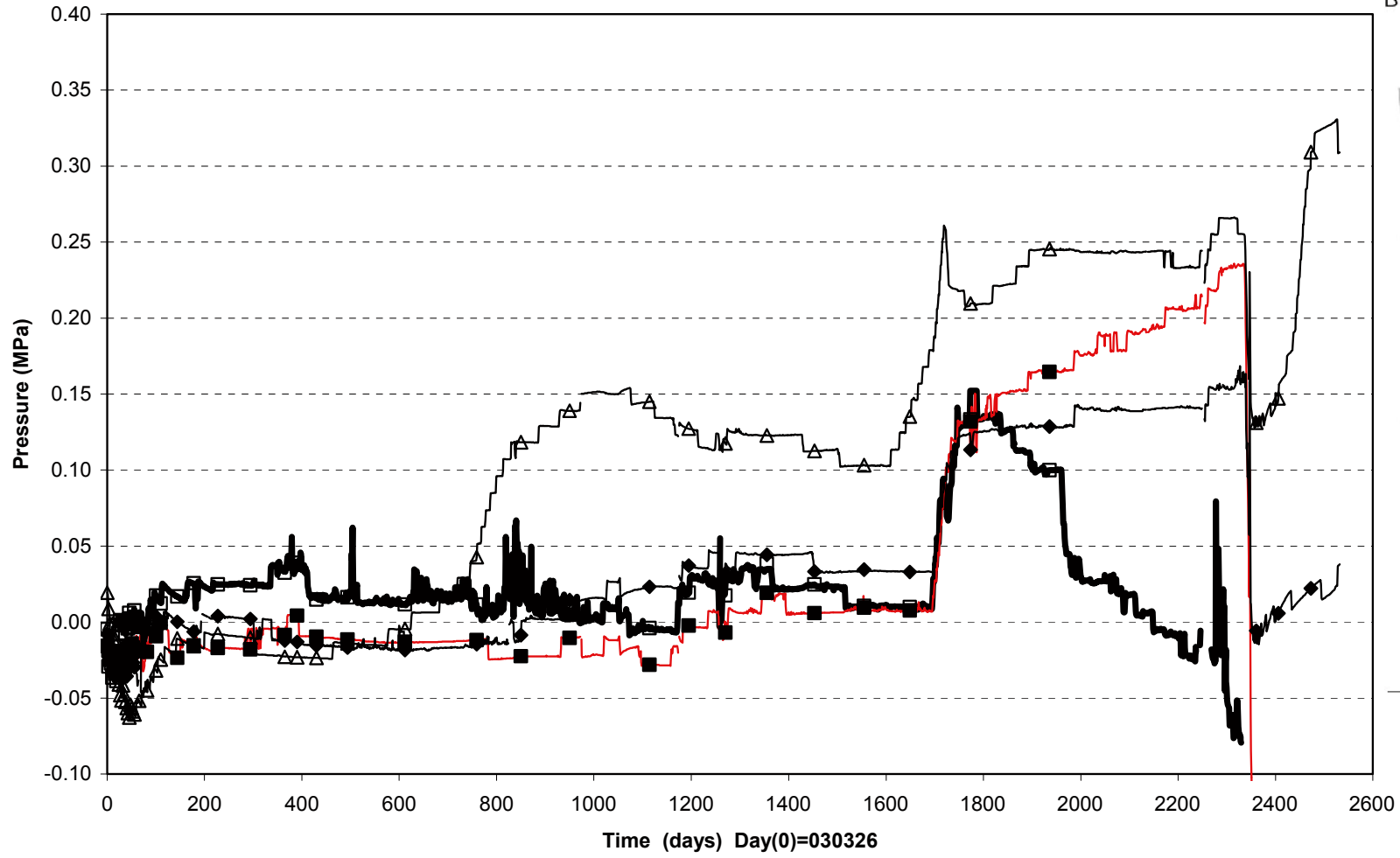
TBT\Cyl.3 (030326-100301) Relative humidity - Vaisala & Rotronic



□ WB231(7250\180°\420) ■ WB232(7250\225°\635) △ WB234(7250\270°\785)

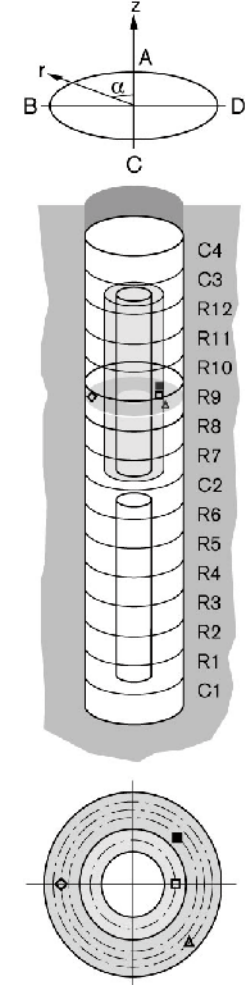
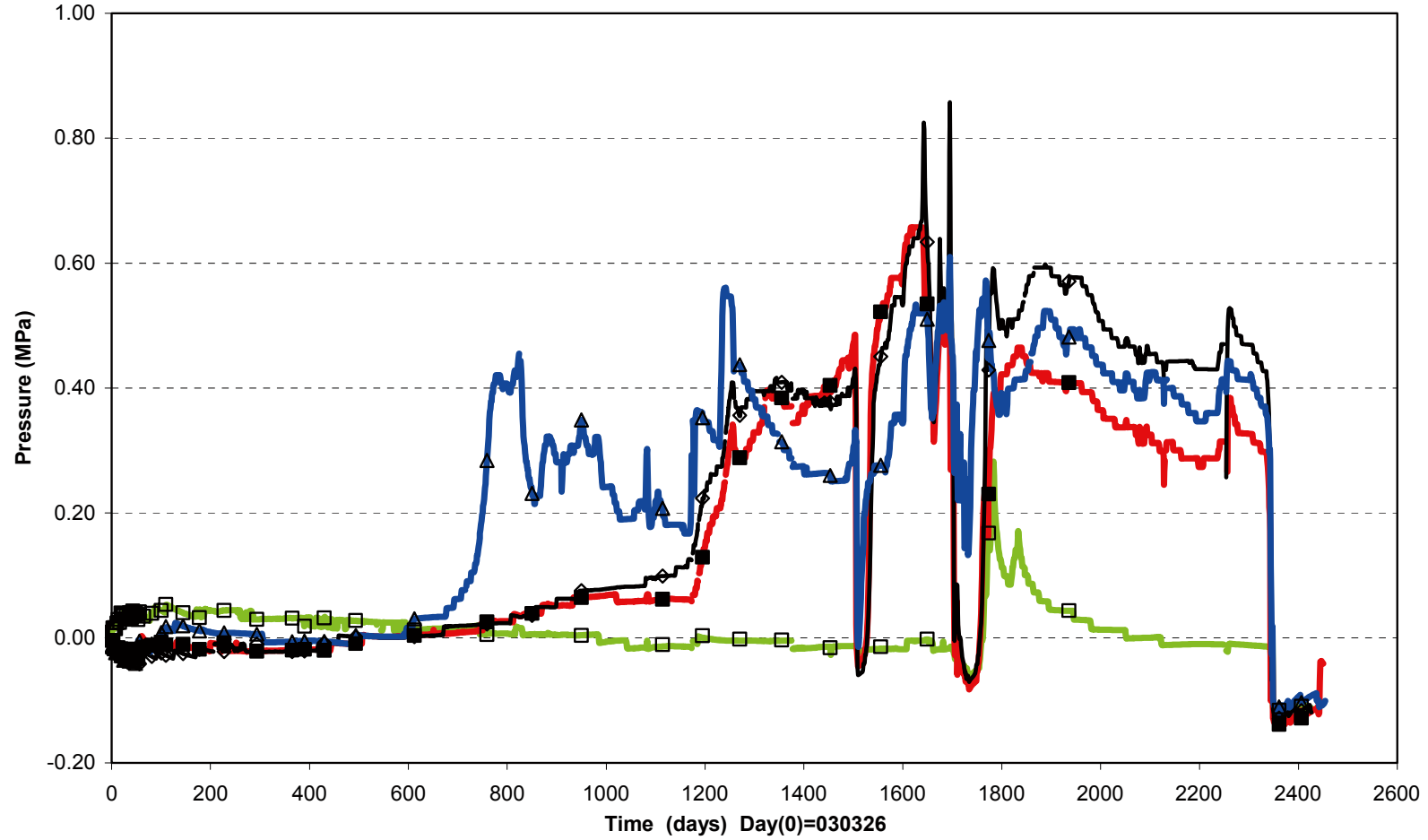


Pore pressure/Ring 3 (030326-100301) Geokon



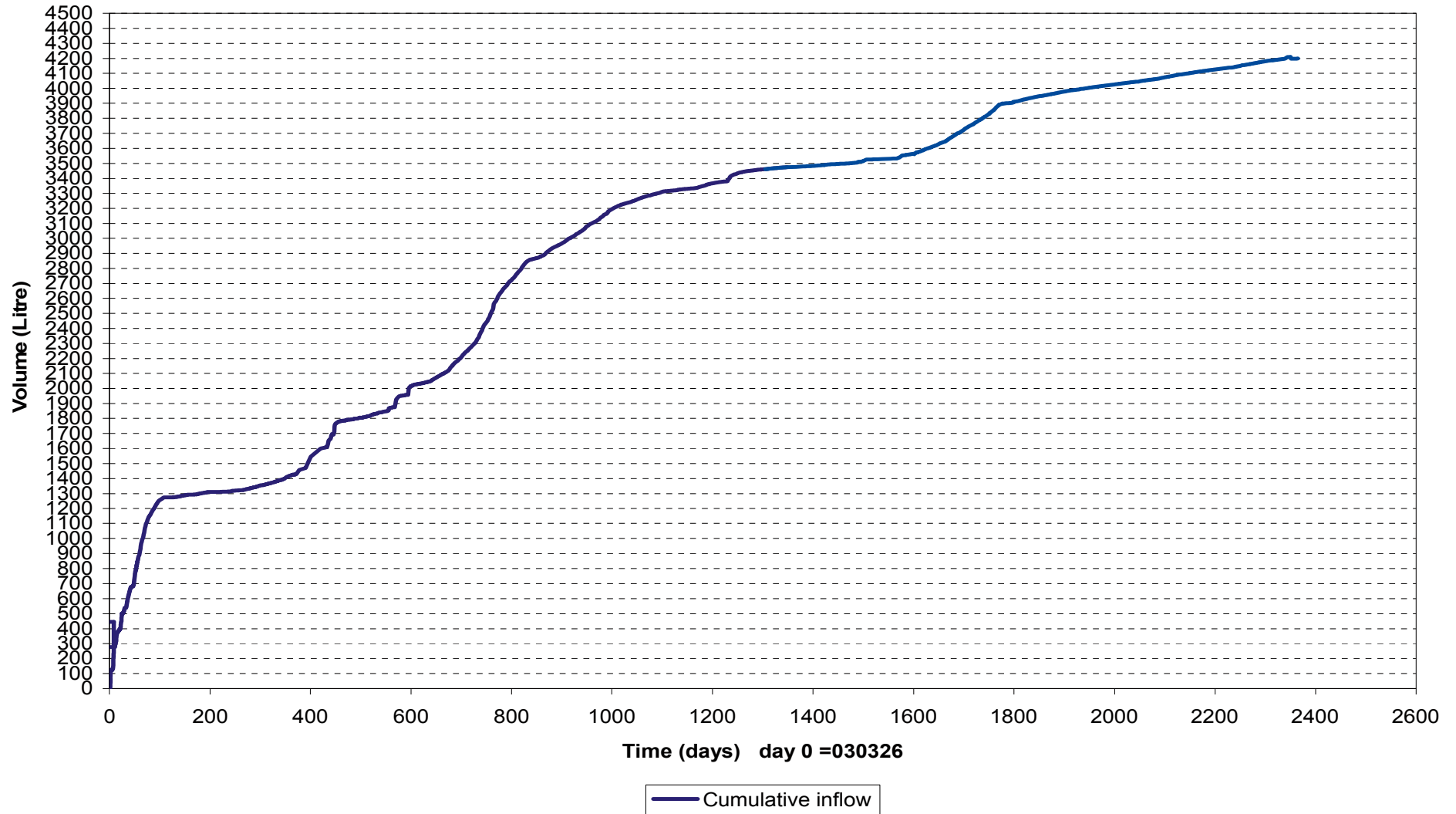
□ UB201(1.750\270°\0.420\R) ■ UB202(1.750\350°\0.535\R) ◆ UB203(1.750\90°\0.635) ▲ UB204(1.750\280°\0.785)

Pore pressure/Ring 9 (030326-100301) Geokon

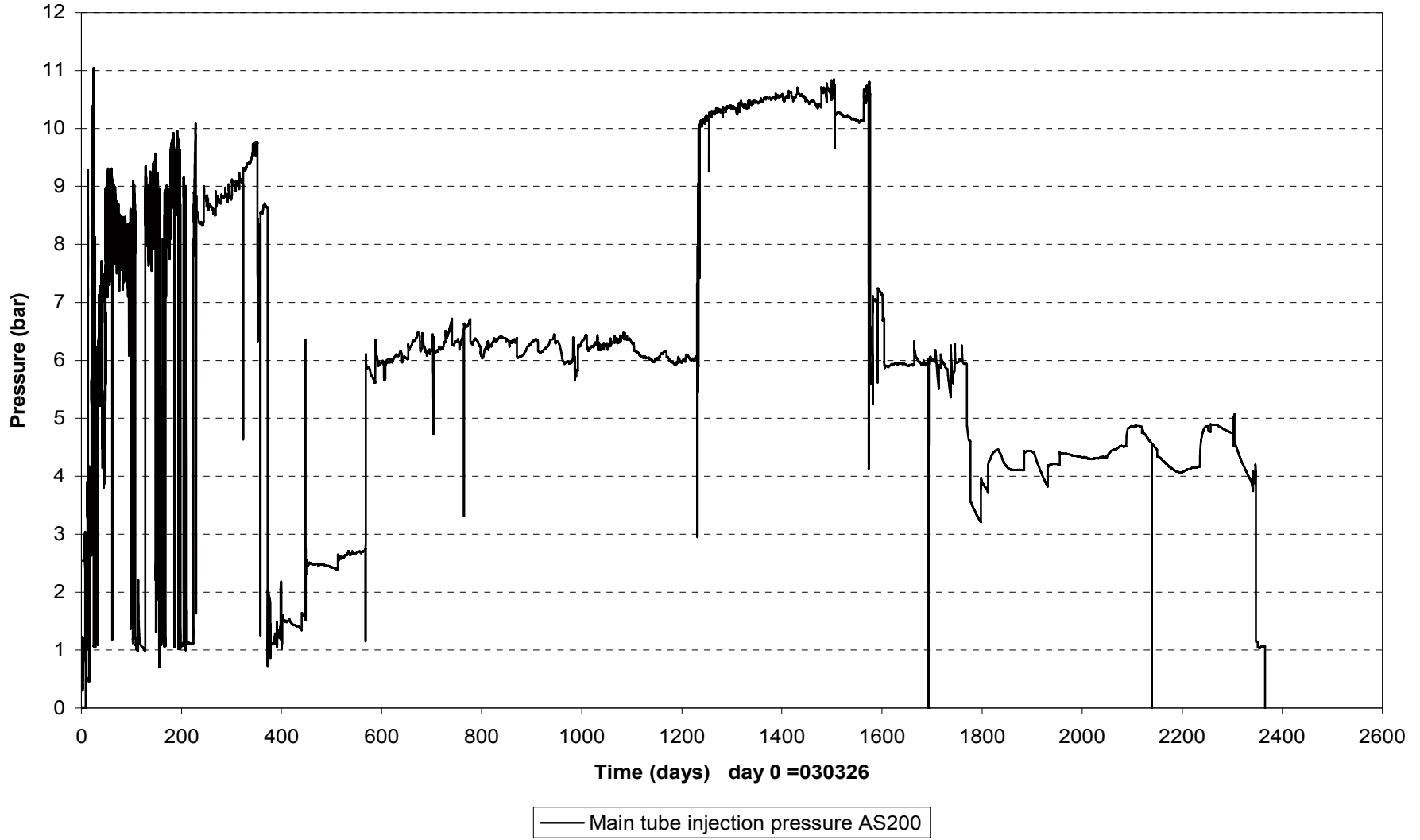


□ UB205(5.250\270°\0.420) ■ UB206(5.250\315°\0.635) ◇ UB207(5.250\90°\0.710) △ UB208(5.250\225°\0.785)

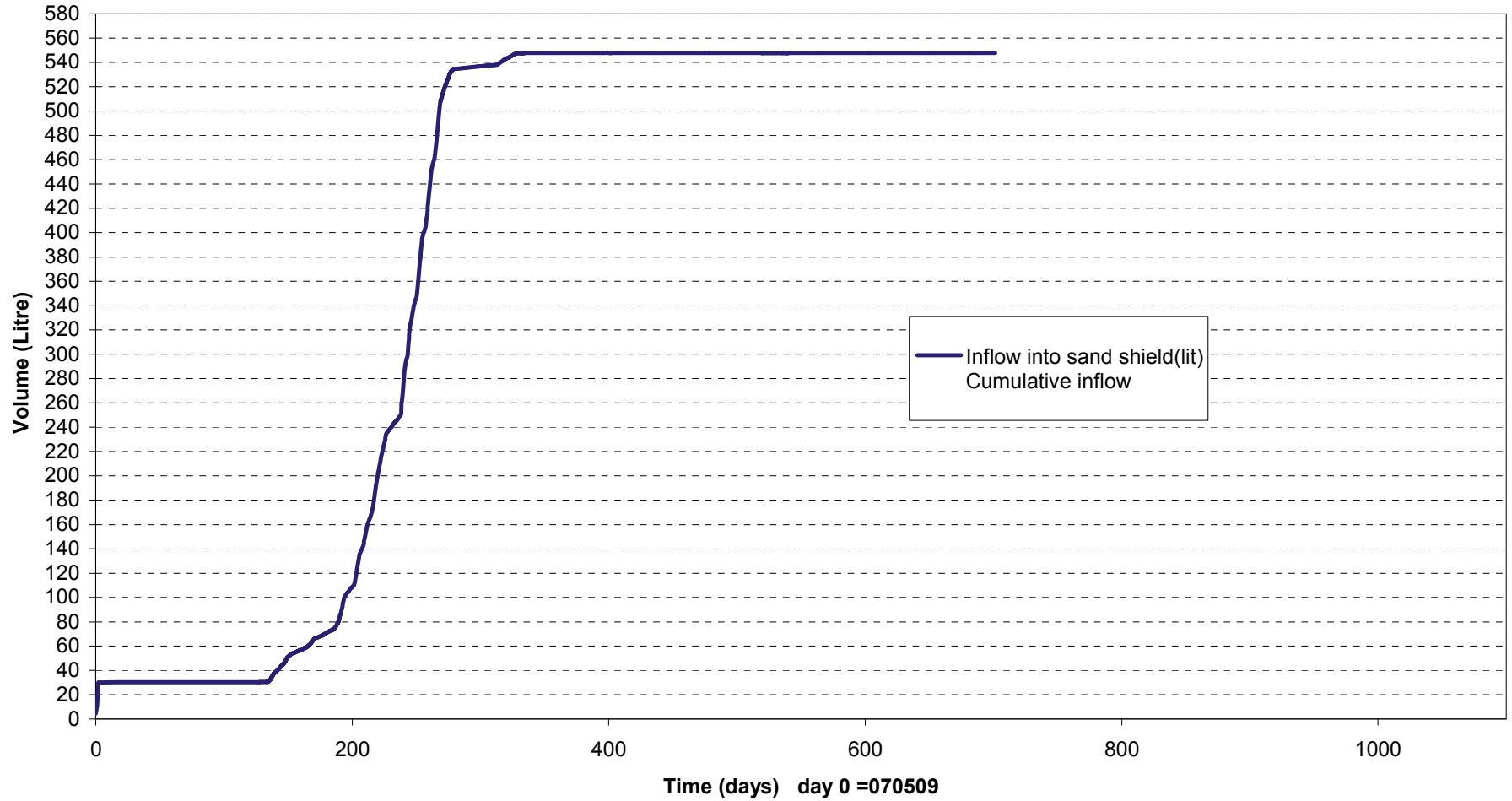
Inflow of water into sand filter (030326-100301)



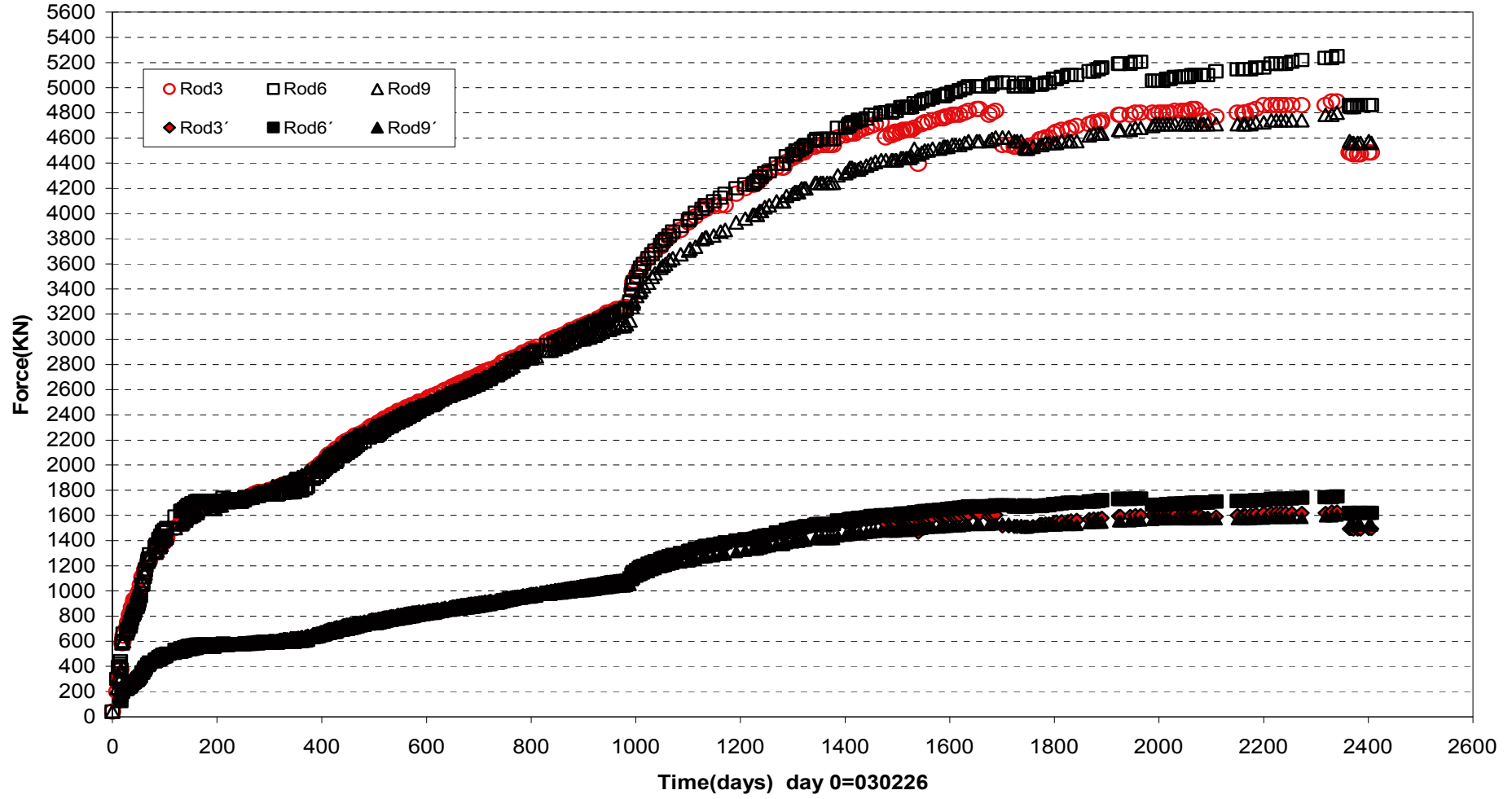
Injection pressure upstream the filter tips (030326-100301)



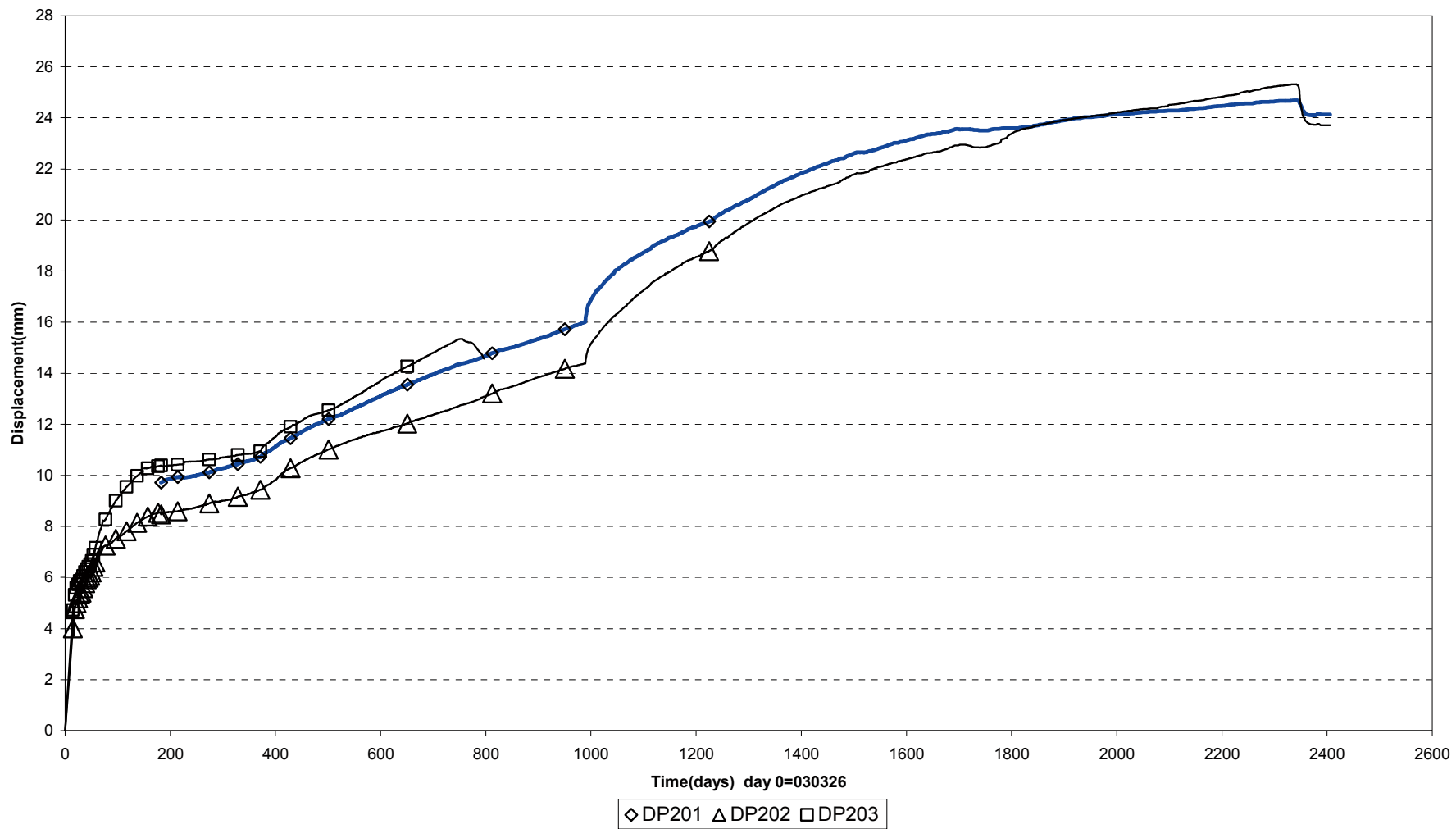
Inflow of water to sand shield (070509-100301)



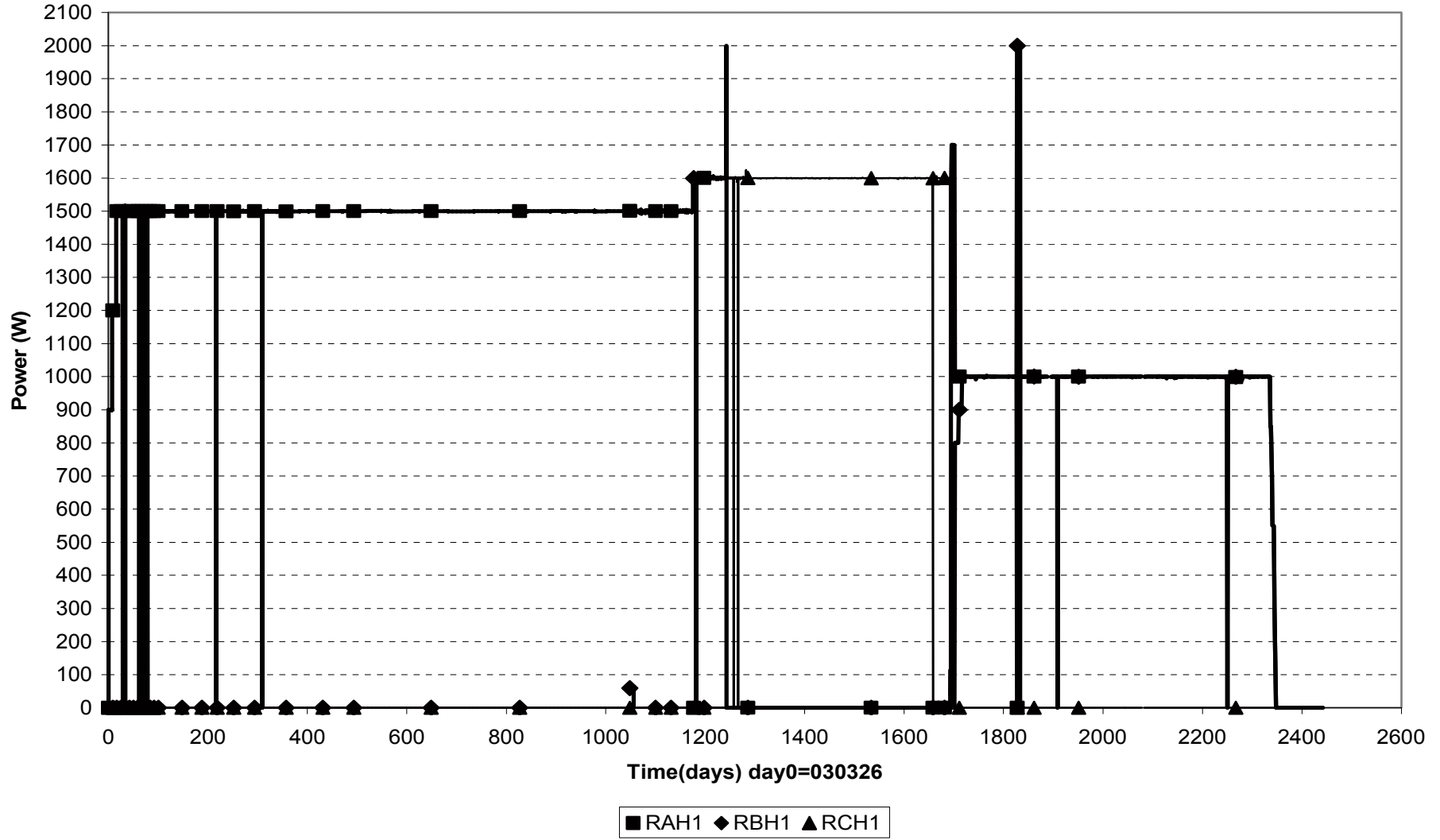
Forces on plug (030326-100301)



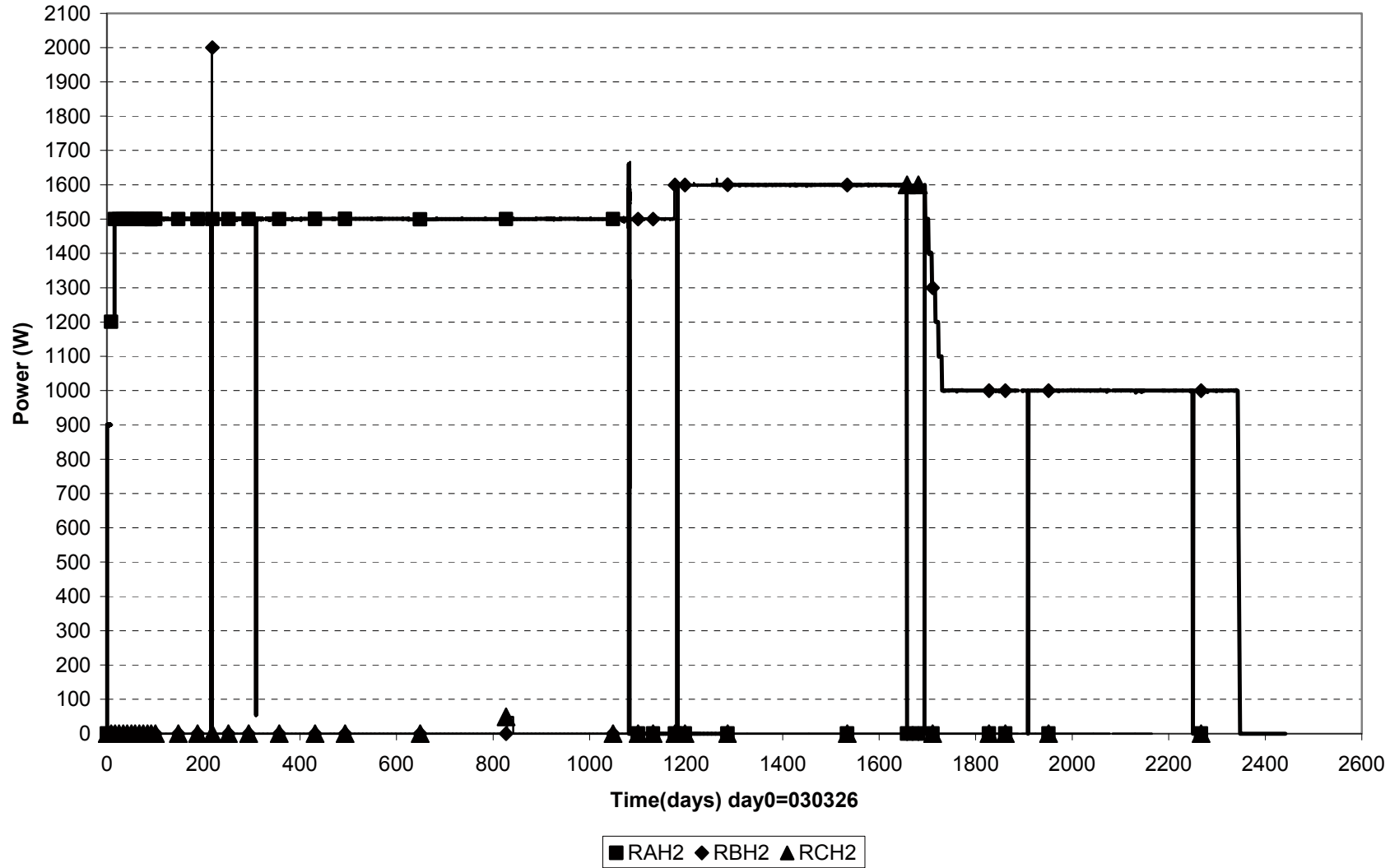
Displacement of plug (030326-100301)



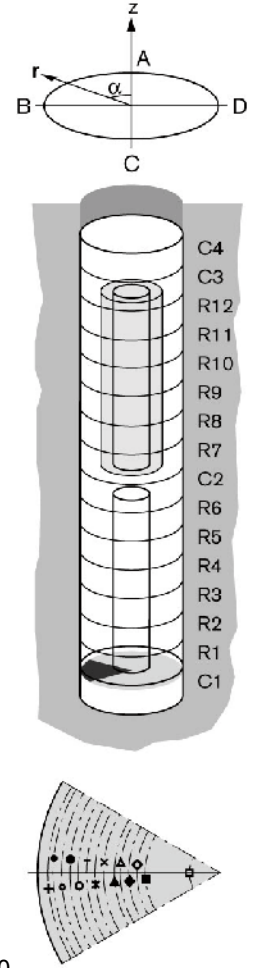
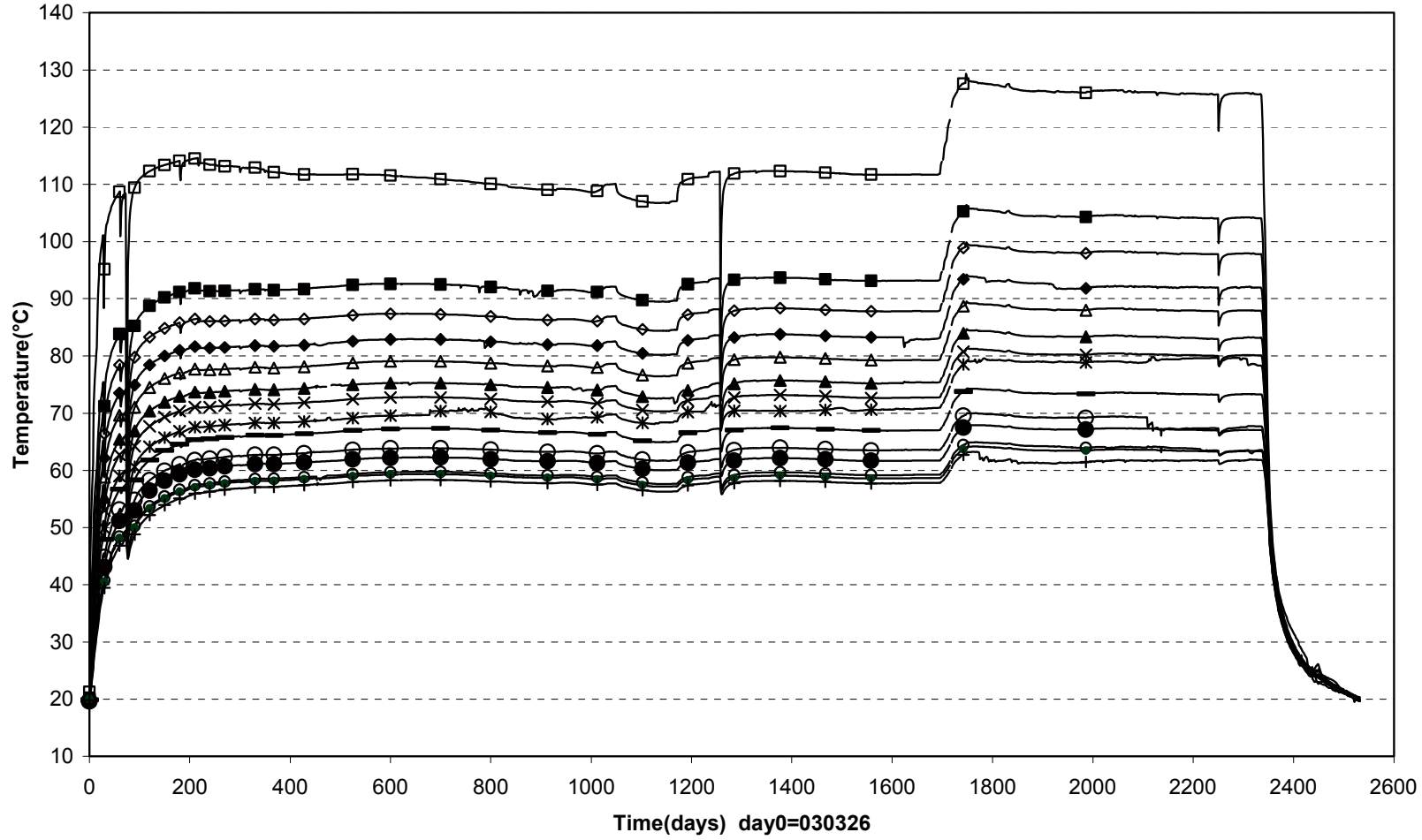
Power Heater 1 (030326-100301)



Power Heater 2 (03026-100301)

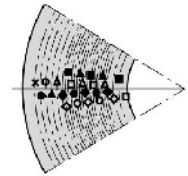
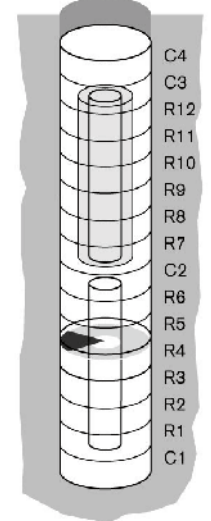
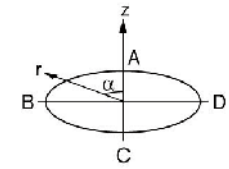
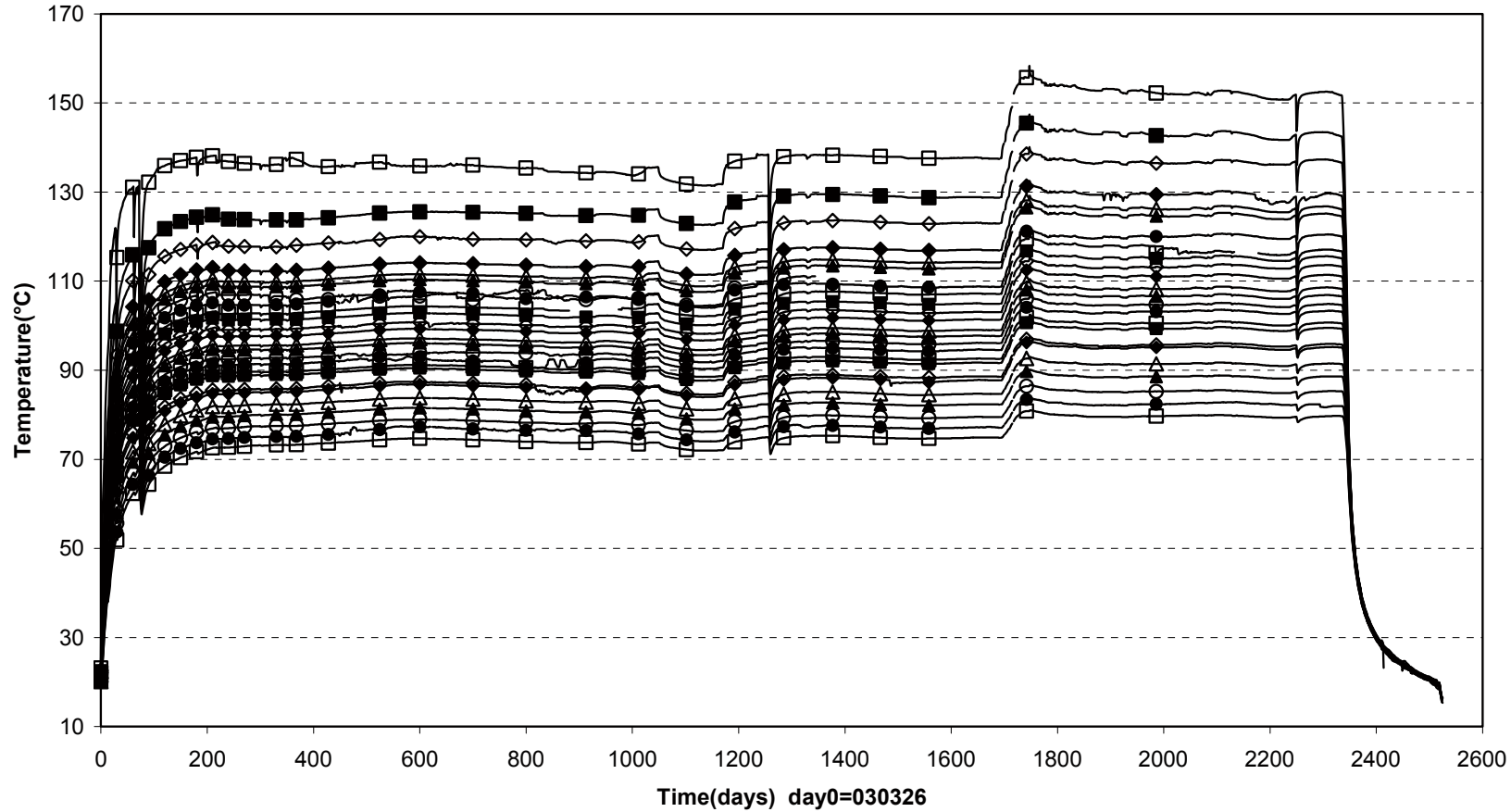


TBT\Cyl.1 (030326-100301)
Temperature - Pentronic



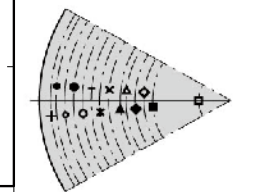
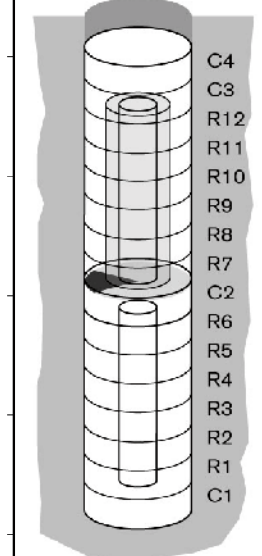
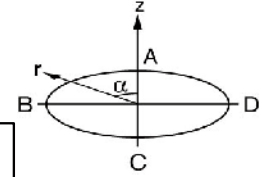
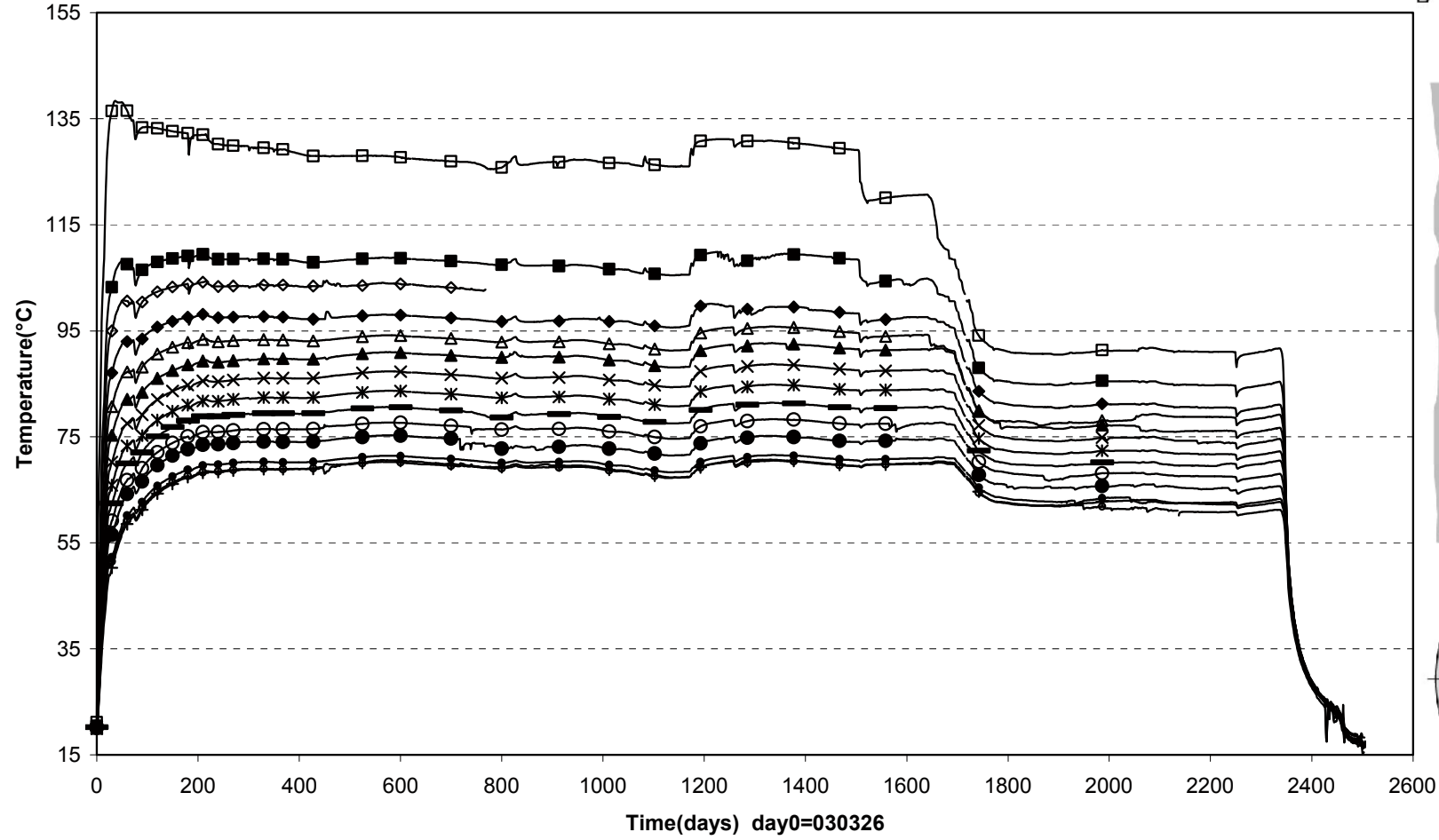
□ TB201(450\90°\150) ■ TB202(450\95°\360) ◇ TB203(450\85°\400) ◆ TB204(450\95°\440) △ TB205(450\85°\480) ▲ TB206(450\95°\520) × TB207(450\85°\560)
 ✖ TB208(450\95°\600) — TB209(450\85°\640) ○ TB210(450\95°\680) ● TB211(450\85°\720) ○ TB212(450\95°\760) ● TB213(450\85°\800) + TB214(450\95°\825)

TBT \Ring4 (030326-100301)
Temperature - Pentronic



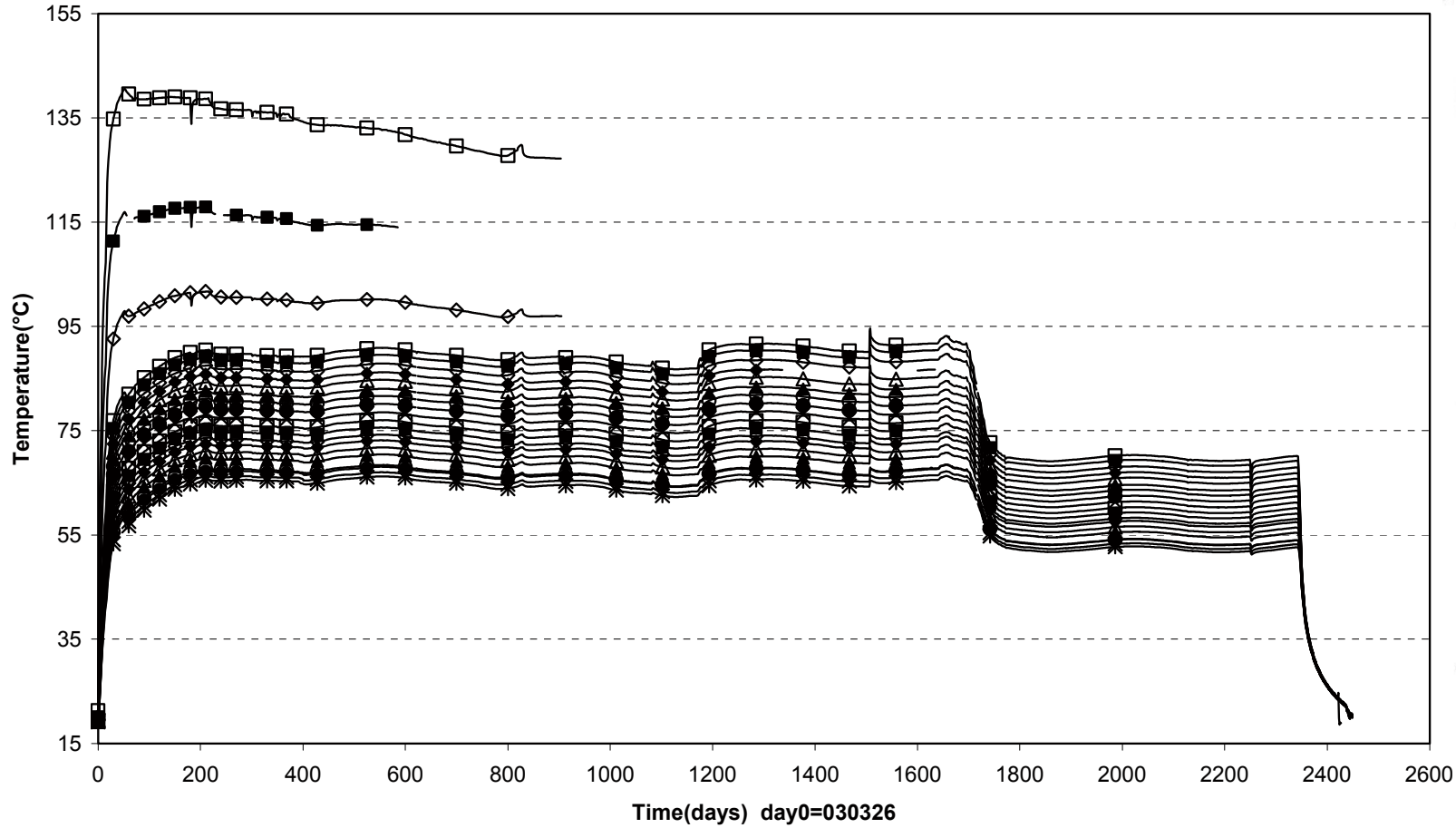
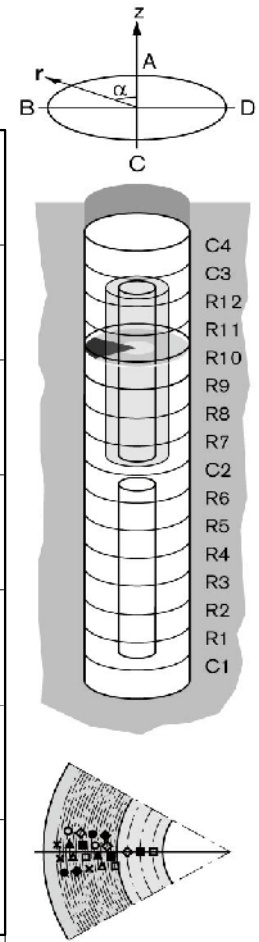
- | | | | | |
|-------------------------|-------------------------|-------------------------|-------------------------|-------------------------|
| □ TB215(2450\97.5°\320) | ■ TB216(2450\82.5°\360) | ◇ TB217(2450\97.5°\390) | ◆ TB218(2450\92.5°\420) | △ TB219(2450\87.5°\435) |
| ▲ TB220(2450\82.5°\450) | ○ TB221(2450\97.5°\465) | ● TB222(2450\92.5°\480) | □ TB223(2450\87.5°\495) | ■ TB224(2450\82.5°\510) |
| ◇ TB225(2450\97.5°\525) | ◆ TB226(2450\92.5°\540) | △ TB227(2450\87.5°\555) | ▲ TB228(2450\82.5°\570) | ○ TB229(2450\97.5°\585) |
| ● TB230(2450\92.5°\600) | □ TB231(2450\87.5°\615) | ■ TB232(2450\82.5°\630) | ◇ TB233(2450\97.5°\645) | ◆ TB234(2450\92.5°\660) |
| △ TB235(2450\87.5°\690) | ▲ TB236(2450\92.5°\720) | ○ TB237(2450\87.5°\750) | ● TB238(2450\92.5°\780) | □ TB239(2450\87.5°\810) |

TBT\Cyl.2 (030326-100301)
Temperature - Pentronic



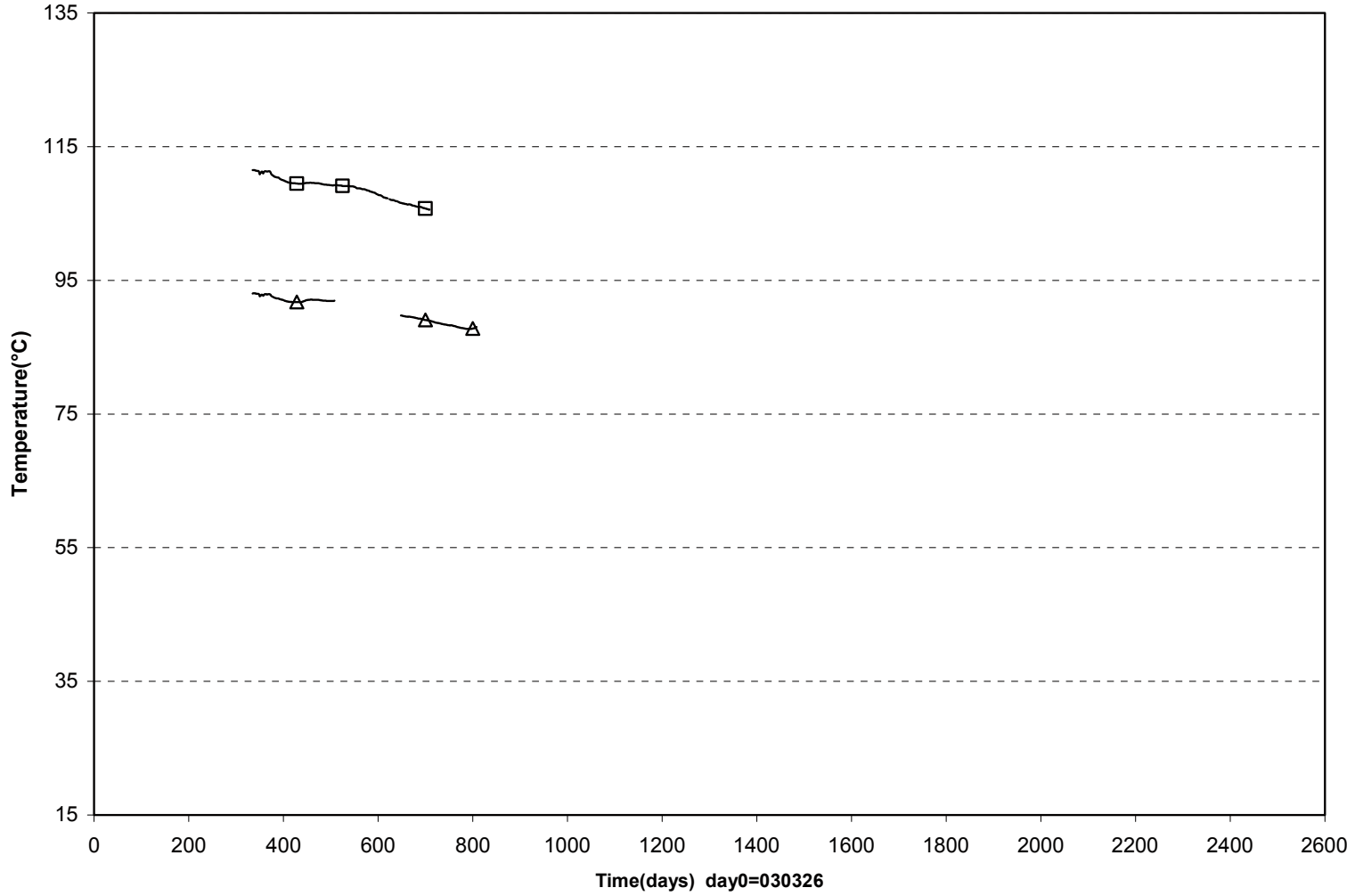
- TB240(3950\90°\150) ■ TB241(3950\95°\360) ◇ TB242(3950\85°\400) ◆ TB243(3950\95°\440) ▲ TB244(3950\85°\480) ▲ TB245(3950\95°\520) × TB246(3950\85°\560)
- × TB247(3950\95°\600) — TB248(3950\85°\640) ○ TB249(3950\95°\680) ● TB250(3950\85°\720) ○ TB251(3950\95°\760) ● TB252(3950\85°\800) + TB253(3950\95°\825)

TBT\ Ring 10 (030326-100301)
Temperature - Pentronic

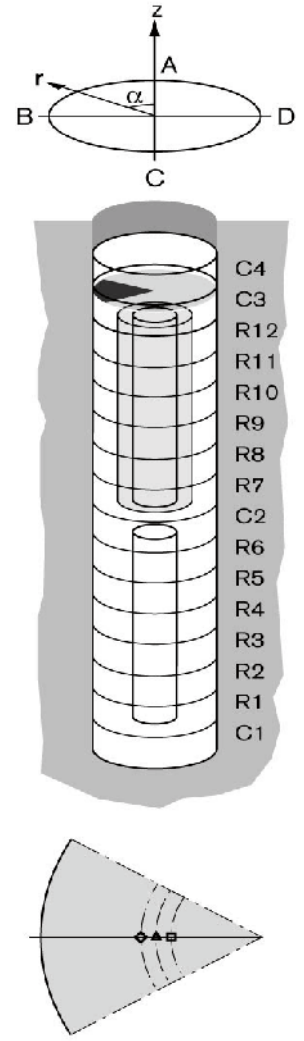


□ TB254(5950\90°\360)	■ TB255(5950\90°\420)	◇ TB256(5950\90°\480)	□ TB257(5950\97.5°\540)	■ TB258(5950\92.5°\555)	◇ TB259(5950\87.5°\570)
◆ TB260(5950\82.5°\585)	△ TB261(5950\97.5°\600)	▲ TB262(5950\92.5°\615)	○ TB263(5950\87.5°\630)	● TB264(5950\82.5°\645)	× TB265(5950\97.5°\660)
□ TB266(5950\92.5°\675)	■ TB267(5950\87.5°\690)	◇ TB268(5950\82.5°\705)	◆ TB269(5950\97.5°\720)	△ TB270(5950\92.5°\735)	▲ TB271(5950\87.5°\750)
○ TB272(5950\82.5°\765)	● TB273(5950\97.5°\780)	× TB274(5950\92.5°\795)	✱ TB275(5950\87.5°\810)		

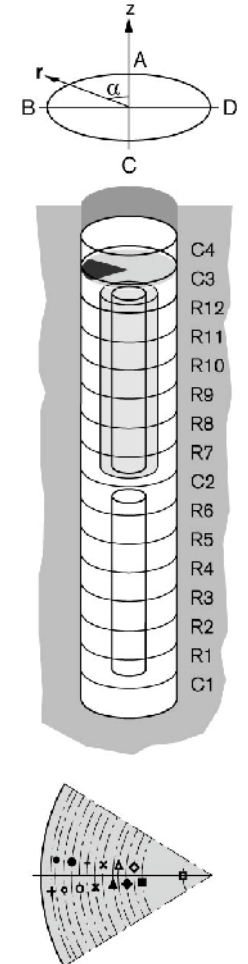
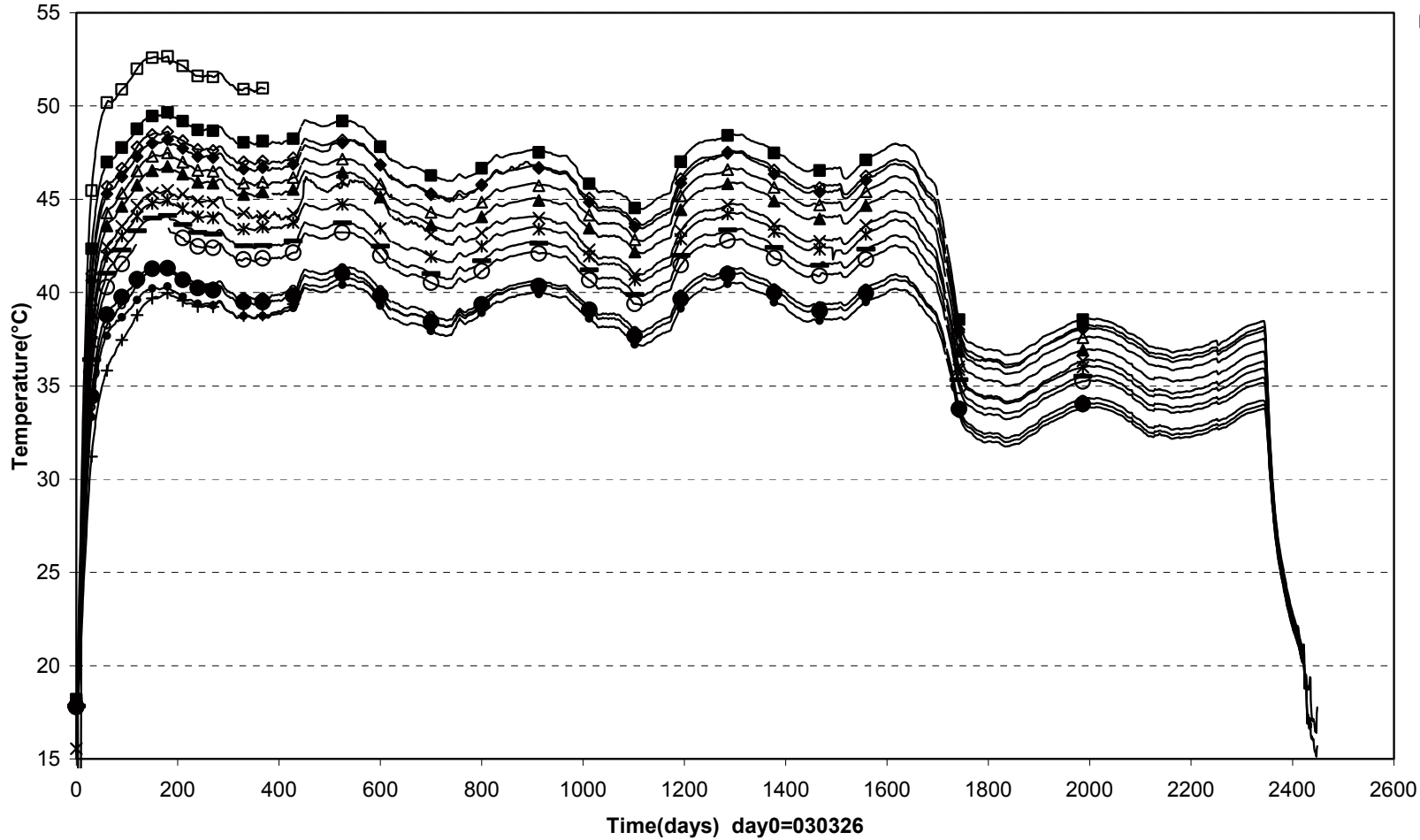
TBT\ Ring 12 (030326-100301) Temperature - Pentronic



□ TB290(6.881\90°\0.360) △ TB291(6.881\90°\0.420) ◇ TB292(6.881\90°\0.480)

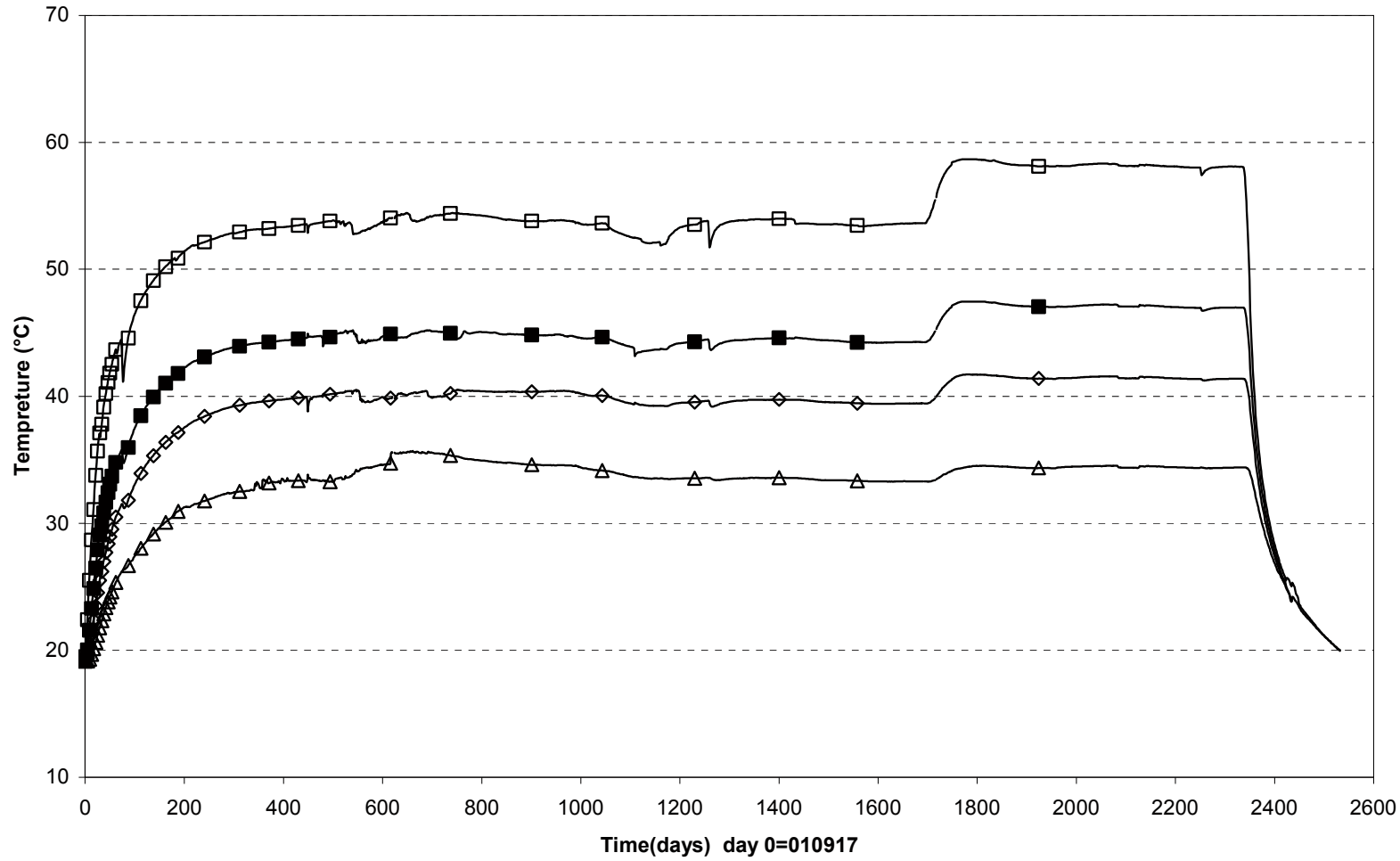


TBT\Cyl.3 (030326-100301)
Temperature - Pentronic

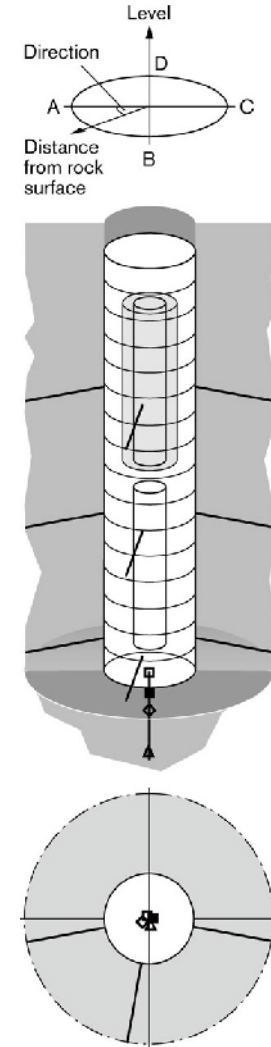


- TB276(7450\90°\150) ■ TB277(7450\95°\360) ◇ TB278(7450\85°\400) ◆ TB279(7450\95°\440) ▲ TB280(7450\85°\480) ▲ TB281(7450\95°\520) × TB282(7450\85°\560)
- × TB283(7450\95°\600) — TB284(7450\85°\640) ○ TB285(7450\95°\680) ● TB286(7450\85°\720) ◊ TB287(7450\95°\760) ● TB288(7450\85°\800) + TB289(7450\95°\825)

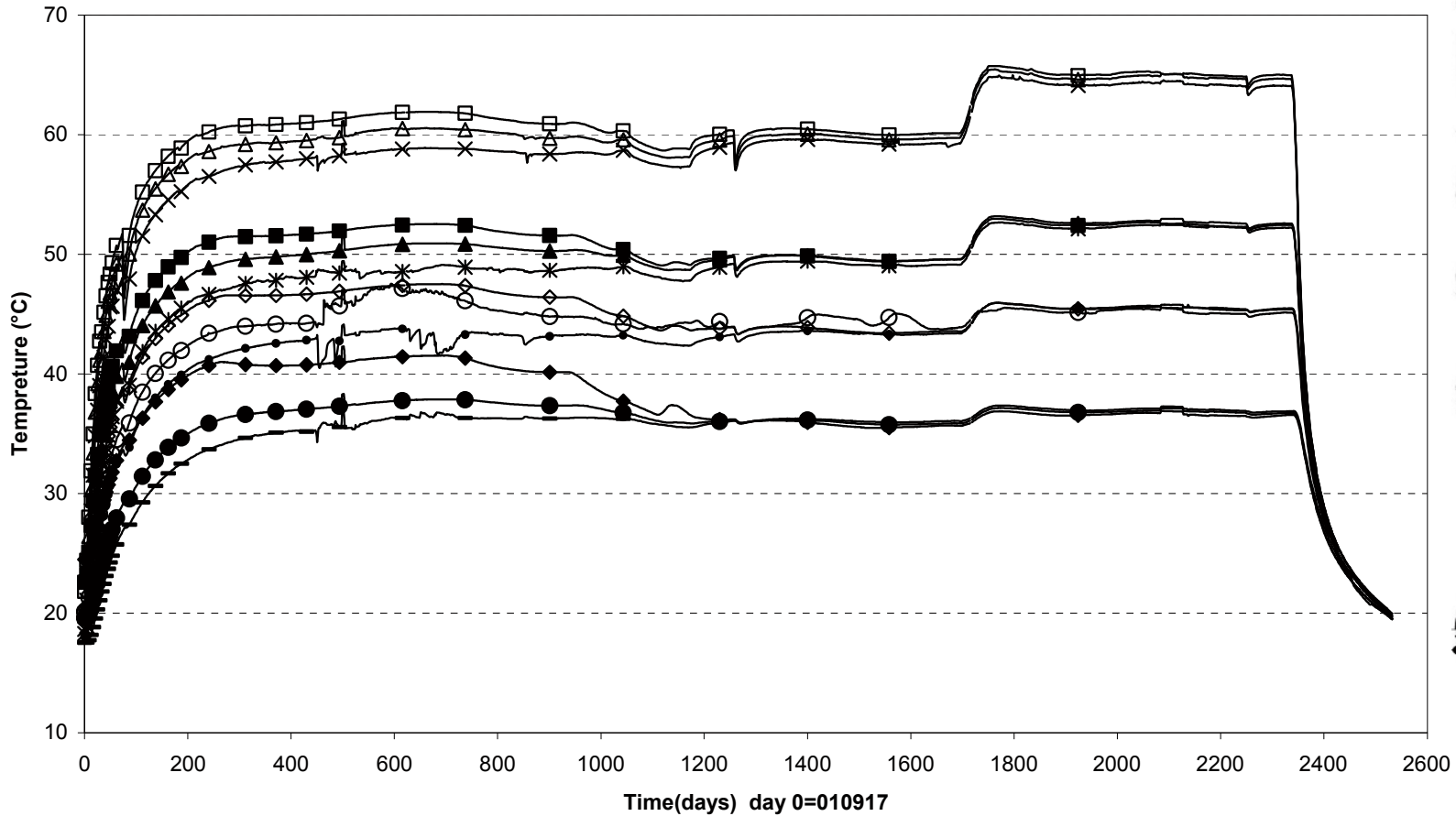
TBT\ Temperature in the rock-below the dep.hole (030326-100301) Temperature - Pentronic



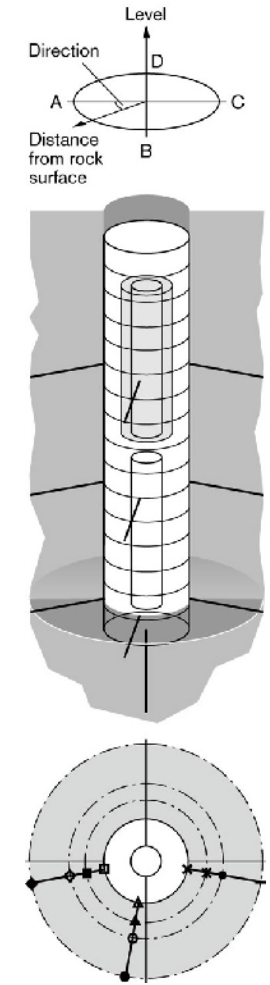
□ TR201(0\centre\0) ■ TR202(0\centre\0.375) ◇ TR203(0\centre\0.750) △ TR204(0\centre\1.500)



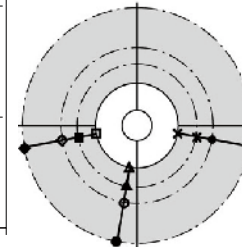
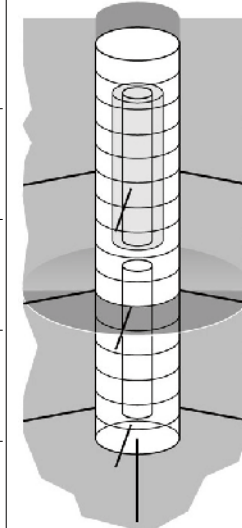
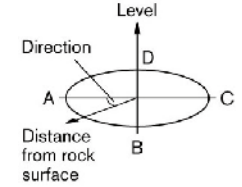
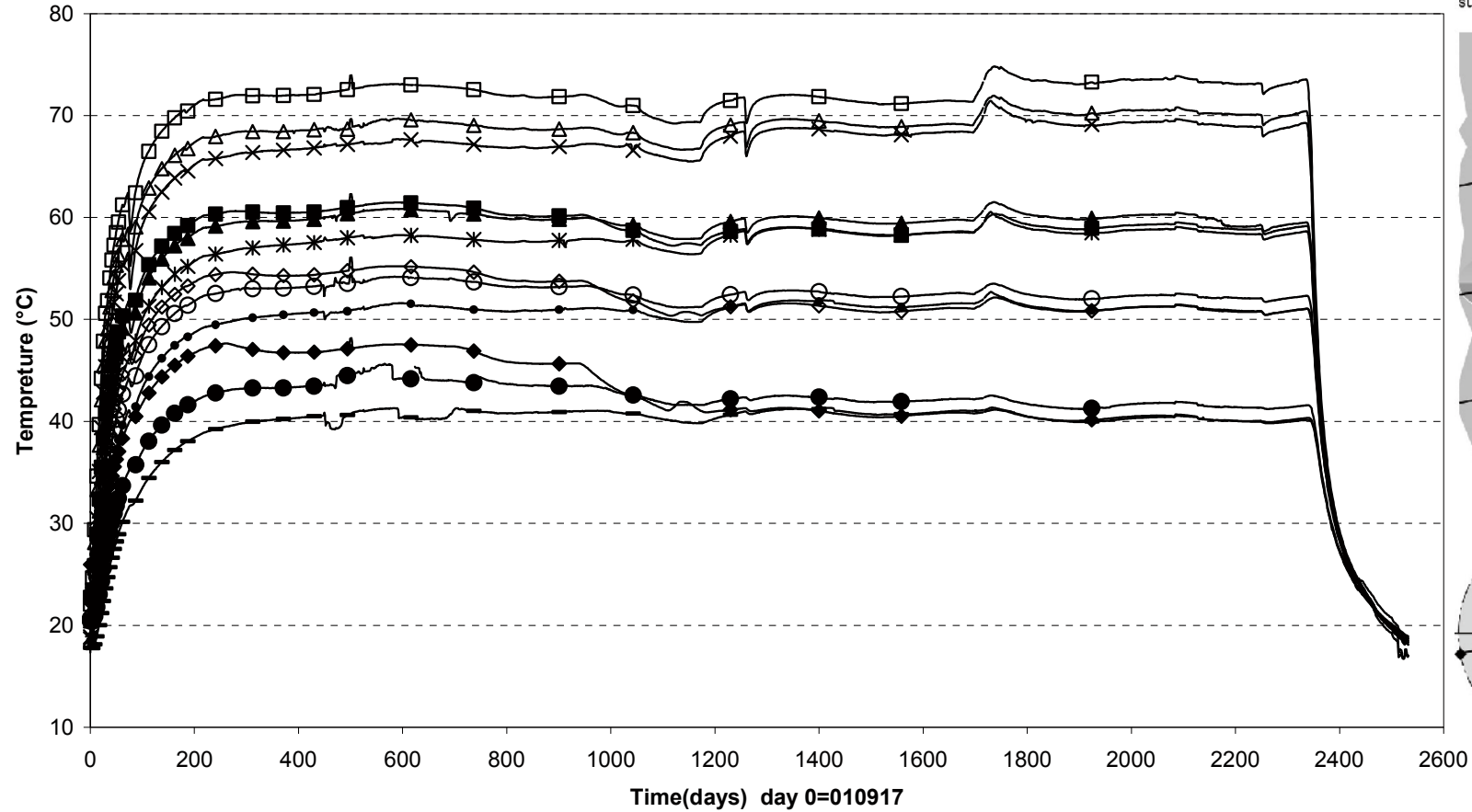
TBT\ Temperature in the rock-level 0.61 m (030326-100301)
 Temperature - Pentronic



Time(days) day 0=010917			
□ TR205(0.61\10°\0.000)	■ TR206(0.61\10°\0.375)	◇ TR207(0.61\10°\0.750)	◆ TR208(0.61\10°\1.500)
△ TR209(0.61\80°\0.000)	▲ TR210(0.61\80°\0.375)	○ TR211(0.61\80°\0.750)	● TR212(0.61\80°\1.500)
× TR213(0.61\170°\0.000)	* TR214(0.61\170°\0.375)	• TR215(0.61\170°\0.750)	- TR216(0.61\170°\1.500)

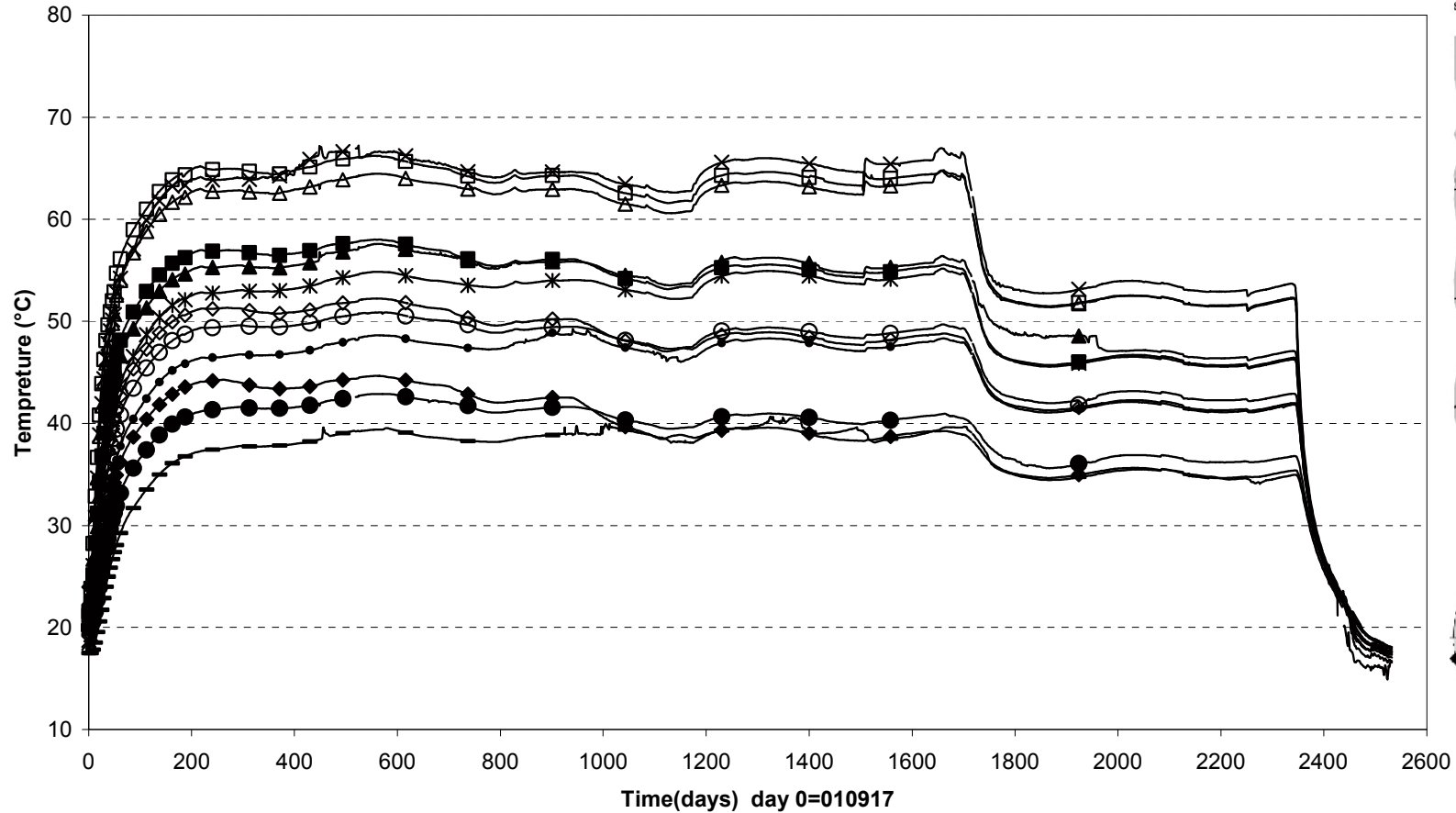


TBT\ Temperature in the rock-level 3.01 m (030326-100301)
 Temperature - Pentronic

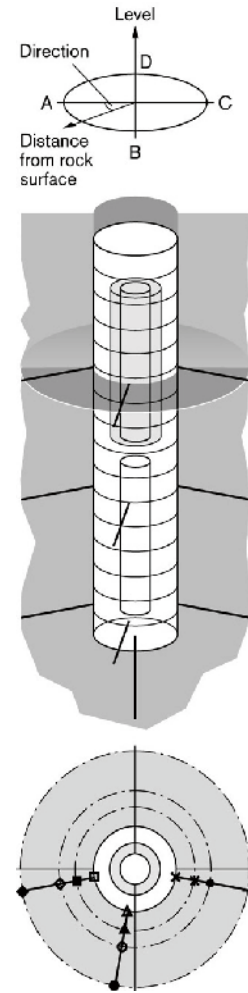


□ TR217(3.01\10°\0.000)	■ TR218(3.01\10°\0.375)	◇ TR219(3.01\10°\0.750)	◆ TR220(3.01\10°\1.500)
△ TR221(3.01\80°\0.000)	▲ TR222(3.01\80°\0.375)	○ TR223(3.01\80°\0.750)	● TR224(3.01\80°\1.500)
× TR225(3.01\170°\0.000)	✱ TR226(3.01\170°\0.375)	• TR227(3.01\170°\0.750)	— TR228(3.01\170°\1.500)

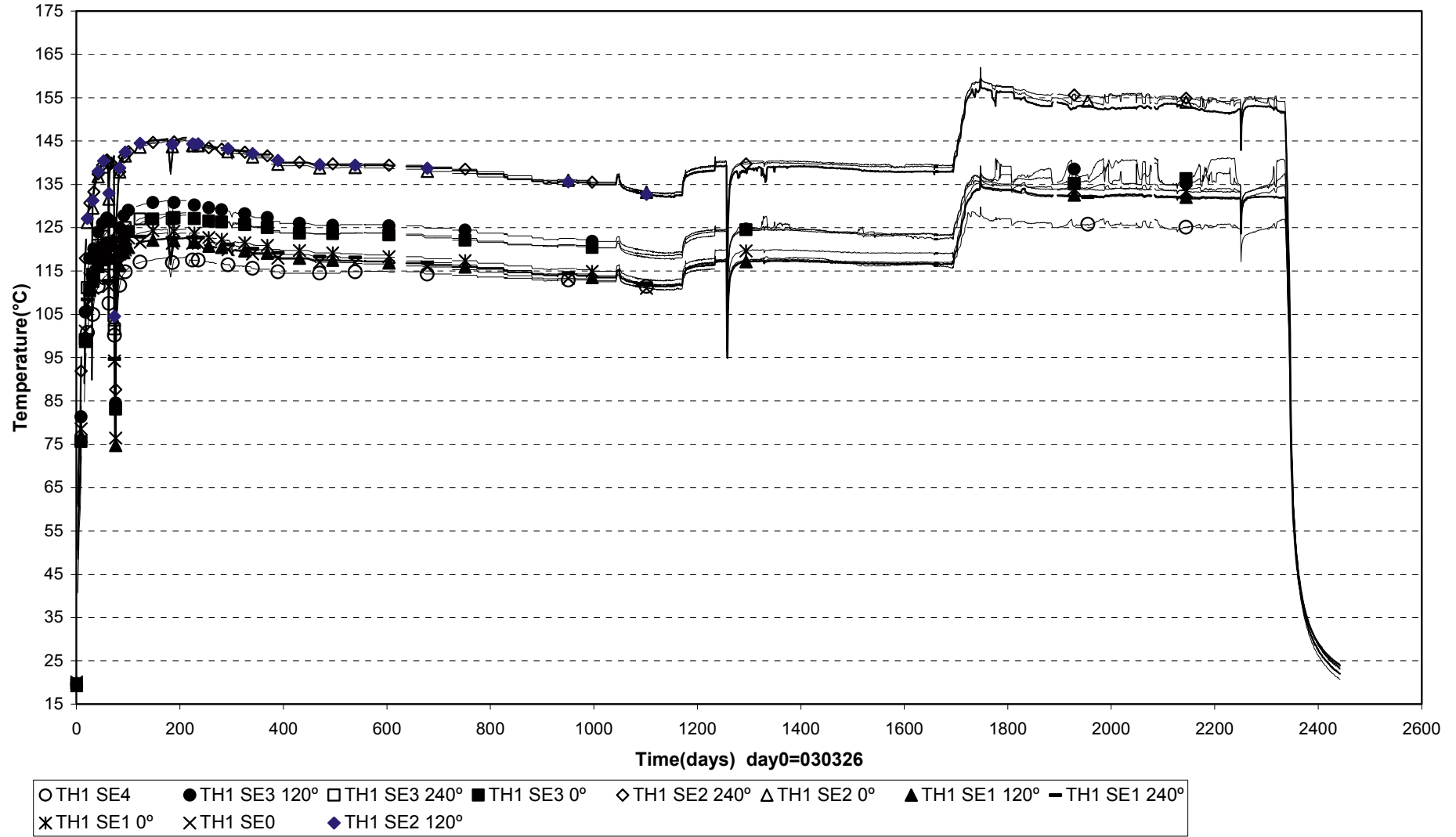
TBT\ Temperature in the rock-level 5.41 m (030326-100301)
 Temperature - Pentronic



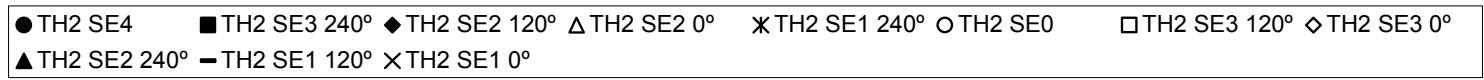
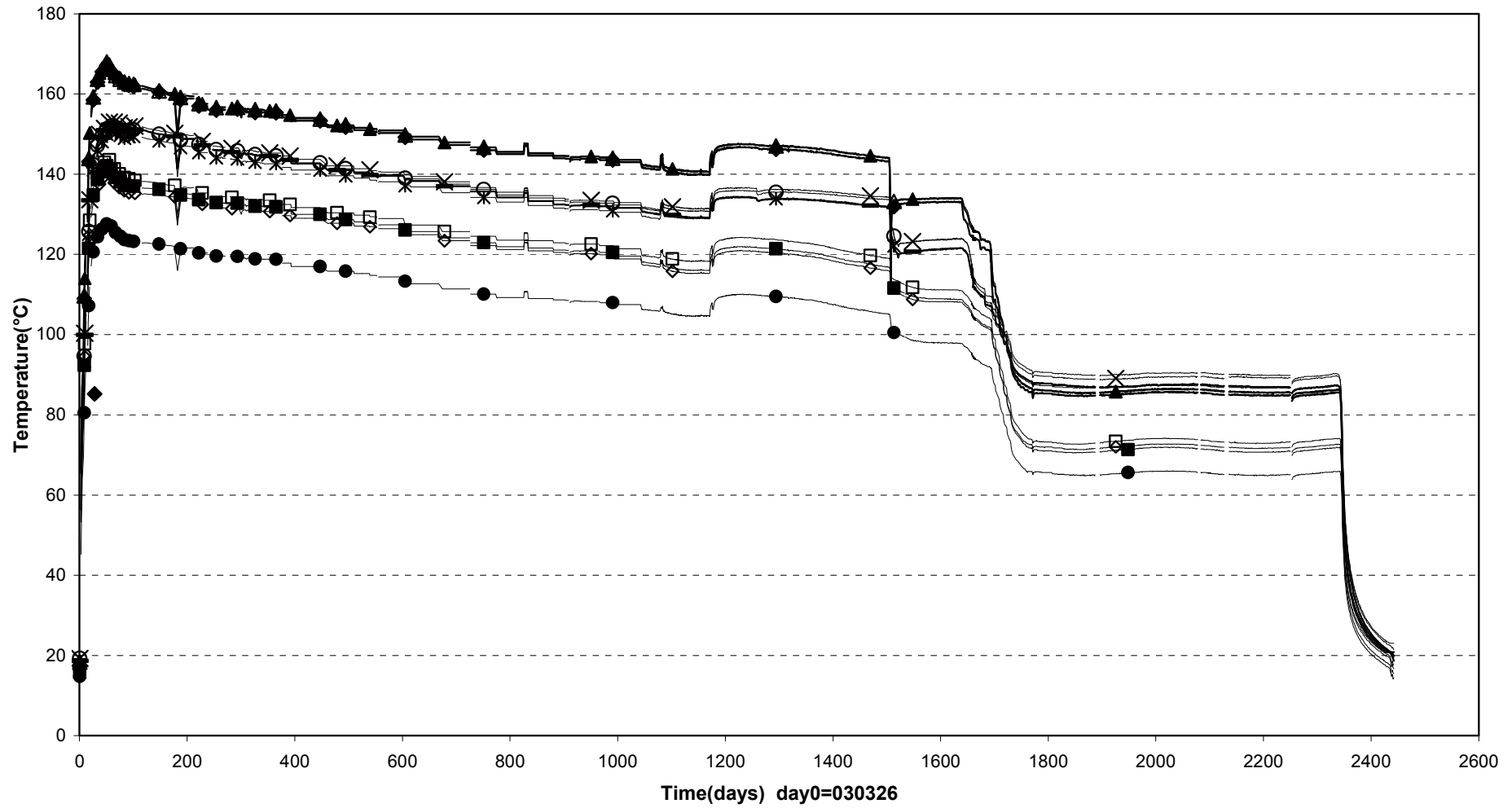
□ TR229(5.41\10°\0.000)	■ TR230(5.41\10°\0.375)	◇ TR231(5.41\10°\0.750)	◆ TR232(5.41\10°\1.500)
△ TR233(5.41\80°\0.000)	▲ TR234(5.41\80°\0.375)	○ TR235(5.41\80°\0.750)	● TR236(5.41\80°\1.500)
× TR237(5.41\170°\0.000)	* TR238(5.41\170°\0.375)	• TR239(5.41\170°\0.750)	- TR240(5.41\170°\1.500)



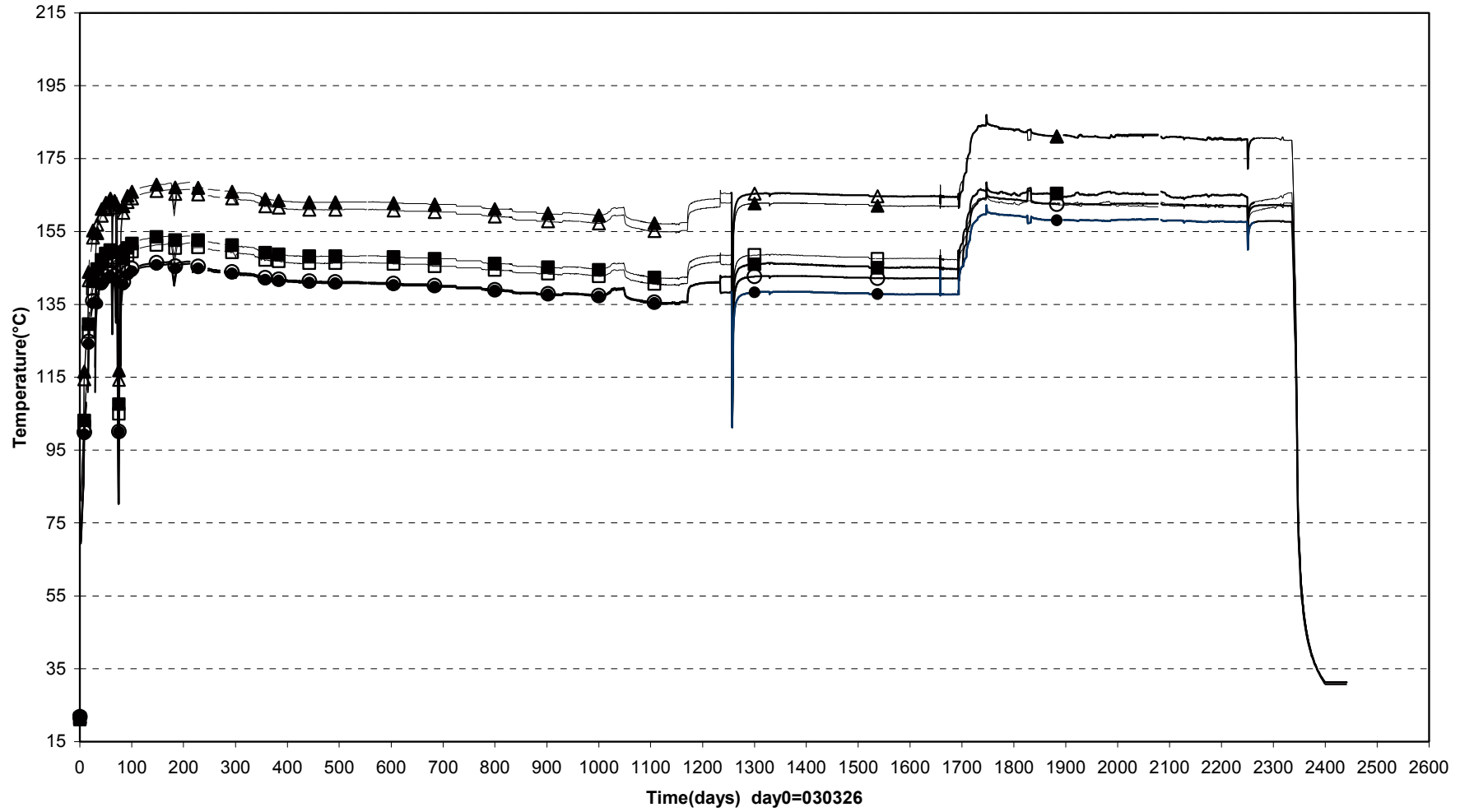
External temperatures Heater 1 (030326-100301)



External temperatures Heater 2 (070504-100301)

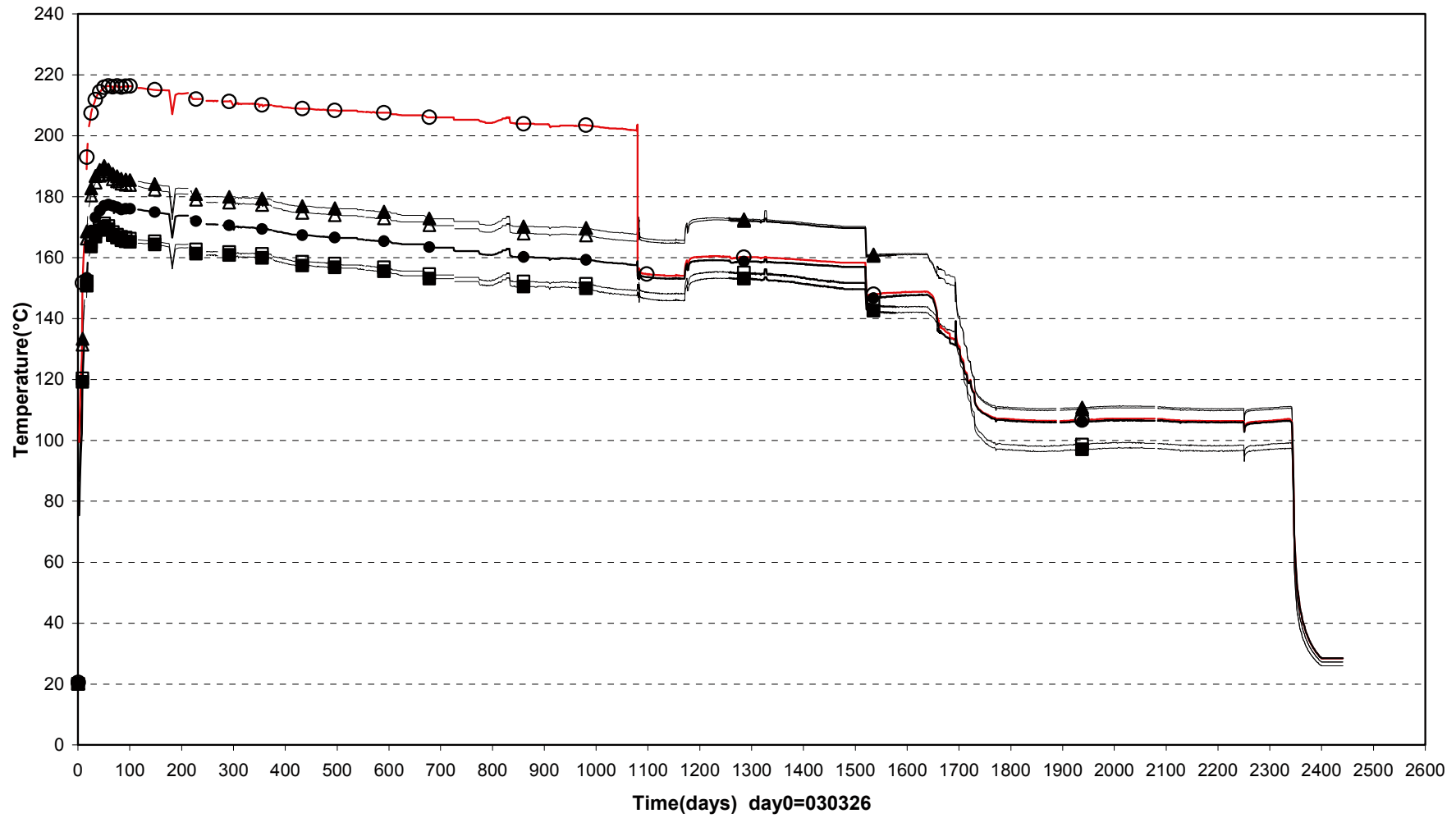


Internal temperatures Heater 1 (030326-100301)



□ TH1 SI1 0° ■ TH1 SI1 180° △ TH1 SI2 0° ▲ TH1 SI2 180° ○ TH1 SI3 0° ● TH1 SI3 180°

Internal temperatures Heater 2 (070504-100301)



□ TH2 SI1 0° ■ TH2 SI1 180° △ TH2 SI2 0° ▲ TH2 SI2 180° ○ TH2 SI3 0° ● TH2 SI3 180°

Sensor validation

Ulf Nilsson, Clay Technology AB

B-1 Introduction

The sensors in the TBT test parcels have been subjected to high temperatures and pressure in addition to saline water. Movements in the buffer during the test may have affected the sensors. Also the act of removing the surrounding material, when the experiment was dismantled, had an effect on the sensors. A number of sensors were in such condition that they were able to be tested. Of the tested sensors that were placed in the buffer the majority of the Geokon pore pressure sensors had small errors, the Geokon total pressure sensors had an offset error smaller than 0.5 MPa. The Druck pressure sensors that were placed topside had, with one exception, errors less than 1%. The thermocouples had an error of less than 2% with one exception. For the tested capacitive RH-sensors the function was outside the stated specifications.

The methodologies of these tests are presented in Section B-2. The first sorting of sensors are described in Section B-3. The results are presented in Section B-4. Examples of damages to sensors are illustrated in Section B-5. Section B-6 presents the complete test results for the Geokon sensors, including the linear regression analyses. A table with the original calibration report is also given. In Section B-7, tables are presented in which the duration (i.e. the day of the last reading), the test results and general comments are given for all Geokon sensors, as well as for all relative humidity sensors. Finally, Section B-8 describes the analyses of the precipitates on one of the filter tips in the sand filter.

B-2 Testing methodology

Pressure sensors

Druck (Type: PTX 610&1400)

These sensors are external pressure sensors and connected to the measured pressure with a pipe or tube. The same port was connected to a GDS ADvanced Volume Pressure Controller which was set to different pressures and the sensor output was read. The GDS ADVPC was calibrated against a Wika CPG 1000 (#1142159) calibrated at SP Technical Research Institute of Sweden. The sensors that were absolute pressure sensors were also tested against vacuum.

Geokon

The sensor was connected to a LC-2A Geokon single channel logger which was coupled to a computer running Logware 2.1.4. The settings for the pressure calculation were taken from the calibration report (linear calculation as in the setup), temperature compensation was not used since both the validation and calibration were made at room temperature. The pressure was delivered from the same GDS ADVPC as in the Druck validation.

Total pressure cells (type: 4800-1X) were immersed in a pressure vessel and the tube with the wire was going through the lid, see Figure B-1. A Swagelok 8 mm coupling sealed the tube, this is the reason sensors with short or no tube could not be tested. The max pressure for the vessel was 4.5 MPa.

Pore pressure cells (Type: 4500 TiX) were tested in a similar fashion but with another pressure vessel where the sensor was going through the lid, only the active parts were immersed, see Figure B-2.

Relative humidity sensors

Three sensor types have been used in TBT. *Vaisala* (model HMP237) and *Rotronic* (model HygroClip IM-1/10; HTS11X/9) are based on the capacitive method for measuring relative humidity, whereas *Wescor* (model PST-55) is a psychrometer. The function of the sensors was tested in a calibration device (Figure B-3), in which the climate was set by a saturated salt solution. Each sensor was tested for three different salt solutions LiCl, NaCl or K₂SO₄, which at room temperature correspond to relative humidity values of approximately 11, 76 and 98%, respectively.



Figure B-1. Test cell with a sensor.

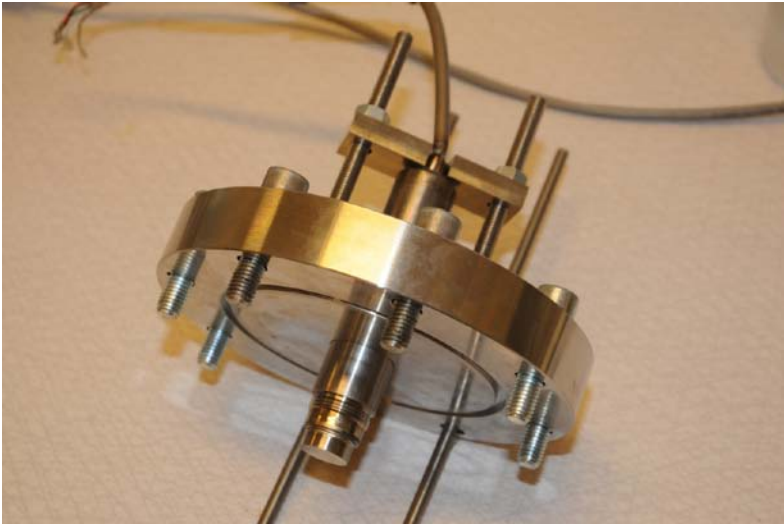


Figure B-2. Test cell lid with a sensor.

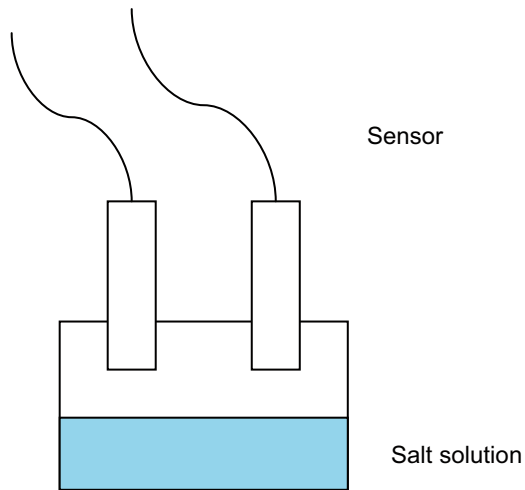


Figure B-3. Calibration device for relative humidity sensors.

B-3 First sorting

When the sensors arrived a quick sorting was made on the basis of which could be directly excluded based on the state of the sensor. Obvious damage, missing cables or parts were reasons why sensors were “scrapped”. Some damage is likely to have occurred during dismantling but others probably happened during the running of the tests.

Pressure sensors Druck

Of 15 received all were deemed testable.

Pressure sensors Geokon Porepressure

Of 7 received sensors, 5 were deemed testable. UB202 had drill damage and could not be tested. For UB205 the cable was missing.

Pressure Sensors Geokon Total pressure

Of 29 received sensors, 14 were initially deemed testable, since they were not superficially damaged. 15 were either missing the cable or had damage on the tube close to the sensor housing.

Relative humidity sensors

Vaisala: Of 10 received sensors, 5 were initially deemed testable, ie complete with no outer damage. When the signal transducer were opened internal corrosion were discovered in two sensors. In two other sensors, faulty signals were measured when these were connected to the power supply. In the end only one was working and tested.

Rotronic: Of 5 received sensors, 2 were tested. The rest showed either 0 (1) or 100% (2) when exposed to 36% and were therefore counted as faulty.

Wescor: Of 8 received sensors, the thermocouple part was found to be ok, but otherwise none were considered to be testable.

Thermocouples (Pentronic , Type K)

These were tested on site, a two point measurement (20°C and 90°C) was made in a water bath.

B-4 Results

Druck

Of the tested Druck pressure sensors all were functioning and 13 had an error of less than 1%. A typical curve is shown in Figure B-4. One sensor CS 202 had an error of 2.5% at zero pressure and less than 1% at pressures above 10 bar, Figure B-5.

Geokon pore pressure

A linear regression curve was made for each of these sensors (Figures B-11 and B-12). In this way both linear error and offset errors could be seen. The tested sensors had a linear error less than 5% and with one exception offset error less than 0.1 MPa. UB 201 had an offset error of -0.36 MPa. See Table B-1.

Geokon Totalpressure

Evaluating these sensors a linear regression curve was made for each. In this way both linear error and offset errors could be seen. Only one of the tested sensors had a linear error less than 5%. The rest of the tested sensors had a linear error of 6 to 10% and an offset error of 0 to -0.64 MPa. This includes the sensors that were damaged by drilling. See also Table B-2. All diagrams are presented in the Section B-6.

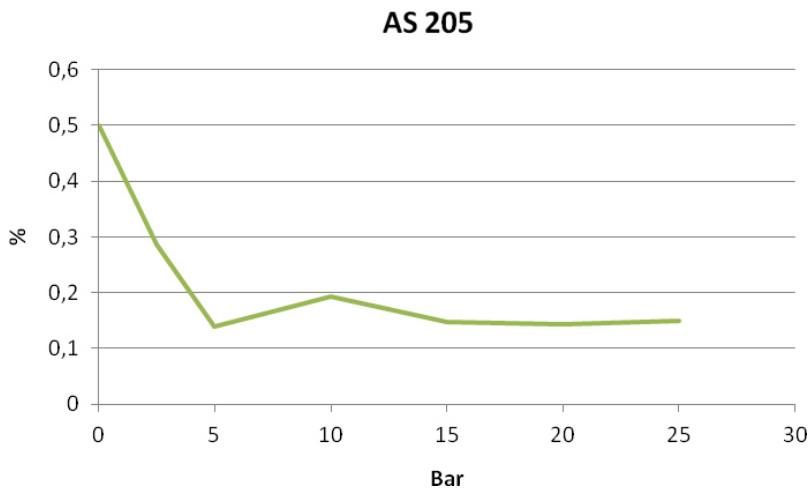


Figure B-4. Error for sensor AS 205 as a function of pressure.

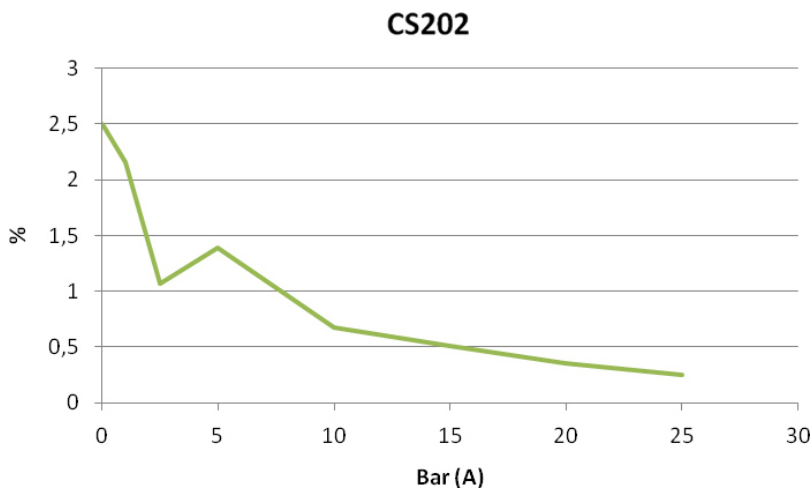


Figure B-5. Error for sensor CS 202 as a function of pressure.

Table B-1. Results from the validation.

Sensor #	Project #	Pass/Fail	Linear error	Offset error	Comment
69714	UB201	Under Spec.	0.974	-0.36	
69713	UB202	Untested			Drill damage
69715	UB203	OK	0.969	0.002	
69709	UB205	Untested			Cable missing
69707	UB206	OK	0.977	-0.04	
69710	UB207	OK	0.983	-0.04	
69708	UB208	OK	0.987	0.07	

Table B-2. Results from the validation: Total pressure sensors.

Sensor #	Project #	Pass/Fail	Linear error	Offset error	Comment
70063	PB201	Under spec.	1.1	-0.38	Polynomial fit better than linear
70065	PB202	Untested			Tube damaged close to sensor
70064	PB203	Fail			Leakage
70053	PB204	Untested			Tube damaged close to sensor
70057	PB205	Untested			Tube damaged close to sensor
70052	PB206	Untested			Cable missing
70048	PB207	Untested			Weld housing/pipe broken
70056	PB207	Untested			Cable missing
70058	PB208	Untested			Tube damaged close to sensor
70055	PB210	Untested			No connection
70059	PB211	Untested			Tube damaged close to sensor
70061	PB212	OK	1.03	0.013	
70061	PB213	Fail			Unstable values
70050	PB214	Under Spec.	1.08	-0.4	
70051	PB215	Untested			Cable missing
70049	PB216	Under Spec.	1.07	-0.34	
70044	PB217	Untested			Tube missing
70039	PB218	Fail			No connection
70054	PB219	Untested			
70043	PB220	Fail			No connection
70046	PB221	Fail			Leakage
70042	PB222	Under Spec.	1.07	0.34	Large cut on the side
70041	PB223	Fail			Unstable values
70040	PB224	Under Spec.	1.08	-0.64	Cut on the side
70047	PB225	Untested			Pipe to bent to test
70045	PB226	Untested			Cable missing
70036	PB227	Untested			Cable missing
70037	PB228	Fail			No connection
70038	PB229	Under Spec.	1.06	-0.07	

Relative humidity sensors

Three sensors were tested in different climates: two Rotronic sensors (WB223 and WB234) and one Vaisala sensor (WB232). The results are illustrated in Figure B-6. The Vaisala sensor was tested at the condition after dismantling, as well as after washing in deionized water, at 11, 76 and 98%. The measured value deviated with approximately 10% at a target relative humidity of 76%. The washing procedure had no apparent effect on the function. The Rotronic sensors both displayed RH 100% at a target value of 76%. All sensors can tentatively be graded “under specification”, since all deviations clearly exceed the stated uncertainties of the sensors (Rotronic: $\pm 1\%$; Vaisala 0–50%: $\pm 1.1\%$, 50–100%: $\pm 1.4\%$).

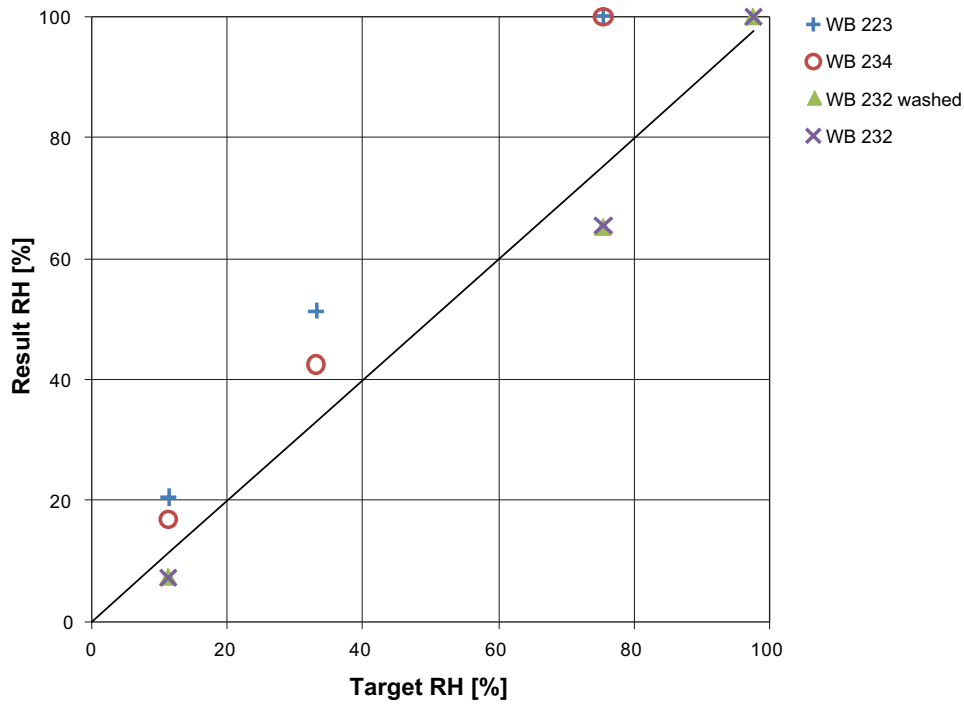


Figure B-6. Measured relative humidity values at different climates for the tested sensors.

Temperature

Of the 23 tested thermocouples only one had large error, TB268 which was functional until the dismantling operation. Results are shown in Table B-3.

Table B-3. Results from validation of thermocouples.

Project #	Pass/Fail	Linear error	Offset error
TB215	OK	0.981	0.184
TB222	OK	0.981	0.551
TB224	OK	0.986	0.269
TB227	Under spec.	0.969	1.723
TB228	OK	0.983	0.216
TB231	OK	0.992	0.359
TB232	Under spec.	0.949	2.304
TB234	OK	0.993	0.111
TB235	OK	0.987	-0.179
TB237	OK	0.992	-0.479
TB238	OK	0.985	-0.354
TB239	OK	0.988	0.104
TB258	OK	0.980	0.414
TB260	OK	0.988	0.364
TB261	OK	0.980	0.467
TB267	OK	0.983	0.233
TB268	Fail	0.058	194.143
TB270	OK	0.987	0.007
TB271	OK	0.994	0.100
TB273	OK	0.987	0.253
TB274	OK	0.983	0.279
TB285	OK	0.980	-0.040
TB287	OK	0.985	-0.110

B-5 Example of damage to sensors

To understand why some sensors have broken, detailed pictures have been taken of the damages. An example of dismantling damage can be seen in Figure B-7. This is from the core drilling of the buffer samples.

The welds and connections are sensitive to movements. Both the weld between the house and the 8 mm tube, see Figure B-8, and the 6 to 8 mm coupling has broken in several sensors, see Figure B-9, especially the Geokon Total pressure sensors. This damage allows water access into the sensor and there cause corrosion and/or short-circuits. As can be seen in the cable also the shielding can be corroded, see Figure B-10. If the damage occurred during the test, dismantling of the test or in later handling cannot always be clear.



Figure B-7. Sensor Geokon 70042 drill damage.



Figure B-8. Sensor 70054, broken in the weld to the housing.



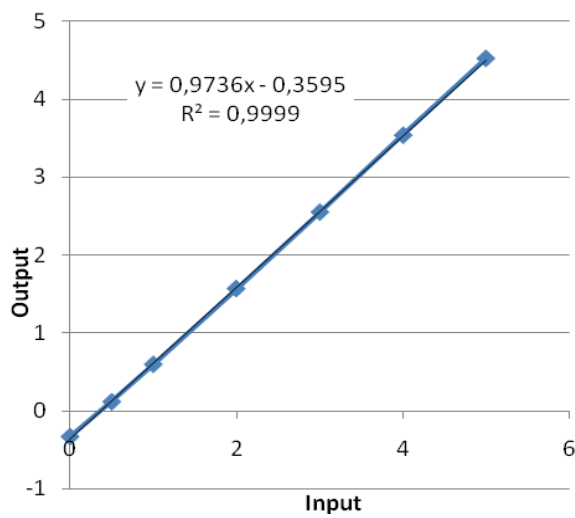
Figure B-9. Sensor Geokon 70064, weld 8 mm to 6 mm tube has broken and water can reach the sensors electronics.



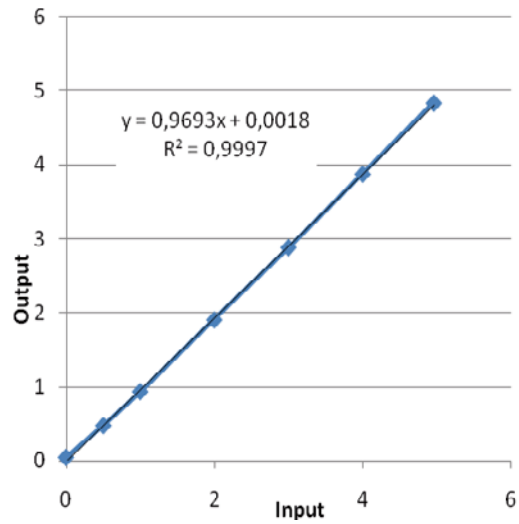
Figure B-10. Sensor cables, the upper showing corrosion in the shield from water. 70039, 70055.

B-6 All Geokon diagrams

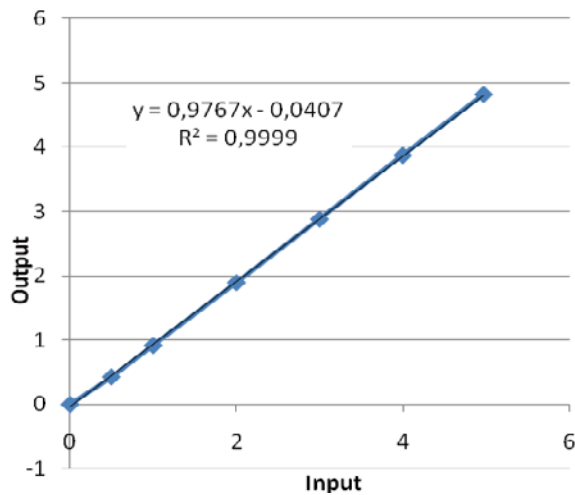
For all diagrams the x-axis represents the applied pressure in MPa and the y-axis the resulting value. A linear regression is calculated.



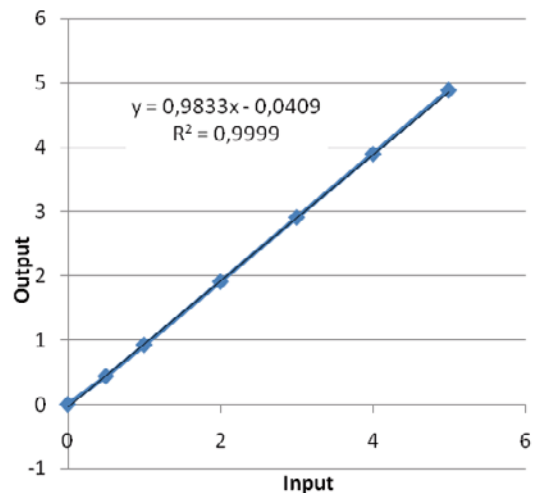
UB 201 #69714



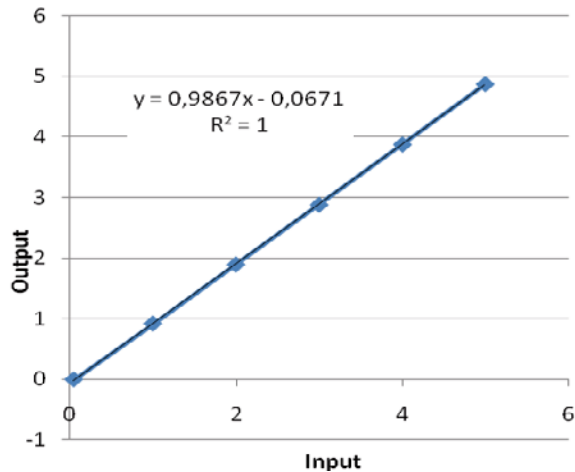
UB 203 #69715



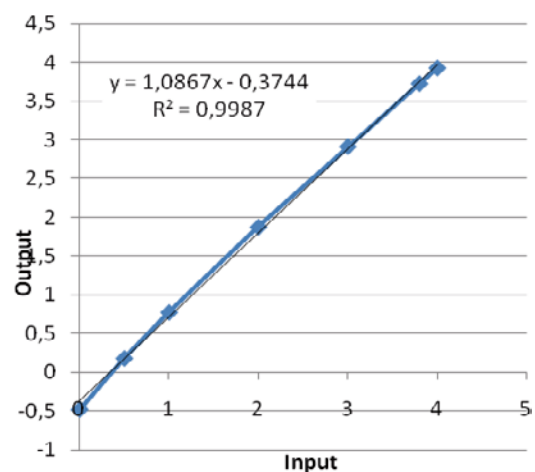
UB 206 #69707



UB 207 #69710

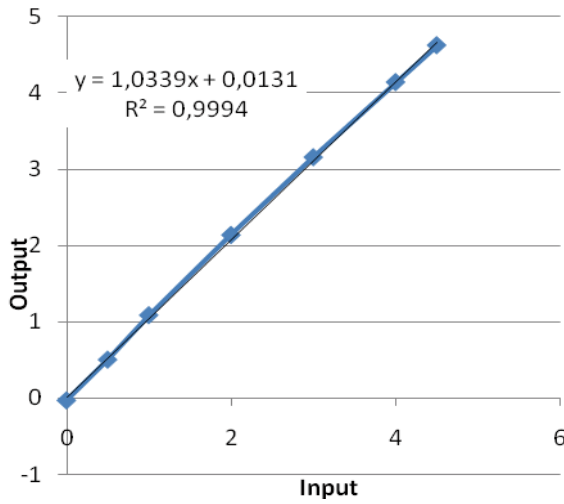


UB 208 #69708

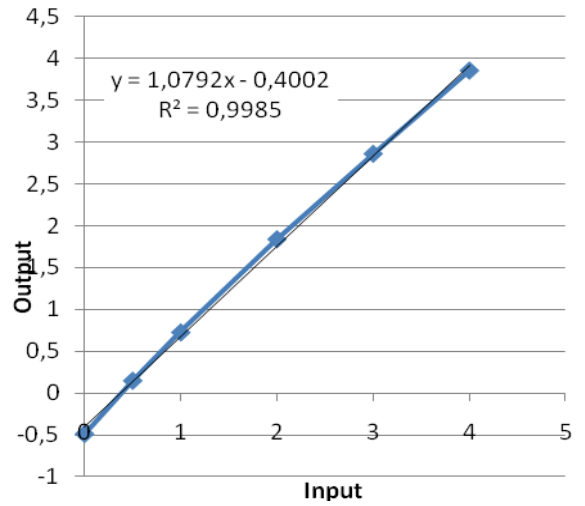


PB 201 #70063

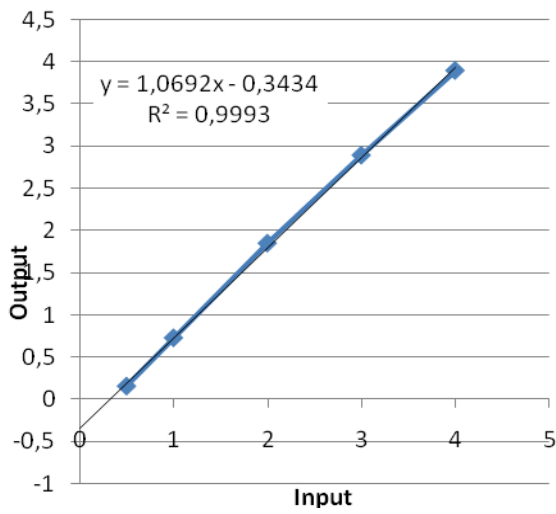
Figure B-11. Regression of input and output from Geokon sensors.



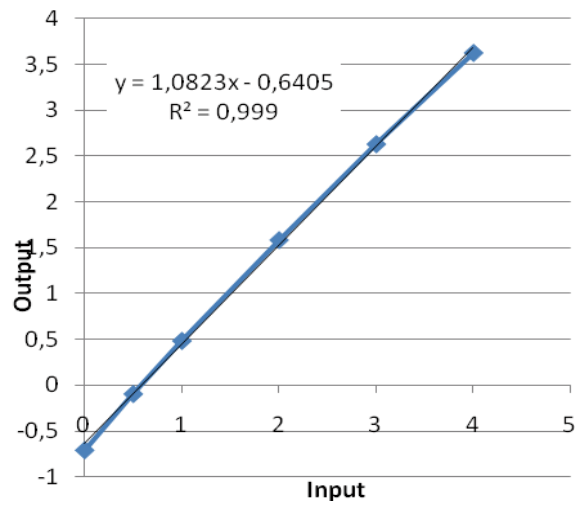
PB 212 #70061



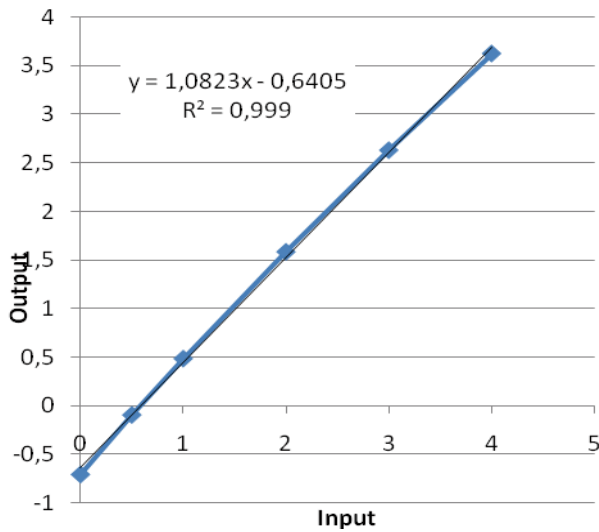
PB 214 #70050



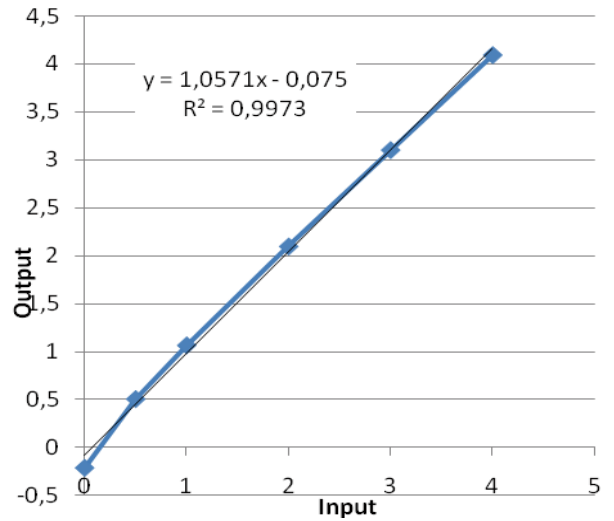
PB 216 #70049



PB 222 #70042



PB 224 #70040



PB 229 #70038

Figure B-12. Regression of input and output from Geokon sensors (cont).

Table B-4. Data from original calibration report.

Serial #	Project #	Linear Gage factor (MPa/digit)	Regression Zero
69714	UB201	0.001390	8,980
69713	UB202	0.001363	7,993
69715	UB203	0.001362	9,102
69709	UB205	0.001387	9,179
69707	UB206	0.001368	9,119
69710	UB207	0.001360	8,802
69708	UB208	0.001364	9,378
70063	PB201	-0.002045	2,817
70065	PB202	-0.002254	3,117
70064	PB203	-0.001948	2,814
70053	PB204	-0.001991	2,884
70057	PB205	-0.002009	3,123
70052	PB206	-0.001997	2,694
70048	PB207	-0.002019	2,826
70056	PB207	-0.002010	2,338
70058	PB208	-0.002021	2,559
70055	PB210	-0.002024	2,953
70059	PB211	-0.001768	3,162
70061	PB212	-0.002052	3,567
70060	PB213	-0.001981	2,885
70050	PB214	-0.002000	3,068
70051	PB215	-0.001980	2,761
70049	PB216	-0.002008	2,978
70044	PB217	-0.002035	2,559
70039	PB218	-0.001992	2,639
70054	PB219	-0.002017	2,808
70043	PB220	-0.002033	3,009
70046	PB221	-0.001985	2,902
70042	PB222	-0.002033	2,941
70041	PB223	-0.001986	2,987
70040	PB224	-0.002113	2,798
70047	PB225	-0.002026	2,732
70045	PB226	-0.002048	2,890
70036	PB227	-0.001996	2,784
70037	PB228	-0.002023	2,893
70038	PB229	-0.002032	3,245

B-7 Last readings and comments

Table B-5. Geokon total pressure sensor: last reading, test results and comment.

Sensor	Day of last reading	Test results	Comments
PB201	2,532	Under spec.	
PB202	2,504	Untested	Cable cut close to sensor
PB203	1,759	Fail	Weld 6–8 mm loose, corrosion in the shield
PB204	2,362	Untested	Pipe damaged close to housing
PB205	814	Untested	Cable cut 1 cm from sensor, drill damage
PB206	325	Untested	Drill damage, no tube, no cable
PB207	229	Untested	Weld pipe/sensor broken when handling
PB208	2,130	Untested	Cable cut close to sensor, drill damage
PB209	2,532	Untested*	Cable missing
PB210	345	Untested	No contact with sensor
PB211	1,358	Untested	Wire and tube cut close to sensor
PB212	2,532	OK	
PB213	2,532	Fail	Damage on the face side
PB214	2,504	Under spec.	
PB215	2,278	Untested	Cable missing
PB216	2,249	Under spec.	
PB217	2,454	Untested	Pipe missing
PB218	1,587	Fail	Bad contact
PB219	2,447	Untested	Not found
PB220	1,515	Fail	Signal $-\infty$
PB221	230	Fail	Weld 6–8 mm loose, corrosion in the shield
PB222	2,426	Under spec.	Large cut on the left side
PB223	1,571	Fail	Unstable negative values
PB224	2,455	Under spec.	Small cut on the left side
PB225	2,455	Untested	Pipe to twisted to allow testing
PB226	2,532	Untested	Cable missing
PB227	686	Untested	Cable missing
PB228	1,378	Fail	No signal from sensor
PB229	2,433	Under spec.	

* PB209 marked as PB207

Table B-6. Geokon porel pressure sensor: last reading, test results and comment.

Sensor	Day of last reading	Test results	Comments
UB201	2,527	Under spec.	
UB202	2,532	Untested	Drill damage on the surface
UB203	2,532	OK	
UB204	2,532	Untested	Not found
UB205	2,426	Untested	Cable missing
UB206	2,450	OK	
UB207	2,426	OK	
UB208	2,454	OK	

Table B-7. Vaisala RH sensor: last reading, test results and comment.

Sensor	Day of last reading	Test results	Comments
WB202	152	Untested	Sensor cable cut
WB206	1,138	Untested	Not found
WB208	335	Untested	Not found
WB210	409	Untested	Sensor cable cut
WB214	141	Untested	Sensor cable cut
WB217	1,237	Untested	Frequency missing T channel
WB221	450	Untested	Corrosion inside box
WB222	620	Untested	Corrosion inside box
WB224	1,098	Untested	Frequency missing T channel
WB227	981	Untested	Frequency missing T channel
WB232	1,118	~Under spec.	

Table B-8. Rotronic RH sensor: last reading, test results and comment.

Sensor	Day of last reading	Test results	Comments
WB201	2,532	Untested	Not found
WB204	2,440	Untested	Sensor cable cut
WB207	244	Untested	Not found
WB209	1,801	Untested	Not found
WB212	1,993	Untested	Connector damaged
WB216	1,654	Untested	Connector damaged
WB219	1,835	Untested	RH 0% at 36%, possible cable damage
WB223	2,449	~Under spec.	
WB225	2,451	Untested	RH 100% at 36%
WB229	2,451	Untested	RH 100% at 36%
WB231	2,454	Untested	Box only
WB234	2,434	~Under spec.	

Table B-9. Wescor RH sensor: last reading, test results and comment.

Sensor	Day of last reading	Test results	Comments
WB203	1,711	Untested	Sliding plateau
WB205	1,602	Untested	Not found
WB211	337	Untested	Not found
WB213	168	Untested	Not found
WB215	698	Untested	Wire cut
WB218	1,262	Untested	No plateau
WB220	237	Untested	Can not zero
WB226	744	Untested	Can not zero
WB228	531	Untested	No plateau
WB230	418	Untested	Can not zero
WB233	1,262	Untested	Can not zero
WB235	1,043	Untested	Can not zero

B-8 Filter tips

The filter tips in the sand filter have exhibited a high flow resistance, and after the dismantling it was apparent that the filter tips have been covered with some type of precipitate (Figure B-13). This material has been analyzed with X-ray diffraction analysis, and the resulting diffractogram is shown in Figure B-14. The results indicated that the sand particles have been “cemented” together by calcite.



Figure B-13. Filter tip from injection point AS205 with precipitates.

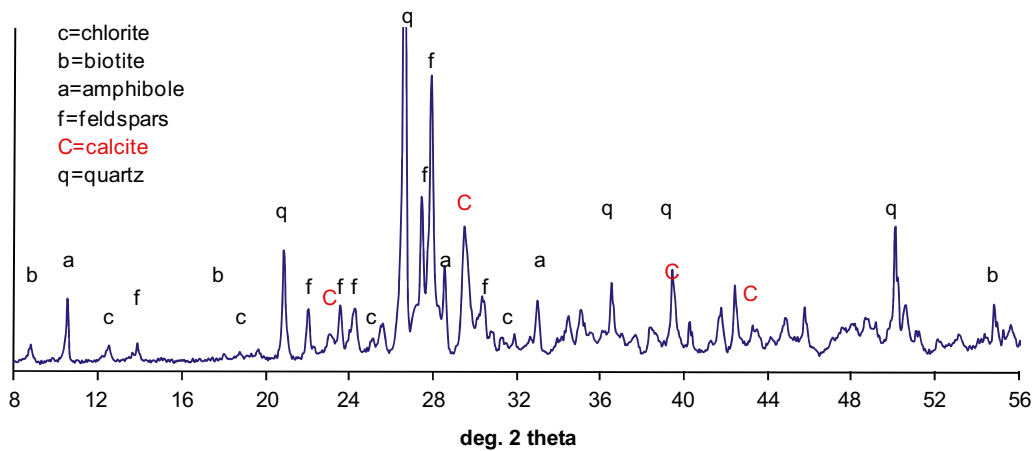


Figure B-14. XRD profile for analyzed precipitate material from AS205 filter tip. Identified minerals indicated at different peaks.